STRENGTH OF SCREW PROPELLERS

B. A. Biskup, et al

Naval Intelligence Support Center
Washington, D. C.

7 July 1975

DEPARTMENT OF THE NAVY
NAVAL INTELLIGENCE SUPPORT CENTER
TRANSLATION DIVISION
4301 SUITLAND ROAD
WASHINGTON, D.C. 20390

22017C

CLASSIFICATION: UNCLASSIFIED

APPROVED FOR PUBLIC RELEASE: DISTRIBUTION UNLIMITED

TITLE: Strength of Screw Propellers

Prochnost' grebnykh vintov

AUTHOR(S): Biskup, B.A., Terletskiy, B.M., Nikitin, M.N., and Popov, S.I.

PAGES: 168

SOURCE: Sudostroyeniye Publishing House, Leningrad, 1963
Pages 2-147 and 161-168

ORIGINAL LANGUAGE: Russian

TRANSLATOR: C

NISC TRANSLATION NO. 3680

APPROVED P.T.K

DATE 7 July 1975

STRENGTH OF SCREW PROPELLERS

(Biskup, B. A., Terletskiy, B. M., Nikitin, M. N., Popov, S. I.; Prochnost' grebnykh vintov, Publishing House "Sudostroyeniye", Leningrad, 1953, 168 pages; Russian)

ABSTRACT

/2*

The book is an attempt to systematize problems related to substantiation and development of practical methods for general strength calculation of ship propellers. Two approaches are presented for determining the strength characteristics of screw propellers: the first is based on taking into consideration static loads on the propeller blade only, while the second takes into account variable (cyclic) forces acting on the screw propeller. The discussion of the calculation method based on static loads (Chapter I) includes: determining the constant component of hydrodynamic loads and centrifugal forces, design calculations of the geometrical characteristics of the blade and of its separate elements, determining the maximum stresses in the propeller blade, and evaluating the strength characteristics of the blade.

Substantiation is given for evaluation of the cyclic strength of a ship propeller. Design calculation diagrams are suggested for determining the external forces acting on screw propeller under various conditions of ship operation. A method is discussed for determining the general safety factor by means of individual coefficients taking into account the conditions of manufacture and service of ship propellers (Chapter II). Information is provided on experimental studies of screw propeller strength under laboratory as well as under operational conditions (Chapter III). Problems of selection and actual strength calculations of propeller elements with detachable blades are discussed in detail. Data on propeller design with optimum strength characteristics and dimensions tested in actual service of such propellers are given (Chapter IV). Information on materials used for manufacturing ship propellers is included, particularly those characteristics which are directly related to propeller strength, as well as the requirements for such materials (Chapter V). 75 figures, 25 tables. Bibliography includes 45 titles.

---

*Numbers in the right margin indicate pagination in the original text.

Reviewers: M. A. Mavlyudov, G. G. Martirosov

Scientific Editor: F. M. Katsman

FROM THE AUTHORS /3

Problems of ship propeller strength attract in particular the attention of shipbuilders and specialists concerned with water transportation. Current trends toward increasing the capacity of power plants and ship tonnage, introducing new materials for ship propellers, and improving their manufacturing technology are only a few areas which require, in one way or another, the analysis of strength problems.

The present state of the art as well as current research in this field are not sufficiently reflected in the technical literature. The published data on strength studies and existing methods of strength calculations are of disconnected, individual character which makes their practical utilization difficult. This fact determined the purpose of this book. The authors have attempted to provide practical guidance for performing strength calculations of ship propellers and to acquaint engineering and technical personnel concerned with propeller strength problems with the main tasks which emerge during the solution of these problems. Considerable attention was devoted to the fatigue or cyclic strength of propeller blades operating in nonuniform velocity fields behind a moving ship.

Chapters I-III of the book (with the exception of Section 11) were written by B. A. Biskup and B. M. Terletskiy jointly; Chapter IV and Section 11 by M. N. Nikitin and Chapter V by S. I. Popov.

PREFACE /4

Screw propellers are the most commonly used ship propelling devices. They possess high propulsive properties and are relatively simple in design. These factors stimulated development of scientific research for the purpose of detailed study of the hydrodynamics of propellers and improvement of their operational reliability.

The screw propeller belongs to that category of a ship's mechanisms, the strength of which affects not only the operational qualities of the ship but also the safety of its navigation.

Usually the ship propeller operates under very severe conditions:

external forces acting on the propeller blades are, as a rule, non-stationary timewise;

the material of propeller blades is subjected to the action of an aggressive medium (sea water) and as a result, the blades may be subjected to electrochemical corrosion failure;

characteristic for modern ship propellers are operational regimes which, because of hydrodynamic loads, may be accompanied by cavitation.

All this determines the character of propeller damages encountered in practical operation of seagoing and river service ships.

Figure 1 illustrates the damage of carbon steel propeller blades caused by electrochemical corrosion. The appearance of this type of damage depends entirely on the material of the blade and its ability to resist the damaging action of electrochemical processes which take place in the water medium surrounding the propeller.

Figure 2 shows typical erosion-type damages caused by cavitation. The intensity of their development depends not only on the ability of the material to resist hydraulic impacts in cavitation, but also on the correct design of the propeller.

Study of the problems of cavitation erosion of screw propellers, which are also important in the task of increasing propeller reliability are discussed in detail in special literature (6), (28).

Corrosion and erosion-type damages of propellers in a number of cases contribute to bending off of blade edges which deteriorates /5
the hydrodynamic properties of the propeller and at a greater extent of such damages results in breakdown of the blades.

Figure 3 illustrates damage of the propeller blade, i.e., bending of its leading edge, as a result of insufficient local strength of the blade. This type of damage is characteristic for wide-blade propellers with a disk-area ratio of 0.9-1.0. At present there is no method for propeller design which provides for equal strength along its surface. The local strength of the blade is provided as a rule by selecting the edge thickness based on operational experience with propellers designed earlier.

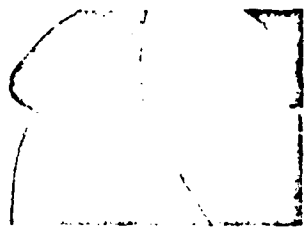

Fig. 1. Electrochemical corrosion of propeller blades

Fig. 2. Erosion of propeller blade

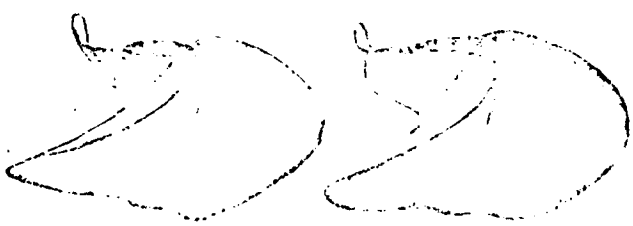

Fig. 3. Bending of propeller blade caused by the action of hydrodynamic forces

This compelled method is particularly unreliable if the parameters which characterize the performance of a new propeller being designed must be extrapolated, e.g., when transmitted power has to be increased or when the propeller being designed must operate under conditions of higher non-uniformity of incident flow.

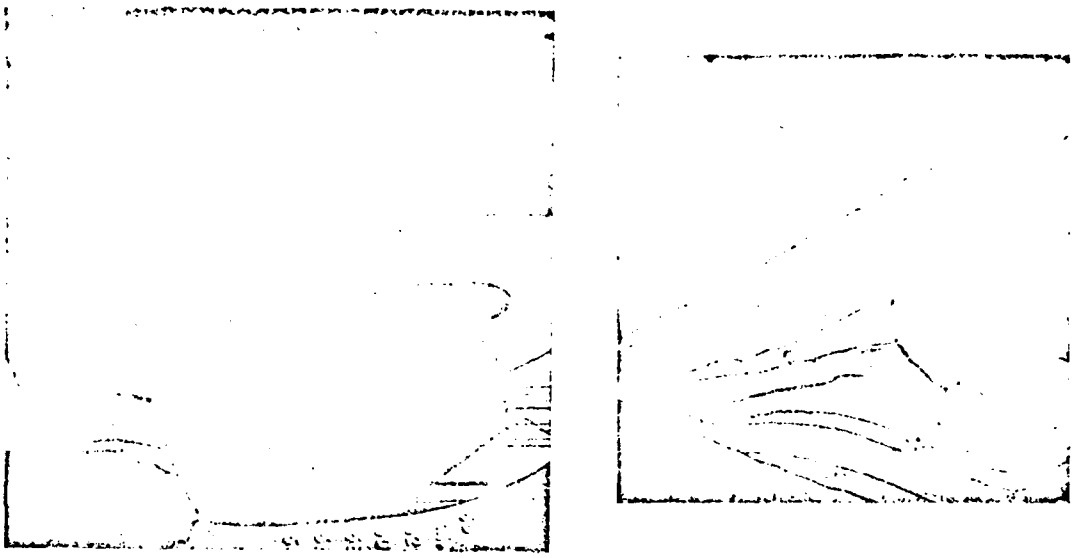

/6

Fig. 4. Fatigue failure of the propeller blade of a high tonnage tanker

Propeller damages caused by insufficient general strength of /7
blades are particularly dangerous and may create a breakdown situation. Fracture (breaking off) of blades occurs as a rule in the root area where the stresses in the cross-sectional areas are highest (Fig. 4). Since the consequences of such damages are very serious, the problems of providing for sufficient strength of blades deserve maximum attention of researchers and designers. At the same time, it is possible to name purely technical and operational economy factors which necessitate general strength calculations of propellers being designed (15). From the technical point of view, the calculation of maximal permissible stresses for a given material under specific conditions of operation makes it possible to assume the minimum thicknesses of propeller blades and in this way to improve the hydrodynamic efficiency of the propeller and at the same time to decrease the probability of cavitation. The resulting decrease of weight and moment of gyration decrease the load on the stern bearing and often makes it possible to avoid operation within the rpm zone that is dangerous in respect to torsional oscillations. Exploitation-economical considerations concern increasing the cruising speed of the ship because of increase of propeller efficiency and saving on the high cost of difficult to obtain materials (bronze, brass, stainless steel).

The load acting on a ship propeller is created by hydrodynamic and inertia (centrifugal) forces.

The hydrodynamic load acting on propeller blades usually is of cyclic character and, more accurately, it has a constant and variable components. This cyclic character of the load is explained by the fact that ship propellers operate in a non-uniform velocity field along the circumference of the propeller disk, which is caused by the hydrodynamic effect of the ship's hull and projecting stern parts. Under such conditions, the angle of incidence of propeller blades changes periodically during propeller rotation and as a result, the corresponding hydrodynamic forces also change.

The load values at certain moments of time may differ considerably from the average values within a time span of one revolution of the propeller. Calculations and experiments indicate that the amplitude of the variable component of hydrodynamic load may in some cases reach 50% of the average full load value. Naturally, the average and instantaneous values of stresses in the blade will be in the same ratio. As an example, Figure 5 /8 illustrates the dependence of normal stresses in the root section of the propeller blade of a high tonnage tanker on the angle of propeller rotation. The graph for this dependence was plotted using data obtained by measuring the relative linear deformations of the actual propeller under regular operational conditions.

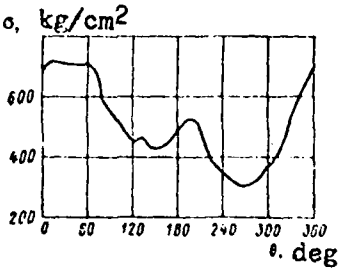

Fig. 5. Change of stresses at a certain point of the root cross section of the propeller blade depending on the angle of propeller shaft rotation

In a general case, the hydrodynamic load acting on the blade may be presented analytically by Fourier series in which the angular coordinate of the blade in the disk of propeller Θ is used as the argument, i.e., the thrust of the blade

$$P_1 = P_0 + \sum_{m=1}^{\infty} (P_{mc} \cos m\theta + P_{ms} \sin m\theta); \qquad (1)$$

Torsional moment

$$M_1 = M_0 + \sum_{m=1}^{\infty} (M_{mc} \cos m\theta + M_{ms} \sin m\theta), \qquad (2)$$

where P_o, M_o - average values of the force and torsional moment of the blade (constant components of the load) within one revolution of the propeller;

P_{mc}; P_{ms}; M_{mc}; M_{ms} - components of the load varying according to harmonic law stipulated by operation of the propeller in a non-uniform velocity field behind the ship's hull.

Historically evaluation of blade strength was carried out assuming that external forces acting on the blade were of statical character, i.e., in equations (1) and (2) only constant components P_o and M_o were taken into consideration. Practically all engineering calculation methods up to the present time (discussed in Chapter I) are based on this assumption. All these methods may be combined into one group of evaluating screw propeller strength by taking into account static loads acting on the blade. The fact that the maximum values of the actual (full) load on the blade may considerably exceed its average values is taken into consideration by introducing a corresponding safety coefficient. This coefficient is selected based on past experience with operation of ship propellers.

Apparently a more accurate method of evaluating propeller strength would be one in which the cyclic character of acting forces would be taken into account in determining external forces. This is particularly important for the high tonnage, mainly single-shaft transport shift in which the propeller operates under conditions of particular non-uniformity of the velocity field.

These circumstances caused the development of a method of calculation (Chapter II) of the cyclic strength, the need for which is demonstrated by the fatigue-type failure of propellers often observed in practice (see Fig. 4), which is caused by the cyclic action of hydrodynamic forces. /9

Requirements which have to be met by ship propellers to provide for their sufficient operational strength play an important role. These concern factors related to the manufacturing technology and repair of propellers, and to the mechanical properties of materials of which propellers are made*. Among the most important are

*Mechanical properties of materials which have to meet necessary requirements are determined with sufficient reliability and stability by testing specimens under conditions approaching those in actual operation of propellers.

perfection of casting technology, uniform cooling of castings, and measures for stress relieving after elimination of blade casting defects by means of welding.

All these factors affecting the strength of ship propellers are taken into account during calculations by means of a safety coefficient, the selection of which is substantiated in Section 9.

The complex character of the state of stress in propeller blades (particularly of wide blades) and the difficulties in analytical studies of stresses with consideration of propeller geometry, stipulated at present the development of experimental methods of studying stresses and deformations of propeller blades. Studies of the state of stress in blades are carried out either using models of propellers or actual propellers. Special features of such studies and some results obtained are discussed in Chapter III.

In addition to solid cast propellers, propellers with variable pitch (VPP), water-jet propellers, and propellers with detachable blades have found wide use. Although the principal approach to their strength evaluation is the same, individual design features of all these types of propellers require solution of some special questions which concern first of all methods of determining forces and calculating of stresses in parts used for fastening blades and the mechanism of propeller drive (propellers with detachable blades and VPP). At the same time, because propellers with detachable blades are used on ships for navigation through ice, the necessity arises to evaluate external forces in the case of impact of propeller blades against floating ice. For the VPP, these problems are relatively fully discussed in special literature (2), (29). For control evaluation of the rotor blades in the design of water-jet propellers, the methodology discussed in (23) is used. Published data on propellers with detachable blades are incomplete and are of disconnected character. This was the reason for including in this book information characterizing special features of design calculation methods for strength evaluation of propellers with detachable blades, including those for operation in ice (Chapter II, Section 11, and Chapter IV). /10

Chapter V contains information on materials used for screw propellers, the rational selection of which determines the reliability of these propellers in operation. Requirements which have to be met by such materials are very strict: resistance against corrosive action of aggressive medium, ability to resist hydraulic impacts in cavitation, and necessity of high fatigue limit in the presence of corrosion and cavitation erosion seats. Therefore, particular attention has always been devoted to the improvement of materials for propellers. New materials which combine high mechanical properties with other properties which meet specific requirements for such propeller materials have found wide use. The composition and mechanical properties of these materials are also included in this book.

CHAPTER I. EVALUATION OF SCREW PROPELLER STRENGTH BY CONSIDERING STATIC LOADS /11

Before starting calculation of propeller strength, the external forces acting on the propeller should be determined.

Evaluation of the general strength of a screw propeller as a rule is carried out for normal operating conditions without taking into account emergency situations (touching the ground when ship accidentally runs aground, impact against large objects which come under the revolving propeller, etc.).

In calculation of propeller strength by static loads, it is assumed that under normal conditions of operation the external load on the propeller is created by a constant component of hydrodynamic forces (see (1) and (2)) and by centrifugal forces of inertia of its blades.

Section 1. Hydrodynamic Forces Which Are Taken Into Account in Strength Calculations of a Ship Propeller Based on Static Loads

Hydrodynamic pressures are distributed in radial direction and in the direction along the elements of the propeller blade. Hydrodynamic forces (which are the product of pressure integration along the chord of the elements) create in the cross sections of the blade and on its surface a system of normal and tangential stresses.

Distribution of pressures along the suction and forcing sides of the element which is formed by the intersection of the blade with the cylinder coaxial with the propeller, as was determined by M. A. Mavlyudov in his experiments with models of propellers, is illustrated in Figure 6. In this figure, the dimensionless pressure coefficient is plotted on the ordinate axis:

$$\bar{p} = \frac{p - p_0}{\frac{\rho}{2}\left[V_p^2 + (2\pi nR)^2\right]}$$

where $p - p_o$ - excessive pressure at the point of the blade element being considered;

V_p - velocity of translation movement of the propeller;

R - radius of the propeller;

n - frequency of propeller rotation;

ρ - density of the medium, /12

while on the abscissa is a chord of the blade element.

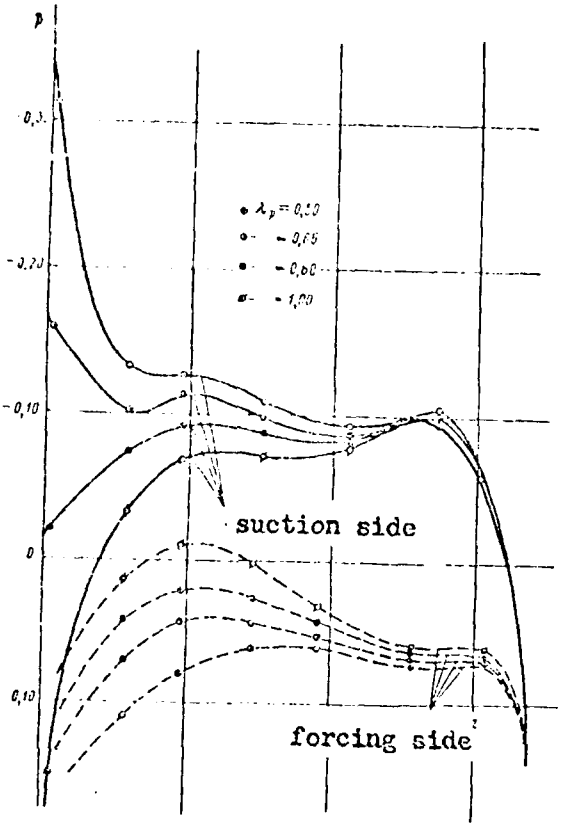

Fig. 6. Distribution of pressure coefficient $\bar{p}$ along the cylindrical cross section of the blade on the relative radius $\bar{r}_0 = 0.8$ with the various advance-diameter ratio λ_p

Evidently, at a given magnitude of hydrodynamic force emerging on the blade element, variation of the distribution of forces along the chord influences only the magnitude of the hydrodynamic moment in respect to a straight line, which is parallel to the blade axis. This moment is balanced by a system of tangential stresses. It was determined that the normal stresses which depend on the resultant force of total pressure, are higher in their magnitude as compared to tangential stresses. Therefore, in strength calculations only /13 the distribution of hydrodynamic pressures in radial direction is taken into account.

Projection of the resultant of pressures on the direction of ship motion represents the average value of the blade force within one revolution of the propeller, while the projection on the direction of propeller rotation represents the tangential force which creates a corresponding torsional moment.

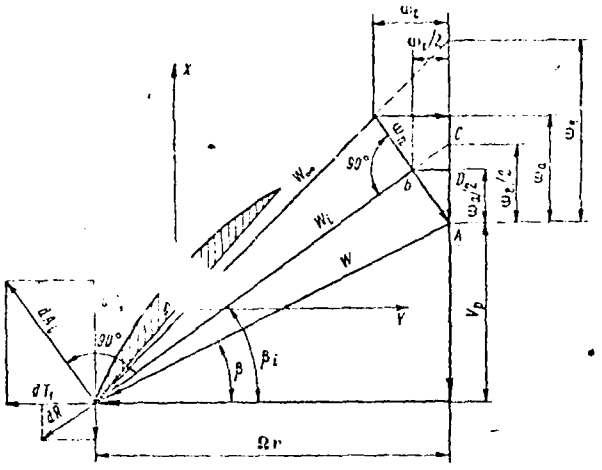

Fig. 7. Diagram of velocities and hydrodynamic forces acting on the elements of a propeller blade in a uniform incident flow

To determine hydrodynamic forces in radial direction we analyze the diagram of velocity and hydrodynamic forces generated at the element of a propeller blade with the relative radius

$$\bar{r} = \frac{r}{R}$$

(Fig. 7). It is assumed that the incident flow is stationary in respect to time. The OX axis coincides with the axis of propeller rotation, and the plane passing through the OY axis is perpendicular to the plane of the drawing and is the plane of rotation. In the relative coordinate system connected with the blade, the parameters of the external incident flow are determined by the velocity of element rotation Ωr ($\Omega = 2\pi n$ - angular speed of propeller rotation) and the speed of forward motion of the propeller V_p. Therefore, the direction of the resultant velocity of external flow W ahead of the propeller, forms with the rotation plane the angle of advance, which may be expressed through a relative advance of the propeller

$$\lambda_p = \frac{V_p}{nD} \quad \text{(D - propeller diameter)} \qquad /14$$

and the relative radius $\bar{r}$ of the position of blade elements along its length,

$$\operatorname{tg}\beta = \frac{\lambda_p}{\bar{r}}. \tag{3}$$

At a considerable distance behind the propeller, the velocity of flow W_∞ will be different as compared with its initial values W because of the appearance of induced velocity $\omega_n = (\omega_a + \omega_t)^{1/2}$, where ω_a and ω_t are axial and tangential components of induced velocity, respectively.

It was theoretically determined that in the plane of a propeller disk, the induced velocity equals 50% of its complete value. Hence, at the area of the blade element under discussion, the velocity of incident flow is determined by a vector W_i, which forms with the rotation plane angle β_i.

At the element of the blade, a lifting force dA emerges which is perpendicualr to the velocity vector W_i, and the force of profile resistance dR directed along velocity vector W_i.

The thrust and tangential force (see Fig. 7) created by the blade element may be found from the equations

$$\left.\begin{aligned} dP_1 &= dA\cos\beta_i(1-\varepsilon\operatorname{tg}\beta_i);\\ dT_1 &= dA\sin\beta_i(1+\varepsilon\operatorname{ctg}\beta_i). \end{aligned}\right\} \tag{4}$$

where $\varepsilon = \frac{dR}{dA}$ - coefficient of the reverse quality of the blade elements.

Assuming that the element is an ideal fluid when $\varepsilon = 0$, we obtain

$$\left.\begin{aligned} dP_u &= \frac{dP_1}{1-\varepsilon\operatorname{tg}\beta_i} = dA\cos\beta_i;\\ dT_u &= \frac{dT_1}{1+\varepsilon\operatorname{ctg}\beta_i} = dA\sin\beta_i \end{aligned}\right\} \tag{5}$$

The lifting force of the element we determine by the Zhukovski formula

$$dA = \rho\Gamma W_i dr, \tag{6}$$

where ρ - density of the liquid;

Γ - circulation of velocity around the blade element.

Let us assume that the elements of the screw propeller at a given condition of operation are selected in such a way that its performance is characterized by minimal inductive losses. Let us note that the assumption made is an initial condition for the design of ship propellers with maximal efficiency.

In a propeller with minimum inductive losses (screw propeller of optimum design), the inductive efficiency of any element of the blade is equal to the inductive efficiency of the entire propeller (3), i.e., /15

$$\eta_{i_r} = \eta_i = \frac{\operatorname{tg}\beta}{\operatorname{tg}\beta_i},$$

or, according to Fig. 7,

$$\eta_i = \frac{V_p}{V_p + \frac{\omega_B}{2}},$$

from this equation

$$\frac{\omega_B}{2} = V_p\left(\frac{1}{\eta_i} - 1\right). \tag{7}$$

But by examining triangles ABD and BCD it follows that

$$\frac{\omega_i}{2} = \frac{\omega_B}{2} \cdot \frac{\operatorname{tg}\beta_i}{1 + \operatorname{tg}^2\beta_i}. \tag{8}$$

Circulation around the element of the blade for an optimum propeller may be determined by equation

$$\Gamma = \frac{1}{Z} 2\pi r \omega_i k, \tag{9}$$

where k - correction of Goldstein-Prandtl, which takes into consideration the effect of the finite number of propeller blades on the amount of total circulation at a given radius;

Z - number of propeller blades.

Substituting equations (6), (7), (8), (9) into (5) and by conversion into dimensionless form of presenting the thrust

$$(dK_1)_1 = \frac{dP_1}{\rho n^2 D^4}$$

and tangential force

$$(dK_T)_1 = \frac{dT_1}{\rho n^2 D^4}$$

created by the blade element, we obtain:

$$\left.\begin{aligned}\left(\frac{dK_M}{dr}\right)_1 &= \frac{1}{Z}\pi^3 r^3 \rho k F(\eta_i, \operatorname{tg}\beta);\\ \left(\frac{dK_{T_i}}{dr}\right)_1 &= \frac{1}{Z}\pi^3 r^3 \rho k F(\eta_i, \operatorname{tg}\beta)\frac{\operatorname{tg}\beta}{\eta_i} = \frac{\operatorname{tg}\beta}{\eta_i}\left(\frac{dK_M}{dr}\right)_1,\end{aligned}\right\} \qquad (10)$$

where

$$F(\eta_i, \operatorname{tg}\beta) = \eta_i(1-\eta_i)\frac{(\eta_i + \operatorname{tg}^2\beta)\operatorname{tg}^2\beta}{(\eta_i^2 + \operatorname{tg}^2\beta)^2}.$$

The values of function F were calculated earlier and are given in Figure 8 depending on the tangent of the relative advance angle β of the element (see (3)) and induced efficiency η_i.

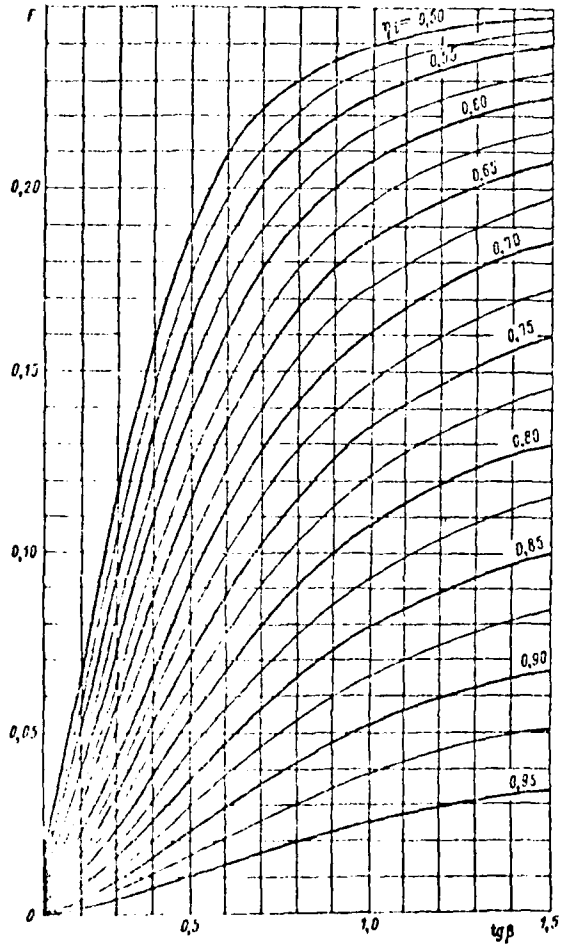

/16

Fig. 8. Graph for the dependence of function F on the angle of relative advance (advance-diameter ratio) β of induced efficiency of propeller η.

In order to approximately take into account profile resistance, it is expedient to present equations (10) in the form: /17

$$\left(\frac{dK_1}{d\bar{r}}\right)_1 = 0{,}98\,\frac{1}{Z}\,\pi\bar{r}^3 kF(\eta_i, \operatorname{tg}\beta), \tag{11}$$

$$\left(\frac{dK_2}{d\bar{r}}\right)_1 = \frac{\operatorname{tg}\beta}{\eta_p}\left(\frac{dK_1}{d\bar{r}}\right)_1, \tag{12}$$

where η_p - efficiency of propeller at a given operation regime.

From the second equation it is also possible to obtain:

$$\left(\frac{dK_2}{d\bar{r}}\right)_1 = \frac{\lambda_p}{2\pi\eta_p}\left(\frac{dK_1}{d\bar{r}}\right)_1, \tag{13}$$

where $\frac{dK_2}{d\bar{r}}$ - coefficient of torsional moment of the blade element.

At a given value of the advance-to-diameter ratio λ_p and coefficient of propeller load according to the thrust

$$\sigma_p = \frac{8K_1}{\pi\lambda_p^2}$$

equations (11) - (13) make it possible to calculate the distribution of hydrodynamic forces along the radius of the propeller in a uniform incident flow or, with some approximation, the distribution of the constant component of the hydrodynamic forces acting on the propeller in a non-uniform velocity field.

Table 1. Calculation of the Distribution of Hydrodynamic Forces Along the Radius of a Propeller

Calculation Formulae	$\bar{r}$						
	0.3	0.4	0.5	0.6	0.7	0.8	0.9
$\operatorname{tg}\beta = \frac{\lambda_p}{\pi r}$	0.497	0.373	0.298	0.249	0.213	0.186	0.166
$F = f(\eta_i, \operatorname{tg}\beta)$ (see Fig.8)	0.1105	0.0790	0.0570	0.0425	0.0325	0.0250	0.0215
$k = f\left(\bar{r}, Z, \frac{1}{\lambda_i}\right)$ (see Fig.10)	0.985	0.975	0.973	0.967	0.940	0.835	0.717
$\frac{1}{Z}\cdot\frac{dK_1}{d\bar{r}} = 0{,}98\frac{\pi\bar{r}^3 Fk}{Z}$	0.0227	0.0374	0.0526	0.0672	0.0794	0.0882	0.0853
$\frac{1}{Z}\cdot\frac{dK_2}{d\bar{r}} = 1{,}00\,\frac{\operatorname{tg}\beta}{\eta_i}\cdot\frac{1}{Z}\cdot\frac{dK_1}{d\bar{r}}$	0.0182	0.0225	0.0253	0.0270	0.0273	0.0265	0.0229

In such a case for finding induced efficiency, the Kramer's diagram is used, which is well known (Fig. 9), and the correction of Goldstein-Prandtl is determined by graphs in Fig. 10. /18

An example of the calculation of hydrodynamic forces distribution along a propeller radius is given in Table 1. The following initial data were given:

Advance-to-diameter ratio $\lambda_p \quad \frac{V_p}{nD} \ldots\ldots 0{,}468$

Coefficient of thrust $K_1 \quad \frac{P}{\rho n^2 D^4} \ldots\ldots 0{,}185$

Number of blades in propeller $z \ldots\ldots 4.$

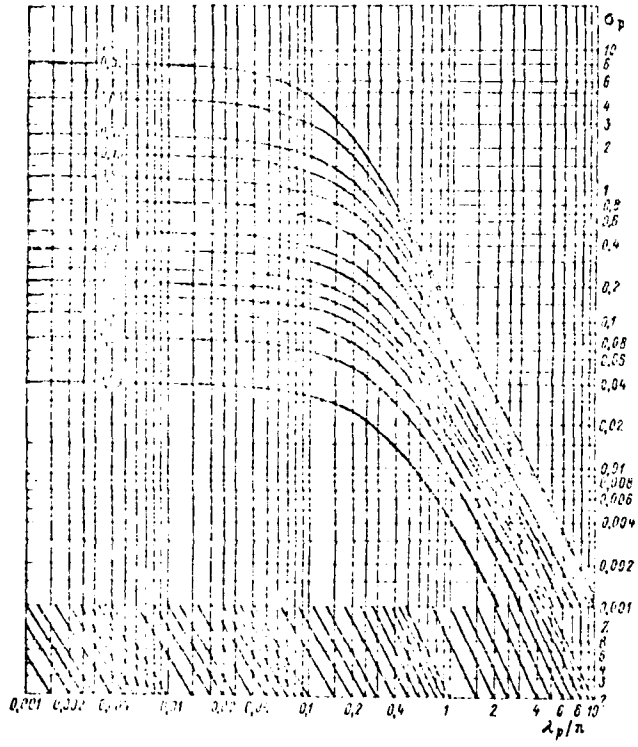

Fig. 9. Kramer's diagram for determining the induced efficiency of a ship propeller

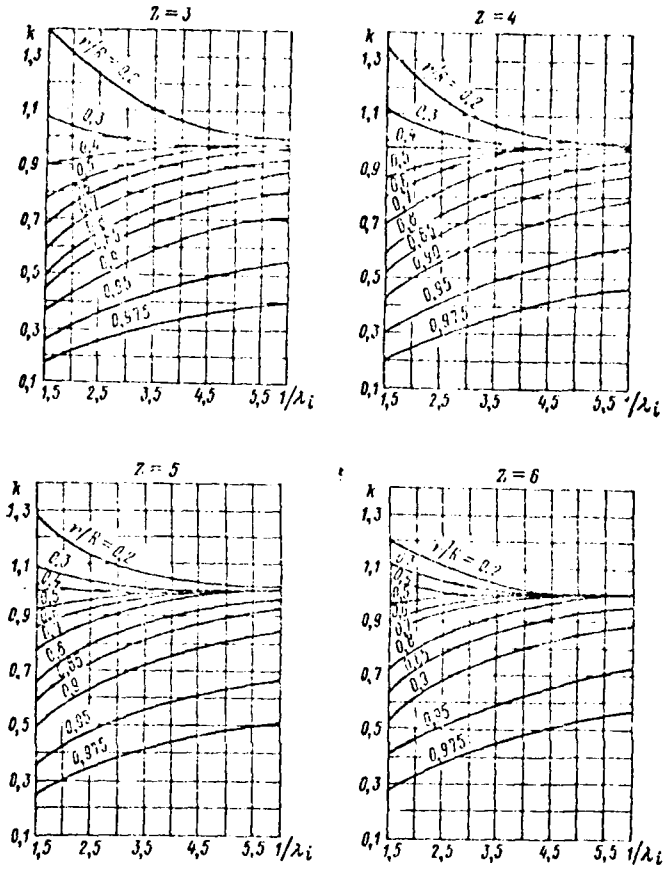

Fig. 10. Goldstein-Prandtl correction for propellers with numbers of blades Z = 3, 4, 5, 6 /19

and also the following auxiliary values were determined: /20

$$\sigma_{pl} = \frac{8K_1}{0{,}98\pi\lambda_p^2} = 2{,}2,$$

$$\eta_i = f\left(Z, \frac{\lambda_p}{\pi}, \sigma_{pl}\right) = 0{,}65 \text{ (see Fig.9)}$$

$$\frac{1}{\lambda_i} = \frac{\pi\eta_i}{\lambda_p} = 4{,}36.$$

Calculation results are shown in the graph in Figure 11.

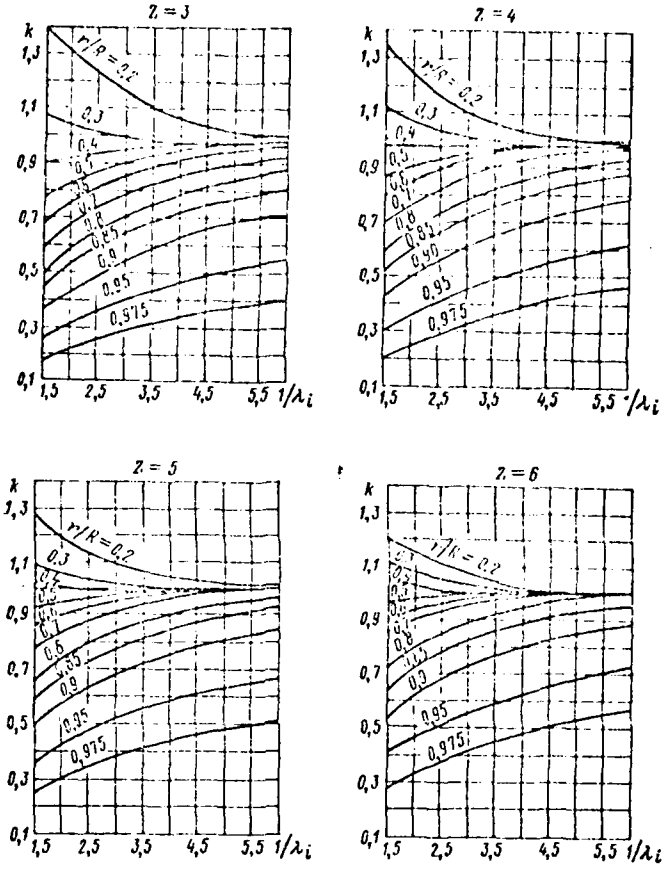

Fig. 10. Goldstein-Prandtl correction for propellers with numbers of blades Z = 3, 4, 5, 6 /19

and also the following auxiliary values were determined: /20

$$\sigma_{pl} = \frac{8K_1}{0{,}98\pi\lambda_p^2} = 2{,}2,$$

$$\eta_i = f\left(Z, \frac{\lambda_p}{\pi}, \sigma_{pl}\right) \quad 0{,}65 \text{ (see Fig.9)}$$

$$\frac{1}{\lambda_i} = \frac{\eta_i}{\lambda_p} = 4{,}36.$$

Calculation results are shown in the graph in Figure 11.

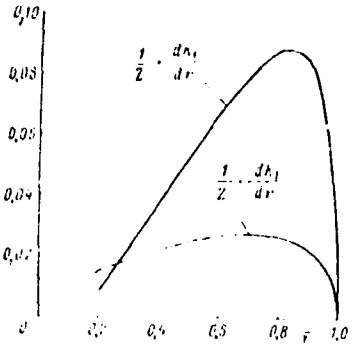

Fig. 11. Distribution of hydrodynamic forces along the radius of a propeller

Taking into consideration that the strength calculations of marine propellers do not require high accuracy in determining external loads, it is expedient to simplify the discussed method of determining hydrodynamic forces acting on the blade.

Calculations demonstrated that within the discussed operational regimes of propellers and variations of their geometrical elements, there were no significant differences observed in the character of distribution of hydrodynamic forces along the radius. This makes it possible, instead of performing calculations for each individual propeller, to establish some general equations which, without essential error, approximate the law governing changes of hydrodynamic load.

In particular, in calculating the general strength of propeller blades, the distribution of hydrodynamic force along the radius is approximated by an analytical dependence of the following type:

$$y = cr^m(1-\bar{r}^n)^p, \tag{14}$$

where c - constant coefficient;

m, n and p - parameters which are determined under condition that equation (14) in the best way reflects distribution of thrust along the propeller radius.

Systematic calculations indicate that for propellers with number of blades Z = 4 and 5, for sea-going transport and industrial ships the following values of parameters may be assumed:

$$m = 2,\ n = 1,\ p = \frac{1}{2}.$$

Substituting these values in equation (14), we obtain an analytical expression which characterizes the distribution of hydrodynamic force along the radius of a propeller. /21

$$\frac{1}{Z}\cdot\frac{dK_1}{d\bar{r}}=c\bar{r}^2(1-\bar{r})^{\frac{1}{2}}. \tag{15}$$

Equation (15) is used in deriving formulae for calculation of stresses in the cross sections of blades.

Section 2. Centrifugal Forces of Inertia

In addition to hydrodynamic forces, the propeller blade is subjected to the action of centrifugal forces of inertia.

On each element of the blade mass dm (Fig. 12) which is located at a distance r from the axis of propeller rotation, the centrifugal force acting in radial direction is:

$$dP=dm\Omega^2 r. \tag{16}$$

Let us analyze a cross section of the blade A-A which is perpendicular to the axis y and is located at a distance $r_i = y_c$ ($r_i < r$) from the axis of propeller rotation.

For the center of gravity of the considered cross section $C(x_c, z_c)$, by projecting it on the coordinate axes x, y, z, we obtain:

$$\left.\begin{aligned}
dP_x &= 0;\\
dP_y &= \Omega^2 y\,dm;\\
dP_z &= \Omega^2 z\,dm;\\
dM_x &= dP_z(y-y_c)-dP_y(z-z_c)=-\Omega^2(zy_c-yz_c)\,dm;\\
dM_y &= -dP_x(z-z_c)-dP_z(x-x_c)=-\Omega^2 z(x-x_c)\,dm;\\
dM_z &= dP_y(x-x_c)-dP_x(y-y_c)=-\Omega^2 y(x-x_c)\,dm.
\end{aligned}\right\} \tag{17}$$

Generally speaking, relationships (17) hold for the body of any form which is rotating about x axis. The special geometrical shape of propeller blades makes it possible, without considerable loss of calculation accuracy, to considerably simplify the calculation formulae by separating principal factors from minor factors.

A propeller blade is a cantilever wing of a finite span. The resultant force of all centrifugal forces of inertia acting on the blade is at a distance from the blade root, and the greatest part of these forces acts in the plane which is close to the plane of minimum rigidity. The maximum stresses in the blade cross sections are normal stresses appearing as the result of the action of tension forces and bending moments, which makes it possible to limit consideration of loads to those causing only normal stresses, as was the case with hydrodynamic forces. In equation (17) such a load is centrifugal force dP_y and bending moments dM_x and dM_z. /22

After integration within the limits $r_i \leqslant r \leqslant R$, we obtain:

$$\left.\begin{aligned} P_y &= \Omega^2 \int_{M_i} y\,dm; \\ M_x &= -\Omega^2 \int_{M_i} (zy_c - yz_c)\,dm; \\ M_z &= \Omega^2 \int_{M_i} y(x - x_c)\,dm. \end{aligned}\right\} \qquad (18)$$

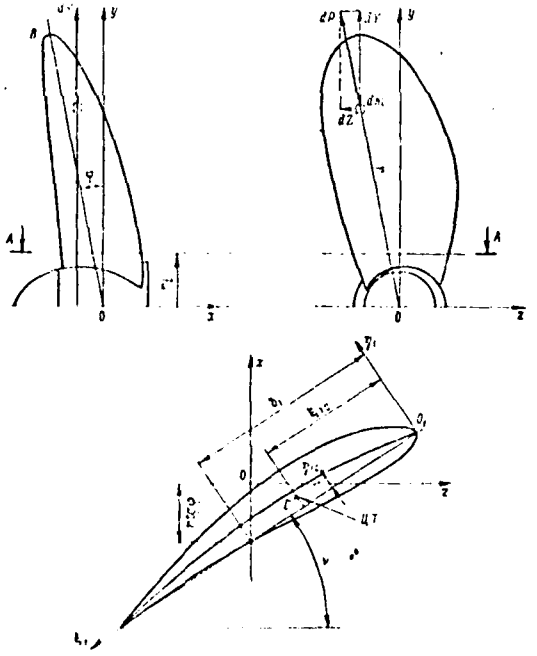

Fig. 12. Diagram for determining centrifugal forces in the blades of a screw propeller

It should be noted that the moments M_x and M_z for blades which do not have rake in respect to the stern ($\hat{\gamma} = 0$, see Fig.12) are very small. By analyzing equations (18), we can see that coordinates $y(y_c)$ are always positive, while coordinates $z(z_c)$ and $x(x_c)$ are positive only for the part of the blade between its leading edge and the Oy axis. Therefore, the moments M_x and M_z for the whole blade will be determined by the difference of similar values and will be therefore small. /23

When the blade has a rake in respect to the x axis, the coordinates $x(x_c)$ will not change their sign in integration of the expression for M_z which, as a result, leads to the relative increase of this moment and to the necessity of taking it into account during evaluation of the effect of centrifugal forces.

Hence, of the components of the load shown in equations (17) which is caused by the action of centrifugal forces of inertia, the most important are the force P_y for blades without a rake, and the force P_y and bending moment M_z for blades with a rake in the direction of the X axis.

To determine the centrifugal force and the bending moment caused by it, the approximate formulae are used in calculation of blade strength.

Assuming that the flat cross section of the blade A-A (see Fig.12) is rightful to the unfolded onto the plane cylindrical cross section, from the general equation (18) we obtain:

$$P_c = P_y = \rho a^3 n^2 \int_{r_i}^{R} Fr dr, \qquad (19)$$

where F - area of unfolded on the plane cylindrical cross section of the blade; diagram for determining area F is given in section 3 below;

r_i - radial coordinate of the cross section being considered.

Equation (19) is used in cases when during calculation it is necessary to find the distribution of centrifugal forces of inertia along the radius of the propeller. When calculation is performed for one cross section near the root of the blade ($r_i \approx 0.2$), a simplified formula may be recommended:

$$P_c = \frac{4\pi^2 n^2}{g} Gr_{c0}. \qquad (20)$$

where G - weight of the propeller blade;

r_{co} - radial coordinate of the center of gravity of the blade. It is assumed that $r_{co} \approx 0.47$ R.

The weight of the blade may be determined by the formula which ensues from the well-known empirical formula of V. V. Kopeyetskiy for the weight of the complete propeller (15):

$$G = \frac{\gamma D^3}{4 \cdot 10^4}\left(\frac{b}{D}\right)\left[6.2 + 2 \cdot 10^4\left(0.71 - \frac{d}{D}\right)\frac{e}{D}\right], \qquad (21)$$

where γ - specific gravity of the propeller material, kg/m^3;

d - diameter of the hub, m;

D - diameter of propeller, m;

b - width of the straightened blade contour at the relative radius $\bar{r} = 0.6$, m;

e - maximal thickness of the blade at the same radius, m.

More accurate methods of determining the weight of the blade and the coordinates of its center of gravity are discussed in Section 3 below. /24

The bending moment resulting from the action of centrifugal forces is found with the help of the approximate formula which is deduced from equation (18):

$$M_c = M_z = \frac{1}{2}\rho\omega^2 n^2 \operatorname{tg}\varphi \int_{r_i}^{R} Fr(r - r_i)\,dr. \qquad (22)$$

When calculation is carried out for the cross section in the area of the blade root, the moment M_c may be found by the following equation:

$$M_c \approx 0.7 P r_{co} \operatorname{tg}\varphi. \qquad (23)$$

Section 3. Geometrical Characteristics of the Cross-Sectional Elements of a Propeller Blade

In strength calculations of a ship propeller, the following geometrical characteristics of its cross section are used: area, coordinates of the center of gravity, and moments of inertia; in addition, for the part of the blade located behind the cross section being considered, the volume and coordinates of its center of gravity are used.

The basis for the profile of the straightened cylindrical cross section of the blade is the profile's chord (Fig. 13).

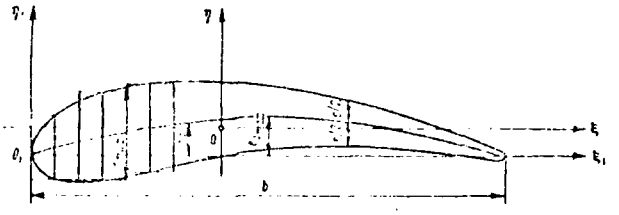

Fig. 13. Geometrical characteristics of a blade cross section

In relation to the chord, the median of the profile is plotted with the ordinates e_0. The curvature of this line is determined as a result of hydrodynamic calculation of the propeller. In most cases the maximum ordinate ($e_{0\ max}$) is located in the middle of the chord b. At both sides of the median the halves of the ordinate values of the standard aerodynamic or segmental profile $\frac{e}{2}$ are plotted. By superposing the origin of auxiliary coordinate system $0, \xi, \eta$, with the leading edge of the chord and by introducing dimensionless values: /25

$$\bar{e} = \frac{e}{e_{max}};$$

$$\bar{e}_0 = \frac{e_{0\,max}}{e_{max}};$$

$$\bar{\xi}_1 = \frac{\xi}{b},$$

where e - current value of the profile thickness;

e_{max} - maximum thickness;

b - length of the profile chord,

we obtain the following formulae for calculating the area and coordinates of the center of gravity of the cross section:

$$F = c_m b \int_0^1 \bar{c} d\bar{\xi}; \tag{24}$$

$$\bar{\xi}_{10} = \frac{c_m b^2}{F} \int_0^1 \bar{c}\bar{\xi} d\bar{\xi}; \tag{25}$$

$$\bar{\eta}_{10} = \frac{c_m^2 b}{F} \int_0^1 \bar{c}\bar{c}_0 d\bar{\xi}. \tag{26}$$

Calculation of the geometrical characteristics of the blade cross section using equations (24) - (26) is performed by the methods of approximate numerical integration, i.e., by methods of triangles, trapezoids, and parabolas (Simpson's). For this purpose, the cross section is divided into separate small areas by ordinates drawn at equal distance. It is expedient to calculate the moments of inertia of the cross section as a sum of moments of inertia of small areas. For example, the moment of inertia about axis $O_1 \xi_1$ is:

$$I_{\xi 1} = \sum_{j=1}^{k} I_{\xi j} + \sum_{j=1}^{k} \eta_{cj}^2 F_j,$$

where $I_{\xi j}$ - moment of inertia of the small area about its own central axis which is parallel to $O_1 \xi_1$ axis;

η_{cj} - ordinate of the center of gravity of this area;

F_j - area of this amall area;

k - number of small areas.

To simplify calculations, it is advisable to replace these small areas by rectangles as shown in Fig. 13.

In this case:

$$I_{\xi 1} \approx \frac{2}{n} c_m^3 b \sum_{j=1}^{\frac{n}{2}} \left| \frac{1}{12} \bar{c}_{2j-1}^3 + (\bar{c}\bar{c}_0^2)_{2j-1} \right|, \tag{27}$$

where n - number of sections into which the chord is divided for calculation of area and coordinates of the center of gravity by equations (24) - (26).

Equation (27) holds if n is an even number. It is recommended to have n = 20. /26

The moment of inertia of the cross section in respect to $O_1\eta_1$ axis is found in a similar way. The formula used for calculation is:

$$I_{\eta_1} = \frac{2c_m b^3}{n^3} \sum_{j=1}^{n/2} \left[\frac{1}{3} + (2j-1)^2 \right] \bar{c}_{2j-1}. \qquad (28)$$

If coordinates of the center of gravity and moments of inertia of cross sections in respect to $O_1\xi_1$ and $O_1\eta_1$ are known, the moments of inertia in respect to central axes $O\xi$ and $O\eta$, which are parallel to $O_1\xi_1$ and $O_1\eta_1$, can be determined:

$$\left.\begin{aligned} I_\xi &= I_{\xi 1} - \eta_{1m}^2 F, \\ I_\eta &= I_{\eta 1} - \xi_{1m}^2 F. \end{aligned}\right\} \qquad (29)$$

The principal central moments of inertia in a general case are determined by formulae:

$$\begin{aligned} I_{\xi_0} &= I_\xi \cos^2\alpha + I_\eta \sin^2\alpha - I_{\xi\eta} \sin 2\alpha, \\ I_{\eta_0} &= I_\xi \sin^2\alpha + I_\eta \cos^2\alpha + I_{\xi\eta} \sin 2\alpha, \end{aligned}$$

where $I_{\xi\eta}$ - centrifugal moment of inertia;

α - angle between main axes and axes ξ and η which is found by equation:

$$\operatorname{tg} 2\alpha = \frac{2I_{\xi\eta}}{I_\eta - I_\xi}.$$

Because the cross sections of a propeller blade have considerable elongation and relatively low curvature, which as a rule does not exceed 2 - 3%, the direction of the main central axis $O\xi_0$ may be considered to be parallel to the chord of the cross section. Then angle $\alpha = 0$, and the moments I_ξ and I_η may be assumed as the principal central moments of inertia. At the same time, centrifugal moment $I_{\xi\eta} = 0$.

The procedure of calculating the area and coordinates of the center of gravity of the unfolded onto the plane cylindrical cross section of the blade by the method of trapezoids is illustrated in Table 2.

In a number of cases the geometrical characteristics of blade cross sections are found by approximate but considerably simpler formulae. For example, cross sectional area may be calculated by formula:

$$F = a_1 c_m b. \qquad (30)$$

Coefficient a_f equals 0.70 - 0.72 for the cross section of the aviation profile and 0.71 - 0.73 for the segmental profile.

Table 2. Calculation of the Geometrical Characteristics of Unfolded Onto the Plane Cylindrical Cross Section of a Blade /27

(b = . . . (m), e_m = . . . (m), n - even number)

i	$\frac{e_i}{e_m}$	$\frac{e_i}{e_m}$	$\bar{e}_i^2$ (гр. 1 × гр. 2)	$\bar{e}_i^3$ (гр. 2 × гр. 3)	$\frac{\bar{e}_i^3}{\bar{e}_0^3}$ (гр. 2)^3, $i = 1, 2, \ldots$	$\frac{1}{12}\frac{\bar{e}_i^3}{\bar{e}_0^3}$ (гр. 6)	$\left(\frac{\bar{e}_i^2}{\bar{e}_0^2}\right)^2$ (гр. 3 × гр. 5)	гр. 7 + гр. 8	$\frac{1}{3}+(i)^3$	гр. 2 × гр. 10
1	2	3	4	5	6	7	8	9	10	11
0					—	—	—	—	—	—
1										
2					—	—	—	—	—	—
3										
. . .										
$n-1$										
n					—	—	—	—	—	—
Σ'		—			—	—	—	Σ_4	—	Σ_5
$\frac{y_0+y_n}{2}$		—			—	—	—		—	
$\Sigma = \Sigma' - \frac{y_0+y_n}{2}$	Σ_1	—	Σ_2	Σ_3	—	—	—		—	

Note: $F = \frac{e_m b}{n}\Sigma_1$; $\bar{\xi}_{s0} = \frac{e_m b^2}{n^2 F}\Sigma_2$; $\bar{\eta}_{h0} = \frac{e_m^2 b}{nF}\Sigma_3$; $I_{\xi 1} = \frac{2}{n} e_m^3 b\Sigma_4$; $I_{\eta 1} = \frac{2}{n^3} e_m b^3 \Sigma_5$.

Table 3 provides values for the coefficient of blade fullness a_f and relative coordinates of the center of gravity of the propeller blade cross sections for propellers of the W series (Wageningen experimental basin, Netherlands). /28

Table 3. Coefficients of Fullness and Relative Coordinates of the Center of Gravity of Blade Cross Sections of W-Series Propellers

r	$\alpha_r = \frac{F}{c_m b}$	$\xi_c = \frac{b_c}{b}$	$\bar{\eta}_c = \frac{\eta_{c0}^*}{c_m}$
0.2	0,692	0,447	0,458
0.3	0,713	0,453	0,440
0.4	0,721	0,455	0,426
0.5	0,722	0,459	0,414
0.6	0,715	0,466	0,407
0.7	0,710	0,481	0,401
0.8	0,714	0,495	0,403
0.9	0,730	0,503	0,405

* Distance between tangential and forcing surface of the blade

Table 4. Calculation of Coordinates of the Center of Gravity of Propeller Blade Cross Sections ($\tan \varphi = \ldots$)

$\frac{r}{R}$	$\frac{r}{D}$	$\frac{H}{D}\left/\frac{r}{R}\right.$	$\frac{t_{0.9}}{D}$	$\frac{t_r}{D}$	$\frac{b_r}{D}$	$\frac{t_r}{b_r}$	$\frac{t_{0.9}}{b_{0.9}}$	$\frac{t_r}{t_{0.9}}$	$\frac{t_r}{t_{0.9}} \cdot \frac{b_{0.9}}{b_r}$	fp. 7 : fp. 11	fp. 12 : fp. 4	fp. 6 : fp. 9	fp. 14 : fp. 15	$\bar{x}_c' = \frac{x_c'}{b}$ fp. 10 − fp. 13 − fp. 15	fp. 12 : fp. 5	fp. 14 : fp. 4	$\bar{x}_c = \bar{x}_c' - \bar{x}_{c0}$ fp. 17 − fp. 18
1	2	3	4	5	6	7	8	9	10	11	12	13	14	15	16	17	18	19
0,2																		
0,3																		
0,4																		
0,5																		
0,6																		
0,7																		
0,8																		
0,9																		

Table 5. Calculation of Volume of the Blade and Coordinates of the Center of Gravity (Propeller Radius R = . . . (m)) /29

$\bar{r}$	F (from Table 2)	$\bar{x}_c$ (from Table 4)	$\bar{z}_c$ (from Table 4)	$\frac{F}{R^2}$	$\frac{F}{R^2}\times\bar{x}_c$ (гр. 3 × гр. 5)	$\frac{F}{R^2}\times\bar{r}$ (гр. 1 × гр. 5)	$\frac{F}{R^2}\times\bar{z}_c$ (гр. 4 × гр. 5)
1	2	3	4	5	6	7	8
1,0							
0,9							
0,8							
. . .							
$\bar{r}_i$							
Σ'		—					
$\frac{y_0+y_n}{2}$		—					
$\Sigma=\Sigma'-\frac{y_0+y_n}{2}$		—		Σ_V	Σ_x	Σ_r	Σ_z

Note: $V=\frac{1-\bar{r}_i}{n}R^3\Sigma_V;\quad x_g=\frac{1-\bar{r}_i}{n}R^4\Sigma_x;\quad y_g=\frac{1-\bar{r}_i}{n}R^4\Sigma_r;\quad z_g=\frac{1-\bar{r}_i}{n}R^4\Sigma_z.$

The volume of the blade or of its separate part which is separated by the cross section being considered is calculated by the formula: /30

$$V=\int_{r_i}^{R}Fdr=R^3\int_{\bar{r}_i}^{1}a_F\bar{c}_m\bar{b}d\bar{r}, \qquad (31)$$

where $\bar{c}_m=\frac{e_m}{R}$ - relative maximum thickness of the cross section;

$\bar{b}=\frac{b}{R}$ - relative length of the chord of the cross section.

The coordinates of the center of gravity of the volume V are determined by coordinates of centers of gravity of cross sections which should be considered in the system O_{xyz} connected with the propeller (see Fig.12).

For the cross section at a distance $\bar{r}$:

$$\left.\begin{aligned}x_c&=r\operatorname{tg}\varphi-(b_1-b\bar{\xi}_{10})\sin\nu-b\bar{\eta}_{10}\cos\nu;\\ z_c&=(b_1-b\bar{\xi}_{10})\cos\nu-b\bar{\eta}_{10}\sin\nu,\end{aligned}\right\} \qquad (32)$$

where ν - pitch angle of the cross section being considered;

b_1 - distance from the leading edge of the profile cross section from the generatrix of the blade.

The sequence of the calculation of coordinates of the center of gravity of cross sections in the O_{xyz} system is determined by Table 4.

The coordinates of the center of gravity of volume V are found by formulae:

$$\left.\begin{aligned} x_0 &= \frac{1}{V}\int_{r_i}^{R} Fx\,dr \qquad \frac{R^3}{V}\int_{\bar{r}_i}^{1} a_r\bar{c}_{ri}\bar{b}\bar{x}_c\,d\bar{r}; \\ y_0 &= \frac{1}{V}\int_{r_i}^{R} Fy\,dr \qquad \frac{R^3}{V}\int_{\bar{r}_i}^{1} a_r\bar{c}_m\bar{b}i\,d\bar{r}; \\ z_0 &= \frac{1}{V}\int_{r_i}^{R} Fz\,dr \qquad \frac{R^3}{V}\int_{\bar{r}_i}^{1} a_r\bar{c}_m\bar{b}\bar{z}_c\,d\bar{r}. \end{aligned}\right| \qquad (33)$$

It is convenient to calculate the blade volume or the volume of the part of the blade located on the radius $r > r_i$ and the coordinates of the center of gravity by the method of trapezoids in the form of Table 5.

Section 4. Calculation of Stresses in Cross Sections of a Propeller Blade

A propeller blade of usual design may be presented as a helicoidal shell of variable thickness rigidly fixed along the inner part of its contour and free along the rest of contour. Calculation of the state of stress of such a shell is a very complex problem, even if initial /31
assumptions for its solution are based on the usual technical shell theory using the hypothesis of straight normals and the condition that there are no normal stresses acting on small areas which are parallel to the median plane of the shell. Such a method of establishing the state of stress in the blade which is of interest first of all because of theoretical considerations, leads to the necessity of solving a complex system of partial differential equations with variable coefficients. Even approximate numerical solutions require the use of high-speed computers.

However, in practical design of screw propellers less accurate methods are used which are not so strict but are considerably less time consuming and are based on several additional assumptions.

The most widely used of these methods are those based on the theory of prismatic rods. Although these methods do not claim to be of high accuracy, they provide sufficiently satisfactory data to inform the designer in his evaluation of the state of stress in the propeller.

These methods are based on the following assumptions:

the blade is considered to be a cantilever rod with variable area of cross section which is rigidly fixed at one end and is subjected to oblique bending under the action of external forces not located in one of the main planes of the blade;

calculation is performed for cylindrical cross sections*

---

*The only exclusion is a method of "Rezing" which was discussed in Section 5. According to this method, stresses are determined not in cylindrical but in flat cross sections.

---

unfolded onto the planes, which are perpendicular to the generatrix of the propeller blade;

one of the main axes of inertia of the cylindrical cross section of the blade selected at random is considered to be parallel to its chord limited to a relatively thin cross section; at the same time, the other main central axis is perpendicular to the chord of the cross section.

Taking into account all these assumptions, the maximum stresses emerging in the blade under the action of external forces may be determined.

The bending moment resulting from the action of the axial (in the direction of the propeller motion) component of hydrodynamic load in any random cross section of the blade at a distance r_p from the axis of propeller rotation is:

$$M_p = \int_{r_p}^{R} \frac{dP_1}{dr} (r - r_p)\, dr, \qquad (34)$$

where dP_1 - thrust of the blade element which may be presented as /32

$$dP_1 = \frac{1}{Z} dK_1 \rho n^2 D^4. \qquad (35)$$

By substituting variable $\bar{r} = \frac{r}{R}$ and substituting formula (35) into (34), we obtain:

$$M_p = \frac{\rho n^2 D^5}{2Z} \int_{\bar{r}_p}^{1} \frac{dK_1}{d\bar{r}} (\bar{r} - \bar{r}_p) d\bar{r}. \tag{36}$$

It is expedient to represent bending moment M_p as a function of the propeller thrust. If K_1 is a coefficient of the propeller thrust at a regime being considered, then, using the evident relation:

$$K_1 = \int_{\bar{r}_0}^{1} \frac{dK_1}{d\bar{r}} d\bar{r},$$

where $\bar{r}_0$ - a relative radius of the propeller's hub, we find:

$$M_p = \frac{K_1 \rho n^2 D^5}{2Z} \cdot \frac{\int_{\bar{r}_p}^{1} \bar{r} \frac{dK_1}{d\bar{r}} d\bar{r} - \bar{r}_p \int_{\bar{r}_p}^{1} \frac{dK_1}{d\bar{r}} d\bar{r}}{\int_{\bar{r}_0}^{1} \frac{dK_1}{d\bar{r}} d\bar{r}}. \tag{37}$$

After substituting into this formula relation (15) and calculating integrals, which are taken in quadratures, we obtain:

$$M_p = \frac{K_1 \rho n^2 D^5}{2Z} G_p(\bar{r}_0, \bar{r}_p). \tag{38}$$

The graph of function $G_p(\bar{r}_0 \bar{r}_p)$ is presented in Figure 14.

Formula (38) makes it possible to calculate the bending moment under the action of axial hydrodynamic forces in any cross section of the blade ($r_0 \leq r_p \leq 1$) for propellers with a relative radius of the hub $0.2 \leq r_0 \leq 0.4$.

Since the maximum stresses appear in the root areas of the blade, usually cross sections of these areas are considered for strength calculations of propeller. As a rule, the relative radius of the hub of solid propellers is $\bar{r}_0 = 0.17 - 0.18$; taking into account that the transition from the blade into the hub has a fillet radius, it is possible to assume, without introducing a significant error, that the cross section which is at the radius of 0.2 should be considered for calculation (dangerous cross section). In addition, taking into consideration that the root area of the blade little influences the thrust, let us assume that $\bar{r}_p = \bar{r}_0 = 0.2$. In such case, formula (37) will be transformed into the following: /33

$$M_p = -\frac{K_1 \rho n^2 D^5}{2Z}\left[\frac{\int_{0.2}^{1} \bar{r}\frac{dK_1}{dr}\,d\bar{r}}{\int_{0.2}^{1}\frac{dK_1}{dr}\,d\bar{r}} - 0{,}2\right]. \tag{39}$$

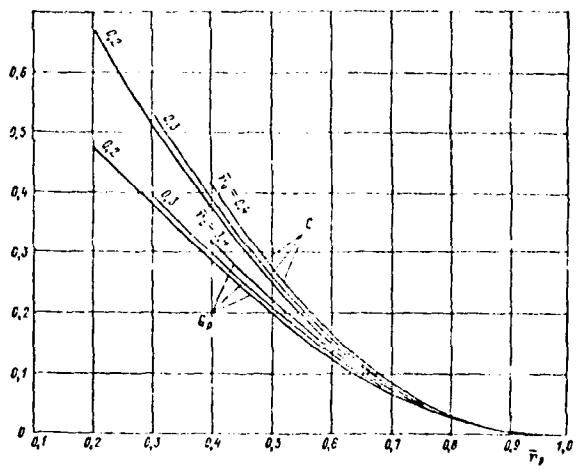

Fig. 14. Graph for functions G_p and G_T

By using formula (15) we obtain a formula for calculating the bending moment created by the action of axial hydrodynamic forces in the dangerous cross section of the blade.

$$M_p = -\frac{1}{Z}\,0{,}238 K_1 \rho n^2 D^5 \tag{40}$$

or

$$M_p = 0{,}475 P_1 R, \tag{41}$$

where P_1 - thrust of each blade of the propeller;

R - radius of the propeller.

The bending moment created under the action of tangential hydrodynamic forces may be calculated in a similar way.

It is evident that /34

$$M_T = \int_{r_p}^{R} \frac{dT_1}{dr}(r - r_p)\,dr, \tag{42}$$

where $dT_1 = \frac{1}{Z} dK_1 \rho n^2 D^4$ - tangential force of the blade element.

Then

$$M_1 = \frac{\rho n^2 D^5}{2Z} \int_{\bar{r}_p}^{1} \frac{dK_T}{d\bar{r}} (\bar{r} - \bar{r}_p) d\bar{r}. \qquad (43)$$

It is expedient to present bending moment M_p resulting from the action of tangential hydrodynamic forces as a function of propeller torque.

If K_2 is the coefficient of torque at the regime under consideration, then using the evident relationship

$$K_2 = \int_{\bar{r}_0}^{1} \frac{dK_2}{d\bar{r}} d\bar{r},$$

and also the expression well known from the hydrodynamics of ship propellers

$$K_2 = \frac{K_1 \lambda_p}{2\pi},$$

and formula (12) we obtain:

$$M_1 = \frac{K_2 \rho n^2 D^5}{Z} \cdot \frac{\int_{\bar{r}_0}^{1} \frac{dK_1}{d\bar{r}} d\bar{r} - \bar{r}_p \int_{\bar{r}_p}^{1} \frac{1}{\bar{r}} \cdot \frac{dK_1}{d\bar{r}} d\bar{r}}{\int_{\bar{r}_0}^{1} \frac{dK_1}{d\bar{r}} d\bar{r}}. \qquad (44)$$

After substituting formula (15) into this and after calculation of integrals

$$M_1 = \frac{K_2 \rho n^2 D^5}{Z} G_1(\bar{r}_0, \bar{r}_p). \qquad (45)$$

The graph for function $G_T(\bar{r}_0, \bar{r}_p)$ is shown in Figure 14.

Formula (45) serves for finding the bending moment created by the action of tangential hydrodynamic forces at any cross section of the blade.

If a cross section located directly at the blade root is being considered in calculations ($r_p = r_o = 0.2$), then formula (44) may be reduced to the form: /35

$$M_T = \frac{K_2 \rho n^2 D^5}{Z} \left| 1 - \frac{0.2 \int_{0.2}^{1} \frac{1}{\bar{r}} \cdot \frac{dK_1}{d\bar{r}} d\bar{r}}{\int_{0.2}^{1} \frac{dK_1}{d\bar{r}} d\bar{r}} \right| . \tag{46}$$

Taking into consideration dependence (15), we obtain:

$$M_T = \frac{1}{Z} 0{,}67 K_2 \rho n^2 D^5 \tag{47}$$

or

$$M_T = \frac{1}{Z} 0{,}67 M, \tag{48}$$

where M - torsional moment of the propeller.

Using formulae (47) and (48), the bending moment created by the action of tangential hydrodynamic forces is calculated in the critical cross section of the blade.

Components of the hydrodynamic bending moment acting in the ACBD cross section of the blade are shown in Figure 15.

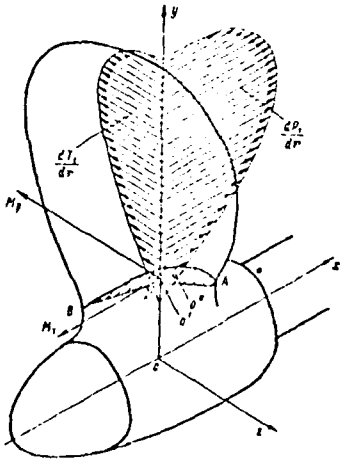

Fig. 15. Components of the hydrodynamic bending moment acting in the ACBD cross section of a blade

In a general case, the point O' to which the hydrodynamic moment is applied does not coincide with the center of gravity of the cross section (point O"). Strictly speaking, the system of stresses emerging in the cross section being considered under the action of hydrodynamic forces should balance not only the bending moment, but also the torsional moment in respect to the center of gravity and shearing force, which leads to the appearance of tangential stresses in the cross section of the blade. As was demonstrated by calculations, these stresses are considerably lower than normal stresses emerging under the action of the bending moment. Therefore, the effect of the torsional moment and shearing force may be disregarded, and it can be assumed that the hydrodynamic bending moment is applied to the center of gravity of the cross section.

In accordance with the above assumptions, let us unfold the cylindrical cross section of the blade on a plane passing through the point O' pependicularly to the blade axis Oy, and in agreement with the discussion in Section 3 we will assume that one of the main central axes of inertia $\xi - \xi$, (axis of minimum rigidity) is parallel to the chord of the cross section, while the other $\eta - \eta$ (axis of maximum rigidity) is perpendicular to the chord (Fig.16). /36

By projecting moments M_p and M_T on the axes $\xi - \xi$, and $\eta - \eta$, we obtain:

$$\left.\begin{aligned} M_\xi &= M_p \cos\nu + M_T \sin\nu, \\ M_\eta &= M_p \sin\nu - M_T \cos\nu. \end{aligned}\right\} \qquad (49)$$

If blades are inclined toward the stern, it is necessary to take into consideration an additional bending moment under the action of centrifugal forces (see (22) and (23)).

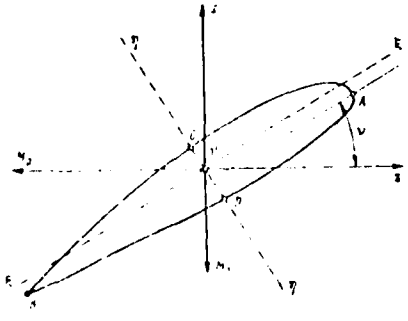

Fig. 16. Main central axes of a blade cross section

Therefore, the total bending moment in respect to the $\xi - \xi$ axis taking into account hydrodynamic and centrifugal forces

$$M_\xi = (M_p + M_c)\cos\nu + M_f \sin\nu, \tag{50}$$

and in respect to the $\eta - \eta$ axis

$$M_\eta = (M_p + M_c)\sin\nu - M_f \cos\nu. \tag{51}$$

In addition to bending moments, the external load on the blade includes tension forces emerging under the action of centrifugal force. The centrifugal force is calculated by formulae (19) and (20).

Knowing the area, moment of inertia, or section modulus of the blade's cross section and using formulae (52) and (53):

$$\sigma_\xi(\eta_{max}) = \frac{M_\xi \eta_{max}}{I_\xi} = \frac{M_\xi}{W_\xi(\eta_{max})} \tag{52}$$

$$\sigma_\eta(\xi_{max}) = \frac{M_\eta \xi_{max}}{I_\eta} = \frac{M_\eta}{W_\eta(\xi_{max})}, \tag{53}$$

where I_ξ, I_η - moments of inertia of the blade cross section in respect to main central axes $\xi - \xi$ and $\eta - \eta$;

ξ_{max}, η_{max} - distances from the neutral axis to the remotest points of the section;

$W_\xi(\eta_{max})$, $W_\eta(\xi_{max})$ - section moduli of the blade cross section for points with coordinates η_{max} ξ_{max}, respectively,

it is possible to determine stresses in points most remote from the neutral axis, which are caused by bending and also tensile stresses caused by the action of centrifugal force: /37

$$\sigma_c = \frac{P_c}{F}. \tag{54}$$

The points most remote from the neutral axis of the cross section under consideration are:

point A, at which tensile stresses caused by moment M_ξ are combined with similar stresses caused by moment M_η and by centrifugal force:

$$\sigma(A) = \sigma_z(\eta_A) + \sigma_u(\xi_A) + \sigma_c; \tag{55}$$

point B, at which compression stresses caused by moment M_η are subtracted from tensile stresses caused by moment M_ξ and by centrifugal force

$$\sigma(B) = \sigma_z(\eta_B) + \sigma_c - \sigma_u(\xi_B); \tag{56}$$

point C, which is subjected mainly to the action of compression stresses caused by moment M_ξ and tensile stresses emerging as a result of the action of centrifugal force:

$$\sigma(C) = -\sigma_z(\eta_C) + \sigma_c; \tag{57}$$

point D at which act tensile stresses caused by moment M_ξ and by centrifugal force:

$$\sigma(D) = \sigma_z(\eta_D) + \sigma_c. \tag{58}$$

Moments of inertia and section moduli in equations (52) and (53) are determined by methods discussed in Section 3. More approximate methods for finding these values may also be recommended. For example, for section moduli in respect to ξ axis:

$$W_\xi(\eta_{max}) = \alpha_\eta b e_m^2; \tag{59}$$

in respect to η axis:

$$W_\eta(\xi_{max}) = \alpha_\xi e_m b^2. \tag{60}$$

The values of α_η and α_ξ coefficients for aviation and segmental profiles with a flat forcing side are given in Table 6 (3).

Calculations indicate that maximum stresses in the blade cross section are the compressive normal stresses at point C. The maximum tensile stresses as a rule emerge in point D. Usually strength calculations of the propeller blade are limited therefore to determining stresses at these points, and therefore the data on section moduli in respect to the ξ axis are needed first of all.

Table 6. Values of α_η, α_ξ for Various Points of Aviation and Segmental Profiles With a Flat Forcing Side

/38

Coefficients	Profiles					
	For points A & B		For point C		For point D	
	segmental	aviation	segmental	aviation	segmental	aviation
α_η	0,11	0,10	0,065	0,085	0,11	0,10
α_ξ	0,07	0,01	"	"	"	"

The sequence of calculation of maximum stresses in cross sections of the blade based on static loads is given in Table 7. As the initial data the following values are used:

Propeller diameter, m . . . . . D

Number of blades . . . . . Z

Relative radius of the hub . . . . . $\bar{r}_0$

rpm . . . . . n

coefficient of thrust . . . . . K_1

coefficient of the moment . . . . . K_2

In addition, the following auxiliary values have to be calculated:

$$\frac{K_{1\rho}n^2D^5}{27} \; ; \quad \frac{K_{2\rho}n^2D^5}{Z} \; .$$

This method may be used for calculation of stresses in various cross sections along the radius, including the most critical cross section at the root of the blade. At the same time, it is possible to select the blade thickness in such a way that distribution of design stresses in the cross section would be relatively uniform.

The maximum stresses obtained as a result of calculations should not exceed the maximum permissible stresses. Selection of permissible stresses for materials from which propellers are manufactured is discussed in detail in Chapter II. The discussion here is limited to the recommended values of permissible stresses tested by experience in operation of various ships and selected in evaluating propeller strength, considering static loads acting on propellers. In Table 8, taken from (15), values of permissible stresses are shown, depending on the material and the number of propellers on a ship, which influences the degree of non-uniformity of the velocity field on the propeller disk and indirectly influences cyclic loads on the blades.

It can be also assumed that the strength of a propeller, based on static loads, is sufficient if the safety factor with regard to tensile strength $\frac{\sigma_b}{\sigma_{max}}$ 8 - 10,

and with regard to the yield point $\frac{\sigma_y}{\sigma_{max}}$ 3,5 - 4,0.

Table 7. Calculation of Maximal Stresses in Cross Sections of a Propeller Based on Static Loads

/39

Designations and Calculating Formulae	Source	Executing Unit	r_p							
			r_0	r_1	r_2	r_3	r_4	r_5	r_6	r_7
b	From the drawing of propeller	m								
c_m	Same	m								
H/D	»	—								
$\nu = \operatorname{arctg} \frac{H/D}{\pi r}$	Same	rad								
$\cos\nu$	»	»								
$\sin\nu$	»	»								
$G_P(r_0, r_1)$	Fig. 14	—								
$G_T(r_0, r_p)$	» »	»								
$M_P = \frac{K_1 \rho n^2 D^5}{2Z} \cdot G_P$	Formula (38)	kg·m								
$M_T = \frac{K_2 \rho n^2 D^5}{Z} \cdot G_T$	Formula (45)	kg·m								
M_c	Formula (22) or (23)	kg·m								
P_c	Formula (19) or (20)	kg								
$M_\xi = (M_P + M_c)\cos\nu + M_T \sin\nu$	Formula (50)	kg·m								
F	Table 2 or Formula (30)	kg·m²								
$W_\xi(C)$	Table 2 or Formula (59)	m³								
$W_\xi(D)$	Same	m³								
$\sigma_c = \frac{P_c}{F} \cdot 10^{-4}$	Formula (54)	kg/cm²								
$\sigma_\xi(C) = \frac{M_\xi}{W_\xi(C)} \cdot 10^{-4}$	Formula (52)	kg/cm²								
$\sigma_\xi(D) = \frac{M_\xi}{W_\xi(D)} \cdot 10^{-4}$	Same	kg/cm²								
$\sigma(C) = \sigma_\xi(C) + \sigma_c$	Formula (57)	kg/cm²								
$\sigma(D) = \sigma_\xi(D) + \sigma_c$	Formula (56)	kg/cm²								

Table 8. Recommended Values of Permissible Stresses, kg/cm^2 /40

Material of Propeller	Permissible stresses in tension		compression	
	Number of propellers on the ship			
	1	2	1	2
LS 55-3-1 brass	400 - 450	450 - 500	450 - 550	550 - 600
LMts 58-2 or LKNMts 3-1-1 stainless steels	650	700	700	750
Carbon steel	400	450	400	450
High strength cast iron	200	225	300	350
Gray cast iron	150	175	300	350
Aluminum-nickel or manganese-aluminum bronzes	600	650	650	700

Section 5. Information on Other Methods Used for Evaluation of Screw Propeller Strength

With the increase in information on the strength of propellers and the development of hydrodynamic calculations based on the vortical theory published by several authors, practical methods of evaluating general strength of propellers have been suggested. The best known of them are the methods of Taylor (44), Romsom (41), Rosingh (42), and Keyser and Arnoldus (38).

Special features of these methods and some formulae used in practical propeller strength calculations by the above methods are discussed below.

Taylor's Method. The first analytical method of stress calculation in propeller blades was suggested in 1920. It was based on general engineering assumptions in strength calculation of propellers (see Section 4). In order to simplify calculation formulae, additional assumptions are made with respect to the distribution of hydrodynamic forces along the radius of a propeller. In particular, it is assumed that the axial components of hydrodynamic forces increase linearly with increasing radius, while the tangential stresses are not changed, i.e.,

$$\left.\begin{aligned} \frac{dP_i}{dr} &= pr_i \\ \frac{dT_i}{dr} &= q \end{aligned}\right\} \qquad (61)$$

Such a schematic presentation of hydrodynamic forces, strictly speaking, is correct only for marine propellers with constant circulation. With such assumptions, bending moments caused by the action of axial and tangential hydrodynamic forces can be found without any difficulties: /41

$$\left.\begin{aligned} M_P &= \frac{PR}{Z}(\bar{r}_{cP}-\bar{r}_p);\\ M_T &= \frac{M}{Z}(\bar{r}_{cT}-\bar{r}_p), \end{aligned}\right\} \qquad (62)$$

where

$$\bar{r}_{cP}=\frac{2+\bar{r}_p^2}{3};$$

$$\bar{r}_{cT}=1-\bar{r}_p+\bar{r}_p^2.$$

Calculation of centrifugal forces as well as determination of bending moments in respect to the main central axes of inertia of the blade cross section and of maximum stresses in the critical cross section do not differ from those discussed in Section 4. It is considered that the strength is sufficient if $\frac{\sigma_0}{\sigma_{max}} \geqslant n$,

where n - safety factor of static strength. For various ship types and service conditions, $6 \leqslant n \leqslant 12$.

The necessity of linear approximation of the distribution of hydrodynamic forces was probably caused by the absence at that time of simple theoretical methods for their determination. However, Taylor succeeded in taking into account the main portion of the action of hydrodynamic forces on the blade. Indeed, a comparison of calculated values of hydrodynamic moments in the cross section at a radius $\bar{r}_p = 0.2$ obtained by Taylor's method and by the vortical theory presented in the form of $M_P = k_P P_1 R$; $M_T = k_T M_1$

indicates that coefficients k_p and k_T are equal, respectively.

	k_p	k_T
According to Taylor	0.469	0.63
According to the vortical theory	0.475	0.67

For comparison of calculated values of bending moments for the section modulus we obtain:

$$M_{max} = (M_P^2 + M_T^2)^{\frac{1}{2}} = \frac{M}{Z}\left[\left(\frac{2\eta_p}{\lambda_p}k_P\right)^2 + k_T^2\right]^{\frac{1}{2}}.$$

For example, for the propeller of a high tonnage tanker, according to hydrodynamic calculations, it can be assumed that $\eta_p = 0.525$ and $\lambda_p = 0.5$. Then the values of bending moment M will be:

According to Taylor	1.68 $\frac{M}{Z}$
According to the vortical theory	1.70 $\frac{M}{Z}$

/42

In this case, both methods produced practically the same results.

Relatively simple methods for determining hydrodynamic forces according to the vortical theory exclude the necessity of using linear approximation. At the same time, the calculation formula (40), (41), (47), (48) are not much more complex than the Taylor's formulae. However, since Taylor's method provides results similar to those obtained by the vortical theory, it is traditionally used for design of ship propellers. It is also significant that the assumptions initially suggested by Taylor are used even at present (see Section 4).

Romsom's Method. This method is a further development of Taylor's method, mainly in the direction of defining more precisely the hydrodynamic forces acting on a blade. The distribution of hydrodynamic load along the radius is determined according to the vortical theory.

In addition, in order to obtain a blade design approaching that of equal strength in bending, Romsom recommends selecting separate elements of the blade attempting to have equal design stresses in cross sections at relative radii $\bar{r}$ which are equal 0.2 and 0.6.

In developing this method, attention was paid to the fact that the moment of inertia of blade cross sections in respect to the η axis almost by the whole order exceeds the moment of inertia in respect to the ξ axis as a result of the relatively small thickness of these cross sections. Therefore, Romsom found it permissible to disregard stresses in the cross section being considered which are caused by bending moment M_η. The advantage of this simplification is supported by experimental data showing that stresses emerging near edges of the blade are negligible in magnitude and almost by one order lower than stresses in the areas where the blade is thick.

Based on the above assumptions and as a result of more precise definitions in calculation of the section moduli of the blade profile, Romsom obtained the following dependences for calculation of maximum normal stresses in cross sections under consideration at the relative radii $\bar{r}$, which are equal 0.2 and 0.6

$$\sigma_p = \frac{C_1 N_e}{\alpha b_m^2 Z}\left(C_2 + \frac{1}{\lambda_i}\right), \tag{63}$$

where N_p - power transmitted to the propeller, hp;

n_m - propeller rpm;

b - length of the straightened cross section, m; /43

e_m - maximum thickness of the blade in cross section, cm;

λ_i - induced relative advance-to-diameter ratio;

$W = \alpha b e_m^2$ - section modulus, cm^3;

C_1 and C_2 - coefficients depending on the pitch ratio with a given cross section of the blade being considered in the calculations.

Graphs for determining coefficients C_1 and C_2 are given in Figure 17. In the same figure is included a graph for the function $X = \frac{1}{\cos^3 \varepsilon}$, which is introduced into the calculation formula in cases when propeller blades are inclined at angle ε.

After a series of experiments in measuring stresses in cylindrical cross sections of blades at a relative radii $\bar{r}$ which are equal 0.2 and 0.6, Romson came to the conclusion that calculation results will in the best way correspond to the measurement data if, in formulae for calculating the section moduli of straightened cylindrical cross sections of the blade, coefficients α in the formula $W = \alpha b e_m^2$ are used according to the following data:

	for $\bar{r} = 0.2$	for $\bar{r} = 0.6$
In tension	0.096	0.100
In compression	0.086	0.080

Inclination of propeller blades, deg.

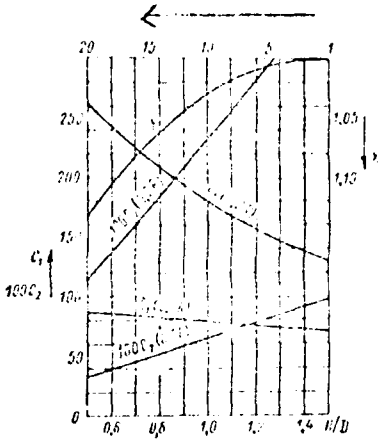

Fig. 17. Graphs for determining coefficients C_1, C_2 and X

Inclination of propeller blades, deg.

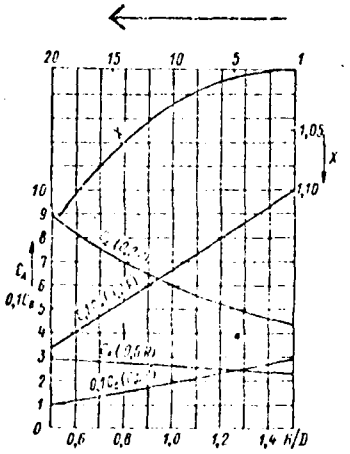

Fig. 18. Graphs for determining coefficients C_A, C_B, and X

When the diagram developed at the Vageningen experimental basin /lll is used for the design of ship propellers, formula (63) is used in slightly modified form:

$$\sigma_p = \frac{C_A \Delta_p}{n D_m^2 Z n_m} \left(C_B + 101{,}5 \frac{\eta_p}{\lambda_p} \right) X, \qquad (64)$$

where C_A, C_B, and X are coefficients similar to coefficients C_1 and C_2, which are found from curves in Figure 18.

Calculation of stresses caused by the centrifugal force of inertia is performed by the approximate method in which bending stresses due to blade inclination are determined at radii $\bar{r} = 0.2$ and $\bar{r} = 0.6$, respectively by the formulae:

$$\sigma_{r(1)} \approx \frac{(n_e D)^2}{10^4}\left(\frac{AC}{\alpha_{(1)}} + 0.58\right) \tag{65}$$

$$\sigma_{r(1)} \approx \frac{(n_e D)^2}{10^4}\left(\frac{AC}{\alpha_{(1)}} - 0.315\right). \tag{66}$$

In these formulae, sign "+" is used for tensile stresses and sign "-" for compressive stresses. Signs in parentheses indicate that the values of coefficients α depend on the character of stresses. This should be taken into consideration in determining these coefficients using data given above.

In order to simplify calculations, coefficients A and C, which are some functions of the pitch ratio H/D, angle of blade inclination, and the relative thickness of its cross sections, are given in graphical form in Figures 19 and 20.

General stresses caused by the action of hydrodynamic and centrifugal forces are found by a simple summation:

$$\sigma_z = \sigma_{zp} + \sigma_{zc}; \quad \sigma_{zp} + \sigma_{zc} = \sigma_{dp} + \sigma_{dc}. \tag{67}$$

where σ_2 and σ_d are maximum tensile and compressive stresses in the cross section being considered.

According to Romsom, propeller strength is considered to be sufficient if:

$$\frac{\sigma_b}{\sigma_{zp} + \sigma_{zc}} \quad \text{or} \quad \frac{\sigma_b}{\sigma_{dp} + \sigma_{dc}} \geq n \geq 8. \tag{68}$$

Romsom's method gains wider and wider use in practical design of ship propellers. The results obtained by this method are similar to those obtained by the method discussed in Section 4, which is apparent since both methods are based on almost the same initial data. /45

Rosingh's Method. Based on experience in operation of ship propellers which demonstrated that breaking off of blades due to insufficient strength often occurs along nearly flat cross sections (Fig. 4), Rosingh developed a method for calculating the static strength of propellers, the main difference of which as compared with other methods is the introduction of geometrical characteristics (areas, moments of inertia) of not cylindrical but flat cross sections of the blade. Rosingh considered that his method would be most effective in strength calculations of propellers with wide blades, because in such blades the difference between the profiles of flat and cylindrical cross sections is particularly pronounced.

In order to present a picture of stress distribution along the complete blade, it is necessary to perform calculations for several groups of cross sections located at different distances from the propeller axis. Each group consists of several cross sections under various angles to the blade axis projected on the transverse plane which is perpendicular to the propeller axis. Since in such a case the volume of calculations is too extensive, the calculation is carried out only for several cross sections directly behind the fillet at the blade root.

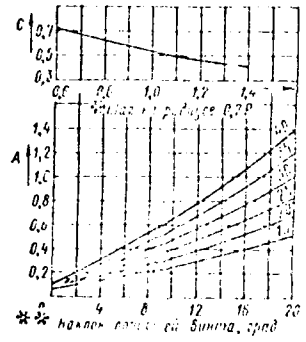

Fig. 19. Graphs for determining coefficients A and C for the cross section at radius $\bar{r} = 0.2$

* Pitch at 0.2 R

**Inclination of propeller blades, deg.

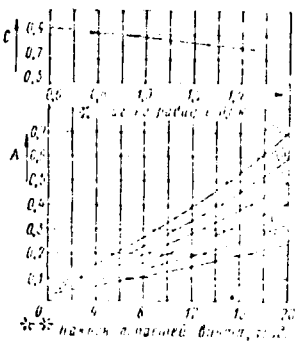

Fig. 20. Graphs for determining coefficients A and C for the cross section at radius $\bar{r} = 0.6$

* Pitch at 0.6 R;

**Inclination of propeller blades, deg.

At first the point is determined at which a resultant of hydrodynamic forces (thrust and tangential force) is applied. In such a case, if the propeller is designed according to the vortical theory, the distribution of the thrust and tangential force on the blade is known*. In this case, with the given values of the thrust and /46

*For the purpose of calculation, the distribution of the thrust and the tangential force may be determined by the method discussed in Section 1.

propeller torque, the points at which resultants of axial and tangential forces are applied may be determined from the equation of moments created by elementary forces.

For finding these points, more approximate methods are also permitted. For example, Rosingh suggested a diagram for approximate determination of the point to which thrust is applied (Fig. 21). For a plane which passes at a distance of $\bar{r} = 0.4$ from the propeller axis, we find that the resultant of thrust is applied at a point located at a distance of 0.73R from the propeller axis and amounts to 92% of the total value of thrust at a design regime of operation*.

*It may be approximately considered that the relative distribution of the thrust along the propeller radius corresponds to the distribution of torsional moment (see (13)). Therefore, the graph in Fig. 21 may also be used for finding the point to which tangential force is applied. Distribution of this force may be found from the formula deduced from formula (12) $\frac{dT}{dr} \sim \frac{1}{r} \frac{dP}{dr}$.

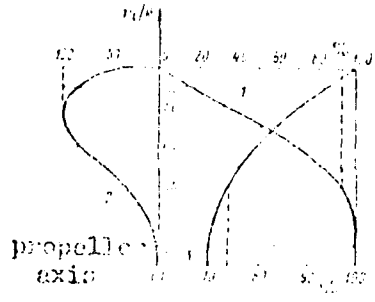

Fig. 21. Graph for approximate determination of thrust and the point of its application.

1 - relative value of the thrust acting in the cross section at a distance r_i from the propeller axis; 2 - distribution of thrust along the propeller radius; 3 - curve of ordinates of the point of thrust application in percent of propeller radius.

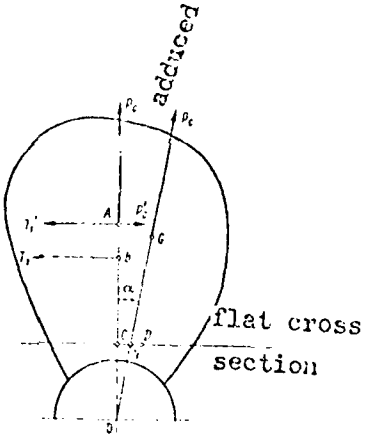

Fig. 22. Adduction of the force acting on the propeller blade to the point A.

Then the centrifugal force P_c, which causes both bending and tension, is determined (in kiligrams-force):

$$P_c = \frac{G_{cb}\omega^2}{g r_0} \qquad (69)$$

where G - weight of blade, kg;

r_G - distance between the center of gravity of the blade and axis of propeller rotation, m;

n_n - propeller rps.

The position of the point to which centrifugal force is applied and which coincides with the center of gravity of the blade when $r > r_0$, is determined by the axial, radial, and transverse coordinates, which were calculated using numerical integration methods (see Sec. 3).

The diagram in Fig. 22 shows: point A to which thrust P_1 is applied*, point B to which tangential hydrodynamic force T_1 is applied,

*Direction of thrust is perpendicular to the plane of drawing.

and point G (which coincides with the center of gravity of the whole blade) to which centrifugal force P_c is applied.

Then, to simplify the calculation, all forces are transferred to point A to which the thrust is applied, maintaining constant the bending moment, which acts in the cross section being considered. For this purpose, the tangential force is decreased in the proportion of $\frac{BC}{AC}$, i.e., $T_1' = \frac{BC}{AC} T_1$. If the point of intersection of the direction of centrifugal force with the blade cross section plane is denoted by letter N, and the center of gravity of the flat cross section of the blade is denoted by letter D, then, by transferring centrifugal force to the point A and maintaining the bending moment constant

$$P_c \frac{ND}{\cos\alpha} = P_{comp} CD,$$

we obtain

$$P_{comp} = P_c \frac{ND}{CD} \cos\alpha. \qquad (70)$$

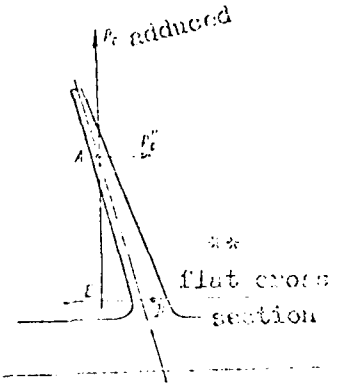

Fig. 23. Diagram for determining the arm of application of arbitrary forces

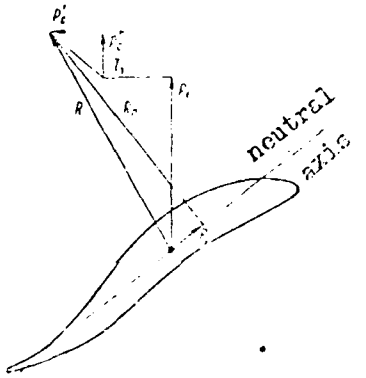

Fig. 24. Diagram of forces which cause bending of the blade

The moment created by force P_c in respect to point D is replaced by moments of some arbitrary forces P_c' and P_c'', which are found (Fig. 22 and 23) from conditions of moments equality: /48

$$\left.\begin{aligned} P_c' AC &= P_{c\,\mathrm{reduced}} CD; \\ P_c'' AE &= P_{c\,\mathrm{reduced}} ED. \end{aligned}\right| \qquad (71)$$

From which

$$\left.\begin{aligned} P_c' &= P_{c\,\mathrm{reduced}} \frac{CD}{AC}; \\ P_c'' &= P_{c\,\mathrm{reduced}} \frac{ED}{AE}. \end{aligned}\right| \qquad (72)$$

A diagram of forces which cause bending of the blade is shown in Figure 24. The resultant of forces T_1, T_1', T_c' and T_c'' may be broken down into normal R_n and parallel R_p to the neutral axis direction, which makes it possible to find the bending moment in the cross section caused by the action of external forces. To find stresses, it is necessary to find the position of the main central axes of inertia and calculate the value of the section modulus for the point most remote from the central axis.

It should be noted that the assumption about parallelness of one of the main central axes of the flat cross section to the chord, used earlier for the cylindrical cross sections unfolded on the plane, in this case would result in a greater error since the flat cross section of the blade is usually of a complex airfoil profile. Therefore, its geometrical characteristics should be determined by general formulae given in Section 3, which makes the calculation more complex.

Koningh's method is more laborious as compared with methods based on consideration of cylindrical cross sections of the blade, mainly due to the complexity of plotting flat cross sections. Koningh's method is very seldom used for the design of screw propellers. However, it is very useful for analyzing the state of stress in blades of high speed ship propellers which operate under heavy load. In most cases, such propellers operate in the cavitation zone, and therefore blades are designed as thin as possible; but they have to meet strength requirements. In such cases, high stresses are tolerated, but their calculation therefore must be as accurate as possible. This method is particularly expedient in performing comparative precise strength calculations for propellers being designed and those which are in operation and provide satisfactory performance.

CHAPTER II. EVALUATION OF SCREW PROPELLERS STRENGTH TAKING INTO ACCOUNT THE CYCLIC CHARACTER OF EXTERNAL FORCES

/49

Section 6. Initial Data on Non-Uniformity of the Velocity Field in the Area of Screw Propeller for Transport Ships with Various Shape of Stern Formations

The reason for periodic variations of hydrodynamic forces at the propeller blades is non-uniformity of external flow incident on the propeller, which is stipulated by the effect of the stern part of the ship and projecting hull parts near propeller.

Data characterising non-uniformity of the incident flow are obtained by measuring velocity fields in the area of propeller location using a model of a ship hull in an experimental water basin. Measurements obtained in the absence of an operating propeller make it possible to obtain data on the so-called nominal velocity field. It is assumed that the effect of the operating propeller on the characteristics of the velocity field non-uniformity may be disregarded and that the non-uniformity of the velocity field obtained in model tests corresponds with the non-uniformity of the velocity field of a real ship.

The weak point of this method is the fact that in determining the parameters of the propeller load, it does not take into account the effect of the propeller load and also of the scale factor on the non-uniformity of the velocity field. However, this is the only method that can be presently used, since existing analytical methods do not make it possible to calculate accurately the flow of a viscous fluid around the stern part of a ship with specific ship lines. On the other hand, measuring the field velocity in the area of propeller location may be considered to be in the category of unique hydrodynamic experiments. The very limited data available testify that the operating propeller may change the initial non-uniformity of the velocity field behind the ship hull. This is particularly pronounced for ships with full lines ($\delta > 0.80$) where at the stern part of the ship, separation of the boundary layer takes place (16). In the case of such ships, because of the suction action of the propeller, a displacement of the area of boundary layer separation toward the stern takes place, which leads to the narrowing of the retarded flow incident on the propeller and the appearance of sharper non-uniformity picks at the propeller disk.

The approximate methods of evaluating the effect of load on the propeller on the non-uniformity of the velocity field (43) show that this effect is quite essential, particularly at inner radii of the propeller disk.

Evidently, for a ship with flow around its stern without separation of the boundary layer and with lower load on the propeller in respect to thrust, the effect of the propeller load on the non-uniformity of the velocity field will be less pronounced. This makes it possible to use the characteristics of the nominal current as the initial data on non-uniformity of the velocity field in the propeller disk. /50

Data on the possibility of using simulation test results on the parameters of velocity field non-uniformity are also very limited. Comparable tests carried out at the Wageningen experimental basin with the use of a series of models of a "Victory" type ship built in different scales, including a large-scale towed model, demonstrated that the effect of the scale factor is not essential.

Data on the non-uniformity of velocity field parameters for the field in which the propeller operates serve as a basis for calculation of periodically varying forces acting on the blade and stresses emerging in the blade under the action of these forces. As noted earlier, these data can be obtained by testing hull models in an experimental basin.

At the initial design stage, parameters on the non-uniformity of the velocity field determined for a prototype ship may be used for evaluation of forces created by the propeller for the same shape of stern parts of ships being built.

It is assumed that slight deviations in the shape of the stern part of a ship would not lead to a considerable change in the nominal velocity field in the propeller disk. Therefore, ships may be broken down into groups with similar characteristics of non-uniformity of the created velocity field.

In considering only single-shaft and double-shaft seagoing ships, the following groups should be separated: with stern-post frame (closed stern), without stern-post frame (open stern), with propeller struts, with shaft bossing.

Block coefficient δ and coefficient τ which reflects the shape of stern frames may be used as parameters characterizing the stern formations of a single shaft ship. A method for determining coefficient τ is shown in Figure 25.

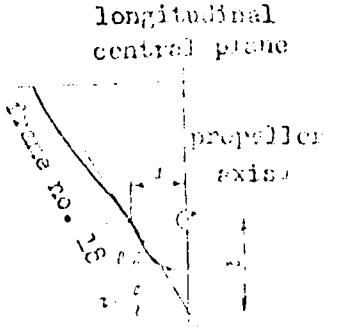

Fig. 25. Determining the frame shape coefficient

Relation between numerical values of coefficient τ and the shape of the stern frames [illegible] /51

U-shape	0.1
Moderately U-shape	0.1 - 0.3
Moderately V-shape	0.3 - 0.4
V-shape	0.4

Typical nominal velocity fields in the area of the propeller for single-shaft transport ships with a stern having a stern post frame (closed stern) are illustrated in Fig. 26 (39).

Graphs in Fig. 26 a, b, and c are plotted for ships which differ by the value of coefficient τ reflecting the shape of stern frames but have the same block coefficient δ.

Graphs in Fig. 26 d, e, f, and g are for ships with different values of both coefficients δ and τ.

In Fig. 27 a and b are shown nominal velocity fields typical for single-shaft transport ships with the closed type of stern (37). Data on non-uniformity parameters are conditionally referred to the ship length along waterline L = 152.5 m (500 feet) and propeller diameter D = 6.1 m (20 feet), $\frac{D}{L} = 0.04$ (Fig. 27, a), and also to L = 183 m (600 feet) and propeller diameter D = 6.7 m (22 feet), $\frac{D}{L} = 0.0365$ (Fig. 27, b).

If the D/L ratio does not coincide with the above values, the values of the radii should be changed according to formula:

$$\bar{r}_1 = \bar{r} \frac{D_1}{D_1 L_1}.$$

where $\bar{r}$, D_1, and L_1 - relative radius of the propeller, its diameter, and the ship length along its waterline, respectively.

Figure 18 shows typical nominal velocity fields in the area of the propeller for two-shaft transport ships (37) with various designs of propeller exposure (housing, propeller shaft strut, combination of both).

In Fig. 26-28 on the x-coordinate is plotted angular coordinate θ*,

*Plotting values of angle θ is started from the upper vertical position in the plane of the propeller disk in clockwise rotation.

and on the y-coordinate relative axial $\bar{V}_a = \frac{V_a}{V}$ (up) and tangential $\bar{V}_\zeta = \frac{V_\zeta}{V}$ (down) components of the velocity field (V-ship speed).

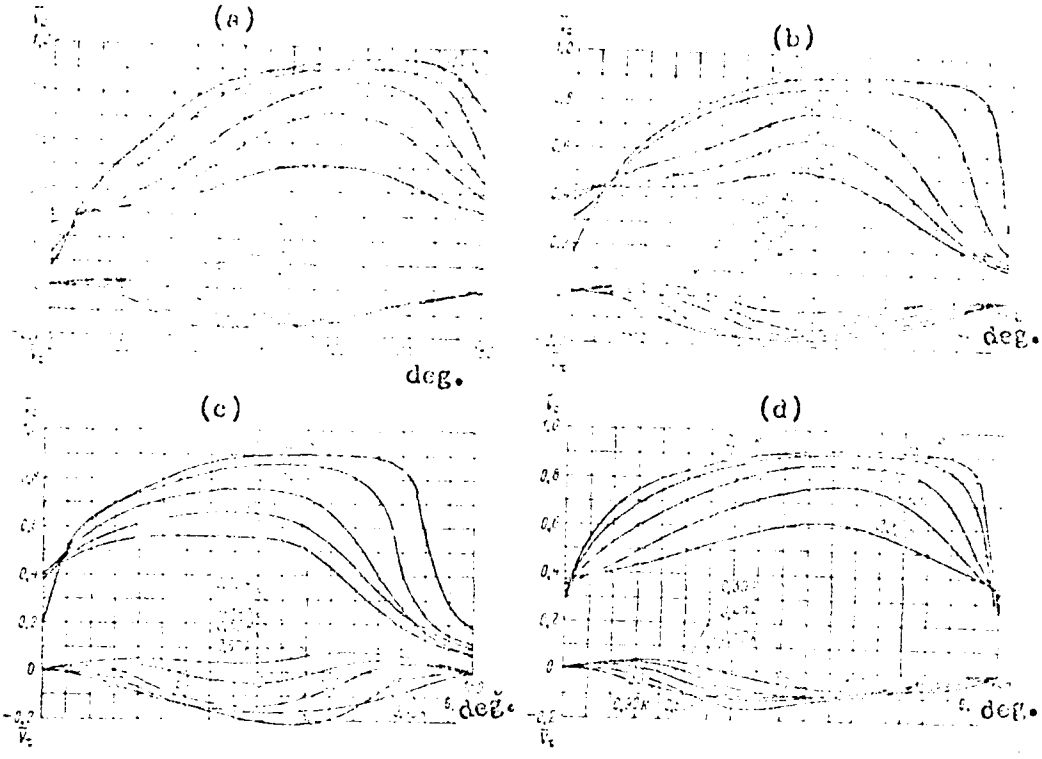

Fig. 26. Nominal velocity fields in the area of the propeller for single-shaft transport ships with a stern having stern post (closed type): /52

a. $\delta = 0.7$, V-shape stern frames, $\tau = 0.55$;

b. $\delta = 0.7$, shape of stern frames intermediary between V and U shape, $\tau = 0.35$;

c. $\delta = 0.7$, U-shape stern frames, $\tau = 0.1$;

d. $\delta = 0.60$, moderate U-shape stern frames, $\tau = 0.20$;

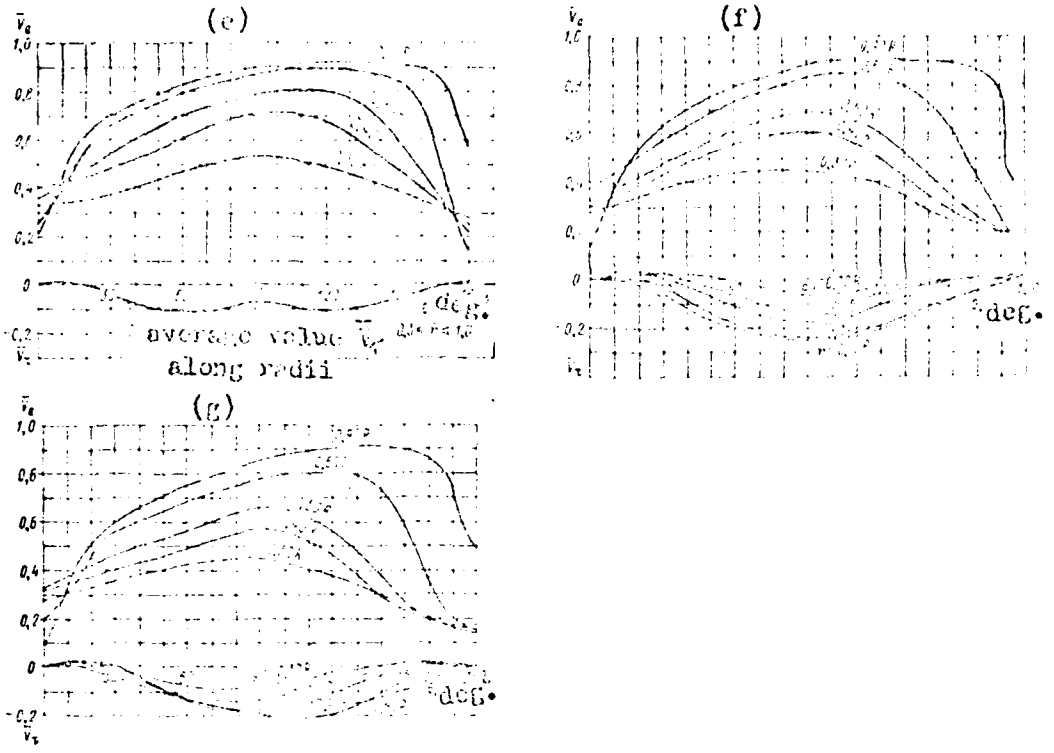

Fig. 26. Nominal velocity fields in the area of the propeller for single-shaft transport ships with a stern having stern post (closed type):

/53

e. $\delta = 0.65$, moderate U-shape stern frames, $\tau = 0.28$;

f. $\delta = 0.75$, moderate V-shape stern frames, $\tau = 0.35$;

g. $\delta = 0.80$, moderate V-shape stern frames, $\tau = 0.40$.

(a)

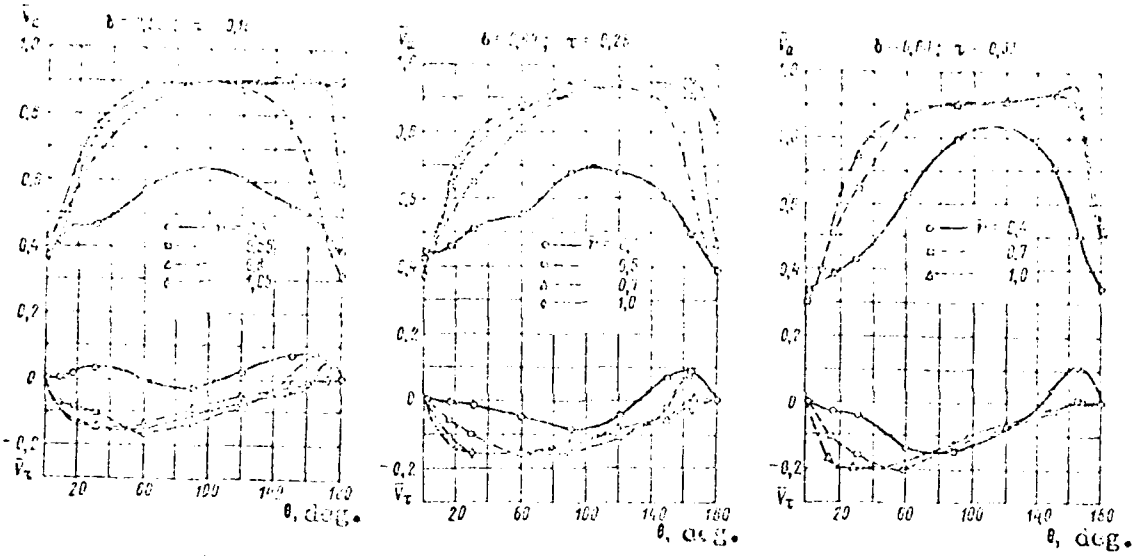

(b)

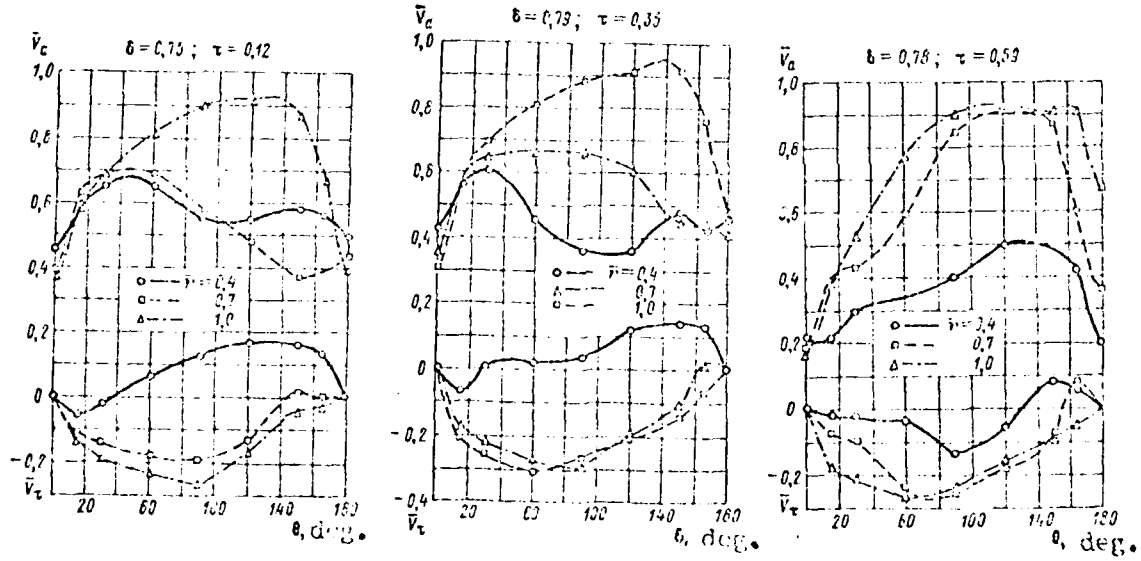

Fig. 27. Nominal velocity fields in the area of the propeller for a single-shaft transport ship with a stern that is without a stern post frame (open type): a. moderate V- and U-shape stern frames; b. V-shape, moderate V-shape, and U-shape stern frames.

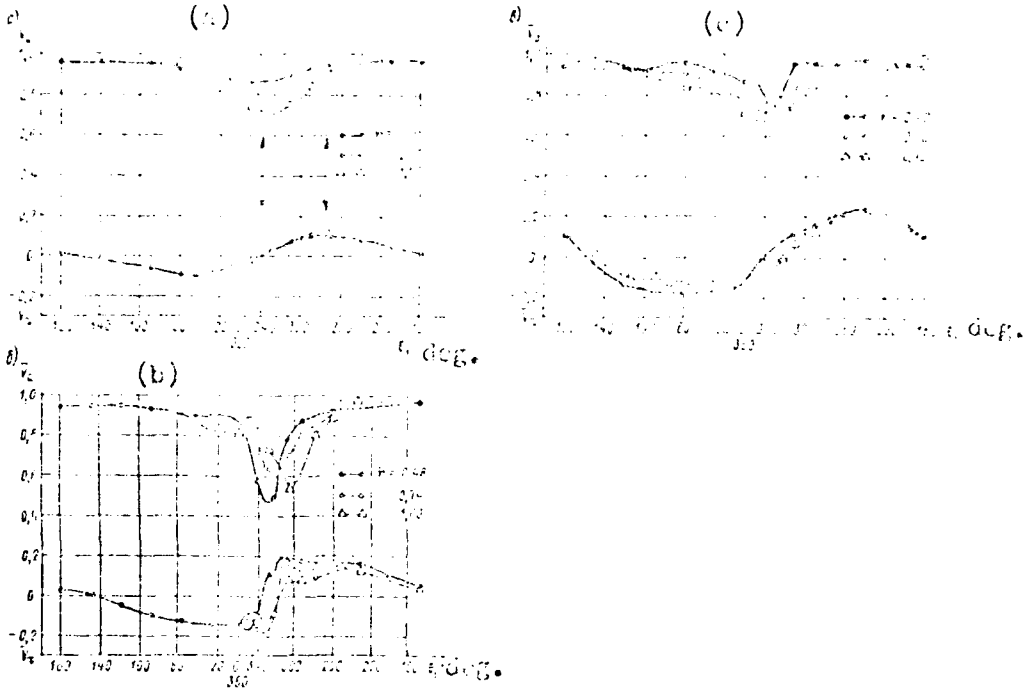

Fig. 28. Nominal velocity fields in the area of the propeller for two-shaft transport ships: a. bossing and propeller shaft struts (arrows indicate planes of struts installation); b. bossing; c. shaft struts.

Section 7. Determining hydrodynamic forces Acting on the Propeller Blade in Operation in a Non-uniform Velocity Field

In a general case, the velocity field in the area of the propeller is characterized by the presence of axial component V_a, tangential V_τ, and radial component V_r. The main role in variations of the angle of incidence of the element and of the hydrodynamic force is played by the axial and tangential components of the velocity fields.

---

*V_a and V_τ are considered to be positive if their vectors coincide with the direction of incident flow and the direction of propeller rotation, respectively.

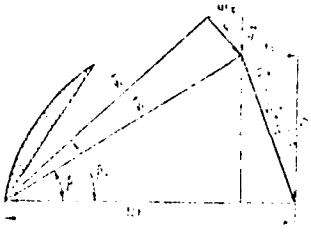

Fig. 29. Diagram of velocity vectors on the blade element of a propeller operating in a non-uniform flow

As seen in the diagram of velocities of blade elements in a non-uniform flow (Fig. 29), in the moment of time characterized by the angle of blade turn to the angular position ζ, the direction of flow incidence is determined by the angle $\beta = \beta(\zeta)$.

$$\operatorname{tg}\beta = \frac{V_a}{\omega r - V_t} = \frac{\lambda}{\pi r} \cdot \frac{V_a}{1 - \frac{\lambda}{\pi r} V_t} \qquad (73)$$

where V - ship speed, $\lambda = \frac{V}{nD}$; $\bar{V}_a = \frac{V_a}{V}$; $\bar{V}_t = \frac{V_t}{V}$.

The instantaneous value of the advance ratio of the element:

$$\lambda_{r\omega} = \pi r \operatorname{tg}\beta = \lambda \frac{\bar{V}_a}{1 - \frac{\lambda}{\pi r} \bar{V}_t} \qquad (74)$$

From the foregoing (see Section 1), it follows that knowing the angle of advance ratio β of an element is sufficient for determining the hydrodynamic load on the propeller in its operation in a uniform incident flow, when the relation between the characteristics of external flow and generated hydrodynamic force is expressed with the help of simple formulas based on the vortical theory of an optimum propeller.

It is impossible to establish similar dependences for a propeller operating in a non-uniform incident flow without introducing additional assumptions, because of the complexity of determining induced velocity ω. The vortical system of a propeller in a non-uniform velocity field is characterized by the presence of free radial and helicoidal vortexes which are caused by periodical change of the circulation of the adjoined vortical system and which induce at the area of velocity system adjoinment and affect the intensity of its circulation. Hence, there is a mutual effect of the adjoined and free vortical systems which depends on the characteristics of the incident flow non-uniformity. Considerably more complex, as compared with operation of a propeller in a uniform flow, is the mutual hydrodynamic effect of propeller blades. Since propeller

/58

blade of finite width which increases with increases in disk ratio, it is necessary to take into account variation of incident flow parameters along the blade element length which is caused by non-uniformity of the nominal field.

The [illegible] indicated above combined with considerable mathematical difficulties in describing physical representation, make of formulating the hydrodynamic forces acting on a propeller in a non-uniform inflow flow considerably more complex. Until the present time, there has been no accurate method for general solution of this problem acceptable for engineering calculations. The only known solutions are those in which more or less substantiated assumptions were introduced. For practical calculations, approximate methods are used for evaluation of the variable hydrodynamic forces created by a propeller. These methods are based on introduced assumptions and hypotheses which shorten considerably the time needed for calculations.

The most widely used is the hypotheses of a quasistationary state, according to which the instantaneous hydrodynamic forces operating on the element of a propeller blade in a non-uniform velocity field are equivalent to the stationary forces acting on the same element during the operation of a propeller in a uniform velocity field under the condition that the instantaneous and stationary velocities of external flow and the angles of incidence in both cases are equal.

Let us analyze equation (7h). Based on the hypotheses of a quasistationary state for a propeller operating in a non-uniform velocity field ($V_a = V_a(\Theta)$ and $V_\tau = V_\tau(\Theta)$), with $\Theta = \Theta_1$ the dependence of the hydrodynamic force (for the element of the blade) on the instantaneous value of the advance/diameter ratio $\lambda_{p0} = \lambda_p(\Theta_1)$ will be the same as for a propeller operating in a uniform velocity when $\bar{V}_a = \bar{V}_a(\Theta_1) = \text{const}$ and $\bar{V}_\tau = \bar{V}_\tau(\Theta_1) = \text{const}$. When the blade is moved into position $\Theta = \Theta_2$, the dependence of the hydrodynamic force on the value of the instantaneous advance/diameter ratio will correspond to the conditions of propeller operation in a uniform velocity field, when $\bar{V}_a = \bar{V}_a(\Theta_2) = \text{const}$ and $\bar{V}_\tau = \bar{V}_\tau(\Theta_2) = \text{const}$, etc.

Thus, the introduction of the quasistationary state hypothesis for determining hydrodynamic forces acting on the blades of a propeller operating in a non-uniform velocity field makes it possible to use the relations existing between the parameters of uniform external flow and hydrodynamic load which are deduced for conditions of a propeller operating in a uniform flow.

The calculation method based on this principle was developed by I. Ya. Miniovich (3). According to the hypotheses of a quasistationary state, the condition which is both necessary and sufficient for equality of hydrodynamic forces acting on the blade element in uniform and non-uniform velocity fields is the equality of the stationary advance/diameter ratio λ_p and the corresponding instantaneous value of the advance/diameter ratio $\lambda_{p\theta}$ determined by equation (74). /59

The latter can be presented in the form:

$$\lambda_{p\theta} = \lambda \frac{1-\psi_a}{1-\psi_\tau}. \tag{75}$$

where $\psi_a = 1 - \frac{V_a}{V}$ - coefficient of the nominal axial wake;

$\psi_\tau = \frac{V_\tau}{\Omega r} = \frac{\lambda}{\pi r} \cdot \frac{V_\tau}{V}$ - coefficient of the nominal tangential wake.

According to Figure 29, it may be considered that at the moment of time being considered, the blade element is rotating at some conditional angular velocity Ω' at rpm n', which corresponds to the actual tangential velocity of flow $\Omega r - V_\tau = \Omega r (1 - \psi_\tau)$.

The values of Ω' and n' are found with the help of the following formulae:

$$\left.\begin{aligned} \Omega' &= \Omega(1-\psi_\tau); \\ n' &= n(1-\psi_\tau). \end{aligned}\right\} \tag{76}$$

In contrast to angular speed of propeller rotation Ω and rpm n, the values of Ω' and n' are variable with time, and in a general case depend on the radius at which the element of the blade is being considered. When the tangential component of the wake velocity is zero, values of Ω' and n' coincide with values of Ω and n.

If the thrust of the element in a non-uniform flow is denoted by dP_1 and the thrust in a uniform flow is denoted by $d\bar{P}_1$, then according to the hypotheses of a quasistationary state, $dP_1 = d\bar{P}_1$ with $\lambda_p = \lambda_{p\theta}$ or, transforming into nondimensional form and taking into account formula (76), we obtain:

$$\frac{dP_1}{\rho(n')^2 D^4} = \frac{d\bar{P}_1}{\rho n^2 D^4}.$$

From this formula:

$$\left(\frac{dK_1}{dr}\right)_1 = (1-\psi_\tau)^2 \left(\frac{d\bar{K}_1}{dr}\right)_1. \tag{77}$$

where:

$$\left(\frac{dK_1}{dr}\right)_1 = \frac{\left(\frac{dP}{dr}\right)_1}{\rho n^2 D^4} \quad \text{и} \quad \left(\frac{d\bar{K}_1}{dr}\right)_1 = \frac{\left(\frac{dP}{dr}\right)_1}{\rho n^2 D^4}.$$

By integrating formula (77) as a function of radius, we obtain the value of propeller blade thrust for a random angular position: /60

$$P_1 = \rho n^2 D^4 \int_{\bar{r}_0}^{1} (1-\psi_\tau)^2 \left(\frac{d\bar{K}_1}{dr}\right)_1 d\bar{r}, \tag{78}$$

where $\bar{r}_0$ - relative radius of the propeller hub.

Similarly the torsional moment of the propeller blade:

$$M_1 = \rho n^2 D^5 \int_{\bar{r}_0}^{1} (1-\psi_\tau)^2 \left(\frac{d\bar{K}_2}{d\bar{r}}\right)_1 d\bar{r}. \tag{79}$$

The values $\left(\frac{dK_1}{dr}\right)_1 = f(\lambda_p)$ and $\left(\frac{d\bar{K}_2}{dr}\right)_1 = f(\lambda_p)$, which characterize the elementary thrust and torsional moment of an individual blade are determined by calculations using the vortical theory of the hydrodynamic characteristics of a propeller operating in a uniform velocity field and the advance/diameter ratio $\lambda_{p0} = \lambda \frac{1-\psi_a}{1-\psi_\tau}$, as shown in Section 1.

For calculations not requiring high accuracy, which also include strength calculations of propeller blades subjected to the action of cyclic loads, it is permitted to substitute the action of the blade by the action of the element located at the center of pressure, i.e., at the radius R_0, called the equivalent radius.

Formulae (78) and (79) in this case will be in the form:

$$P_1 = \frac{\rho n^2 D^4}{Z} (1-\psi_{\tau R_0})^2 \bar{K}_1, \tag{80}$$

$$M_1 = \frac{\rho n^2 D^5}{Z} (1-\psi_{\tau R_0})^2 \bar{K}_2, \tag{81}$$

where $\bar{K}_1$ and $\bar{K}_2$ - coefficients of thrust and torsional moment of the entire propeller.

$\bar{K}_1$ and $\bar{K}_2$ are determined by the curves of propeller action in free water under the condition that:

$$\lambda_{p0} = \lambda \frac{1-\psi_{aR_0}}{1-\psi_{\tau R_0}} = \lambda \frac{\bar{V}_{aR_0}}{1-\frac{\lambda}{\pi R_0}\bar{V}_{\tau R_0}},$$

where ψ_{aRo} and $\psi_{\tau Ro}$ - coefficients of axial and tangential nominal wakes at the equivalent radius $\bar{R}_0 = \frac{R_0}{R} = 0.67$.

Calculation by formulae (80) and (81) is less time consuming since, in this case, calculations based on the vortical theory of load distribution along the radius and subsequent integration of hydrodynamic forces along the blade are not necessary. /61

Formulae (78) and (79) as well as (80) and (81) are used for determining varying hydrodynamic forces on propeller blades in engineering strength calculations for conditions of cyclic loads. Formulae (78) and (79) take into account more accurately special features of the non-uniformity of the velocity field for a specific ship. It is expedient to use formulae (80) and (81) for rough estimates of variable hydrodynamic forces.

A number of studies may be mentioned which were carried out during past years (e.g., (36) and (19)), the data of which testify that it is expedient to introduce some corrections into formulae (78) - (81) in order to improve accuracy in the calculation of hydrodynamic forces acting on the blade. First of all, it concerns defining more precisely the effect of the angle of flow incidence on the propeller.

The coefficient of tangential nominal wake in equations (78) - (81) is in general determined by the inclination of incident flow. F. Gutsche (36), on the basis of results of his systematic experimental studies of the hydrodynamic characteristics of propellers in an inclined flow, considers it expedient to present formula (75) in the form:

$$\lambda_{p\theta} = \lambda \frac{1}{1 - C\psi_i}.$$

The values of coefficient $C \approx 2$ was determined from conditions of similarity of calculated and experimental data.

A similar conclusion on the necessity of increasing the variations of the advance/diameter ratio as compared with that determined by the hypotheses of quasistationary state in the operation of a propeller in an inclined flow was reached by V. B. Lipis.

Taking into consideration the above discussion, it seems to be expedient to introduce corrections also into formulae (78) - (81). Based on systematic calculations and comparing them with the available experimental data, it was found expedient to present formulae for calculating the hydrodynamic load on propeller blades in the following form:

$$P_1 = \rho n^2 D^4 \int_{\bar{r}_0}^{1} (1 - C\psi_\tau)^2 \cdot \left(\frac{d\bar{K}_1}{d\bar{r}}\right)_1 d\bar{r};$$

$$M_1 = \rho n^2 D^5 \int_{\bar{r}_0}^{1} (1 - C\psi_\tau)^2 \cdot \left(\frac{d\bar{K}_2}{d\bar{r}}\right)_1 d\bar{r} \qquad (82)$$

or

$$P_1 = \frac{\rho n^2 D^4}{Z} (1 - C\psi_{\tau R_*})^2 \bar{K}_1;$$

$$M_1 = \frac{\rho n^2 D^5}{Z} (1 - C\psi_{\tau R_*})^2 \bar{K}_2, \qquad (8 \quad /62$$

taking into account that

$$\lambda_{pa} = \lambda \frac{1 - \psi_{aR}}{1 - C\psi_{\tau R_*}} = \lambda \frac{\bar{V}_{aR_*}}{1 - C\frac{\dot{f}}{\pi \bar{R}_0} \bar{V}_{\tau R_*}},$$

where coefficient $C \approx 1.5$.

Formulae similar to (83) are further used for determining the variations of hydrodynamic load acting on the blade for calculating the cyclic strength of a propeller operating in a non-uniform velocity field.

It should be noted that for single-shaft transport and industrial ships, where the non-uniformity of the velocity field is created mainly by the axial component, the effect of flow inclination is not as clearly pronounced. Therefore, individual calculation results by formulae (80), (81), and (83) may differ slightly from each other.

A more significant effect of flow inclination is manifested in the creation of non-uniformity of the velocity field at ship propellers in the case of two-shaft or multi-shaft ships with a transom stern, and also at propellers of high-speed ships with extensive inclination of the line of shafting. In such cases, it is necessary to define more accurately the hydrodynamic forces determined on the basis of the quasistationary state hypothesis.

The component of hydrodynamic load caused by the inclination of incident flow also includes additional forces emerging at the propeller blades as a result of pitching and rolling on the high seas. It is expedient to calculate these hydrodynamic forces also by formulae (82) and (83).

Section 8. Strength Calculation of Propeller Blades In the Presence of Variable Loads

The formulae (78) - (83) obtained above are used for determining external forces in engineering strength calculations of propellers under the action of variable loads. These formulae can be used if the following data are available:

action curves of the propeller tested in free water;

parameters determining the main geometrical elements of the propeller (diameter, number of blades, characteristics of their cross sections) and the regime and conditions of propeller operation (rpm, ship speed, etc.);

information on the distribution of the nominal wake behind the ship hull in the propeller disk; if such information for the ship being considered is not available, the approximate characteristics of non-uniformity of the ship's velocity field, discussed in Section 6, may be used. /63

The initial data listed above make it possible to calculate the instantaneous values of the thrust and torque of the propeller blade for a number of its angular positions during one full revolution. In particular, the extreme values of thrust and torsional moment of the blade ($P_{1\,max}$ and $P_{1\,min}$, $M_{1\,max}$ and $M_{1\,min}$) as well as the amplitude variations of the thrust and torsional moment of the blade during one revolution are determined:

$$\left.\begin{aligned} P_a &= \frac{1}{2}(P_{1\,max} - P_{1\,min}); \\ M_a &= \frac{1}{2}(M_{1\,max} - M_{1\,min}) \end{aligned}\right\}$$

or in dimensionless form:

$$\left.\begin{aligned} \Delta K_1 &= \frac{1}{2}(K_{1\,max} - K_{1\,min}); \\ \Delta K_2 &= \frac{1}{2}(K_{2\,max} - K_{2\,min}). \end{aligned}\right\} \qquad (84)$$

Calculations and experimental determination of the vibration frequencies of propeller blades in water show that the ratio between natural vibrations of blades and those forced by hydrodynamic forces during the operation of a propeller in a non-uniform flow behind a ship hull is such that the critical frequencies are much higher than the frequencies induced by forces corresponding to operational regimes. Therefore, if hydrodynamic loads acting on the blades of a propeller operating behind a ship hull are of periodical character, then the stresses and deformations will change with the same periodicity (with a coefficient of dynamic character equal to one).

Taking into consideration the proportionality between external loads and the stresses created by them, as well as the character of the variation of external forces during one revolution of a propeller, the stresses in cross sections of a propeller may be presented as varying according to an assymmetric cycle consisting of a constant average stress within one cycle σ_m and a stress periodically varying with the amplitude σ_a. Since the study of fatigue is carried out with a sinusoidal form of the stress curve, and the result obtained are applicable without any corrections to other laws of their fluctuations, then analogically it is considered that the frequencies and amplitudes of cyclic stresses in propeller blades are stipulated by the amplitudes and period which are characterized by the parameters of wake, and fluctuation of the thrust and torsional moment, according to a harmonic law.

In order to obtain the dependence for evaluation of stresses under condition of assymmetric cycle, let us use experimental results of testing the cyclic toughness of structural materials (22). Data of these studies make it possible to formulate the following hypotheses: /64

the maximum amount of work absorbed by the material* without

---

*by the term material, a metallic alloy is understood.

---

failure because of hysteresis phenomenon is a constant value which does not depend on the assymmetry index of the cycle;

with stresses equal to the fatigue limit, the width of the hysteresis loop is proportional to the maximum stress of the cycle.

From the first hypothesis it follows that if for some material the area of hysteresis loop corresponding to the fatigue limit of symmetrical cycle S_w is equal to some quantity, then for the same material this area at some maximum stress in the assymmetric cycle will be equal to the same quantity. If we denote by S_s the area of the initial hysteresis loop for maximum stresses of an assymmetric cycle with an assymmetry index s, then based on the first hypothesis

$$S_w = S_s = \text{const.}$$

and because

$$S_w \quad A\sigma_{-1}\Delta_w \tag{85}$$

where Δ_w - the width of the hysteresis loop, then based on the second hypothesis, we obtain

$$\Delta_w = B\sigma_{-1}. \tag{86}$$

From formulae (85) and (86) it follows:

$$S_s = AB\sigma_{-1}. \tag{87}$$

where A and B are proportionality coefficients.

For an assymmetric cycle with components of maximum stress σ_m and σ_a, according to the first hypothesis $S_s = A\,\sigma_a\,\Delta_a$, where Δ_a - cyclic toughness of the material with an assymmetric cycle; according to the second hypothesis $\Delta_a = B\,(\sigma_m + \sigma_a)$, and therefore

$$S_s = AB(\sigma_m + \sigma_a)\sigma_a. \tag{88}$$

However, according to the first hypothesis, $S_w = S_s = \text{const}$, and comparing equations (87) and (88), we obtain:

$$\sigma_{-1}^2 = \sigma_a^2 + \sigma_a\sigma_m. \tag{89}$$

This is the desired expression connecting the fatigue limit in a symmetric cycle with components of maximum stress in an assymmetric cycle, when the average stress of the cycle is positive, i.e., tension. The right part of formula (89) can also be expressed through extreme stresses of the cycle taking into account that the average and the amplitude stresses are related according to the following dependences: /65

$$\sigma_m = \frac{\sigma_{max} + \sigma_{min}}{2}, \quad \sigma_a = \frac{\sigma_{max} - \sigma_{min}}{2}.$$

In this case, equation (89) will acquire the form of:

$$2\sigma_{-1}^2 = \sigma_{max}^2 - \sigma_{max}\sigma_{min}. \tag{90}$$

It should be noted that the obtained dependences (89) and (90) are only approximate but the resulting error is negligible and contributes to a safety factor increase, which is supported by numerous experimental data. The advantage of formulae (89) and (90) is in the fact that they provide the possibility of evaluating variable stresses at any number of cycles by a single property of the material, i.e., the fatigue limit with a symmetrical cycle.

When equations (89) and (90) are used for calculating of cyclic strength in the case of a simple asymmetric cycle, they can be presented in the following form:

$$\frac{\sigma_{-1}}{n_\sim} \geqslant \sqrt{\sigma_a^2 + \sigma_a \sigma_m}; \quad \frac{\sigma_{-1}}{n_\sim} \geqslant \sqrt{\frac{\sigma_{max}^2 - \sigma_{max}\sigma_{min}}{2}}; \tag{91}$$

$$\frac{\sigma_s}{n_T} \geqslant \sigma_{max} = \sigma_m + \sigma_a, \tag{92}$$

where $n_\sim$, n_T - safety factors;

σ_{-1} - fatigue limit of material;

σ_s - yield point of material.

Either of formulae (91) limits to a certain extent the amplitude and the average or extreme stresses of an asymmetric cycle if a specific part is designed for cyclic strength. Fulfillment of this requirement guarantees the absence of fatigue failures of the structure designed with various safety factors. Formula (92) determines the maximum stress of the cycle with a permissible safety factor, which if exceeded does not guarantee the absence of residual strains in the part. Consequently, formula (92) expresses the condition of static strength of the blade, while formulae (91) evaluate cyclic strength.

In some cases, it is more convenient to perform calculations by using equations that show the relationship between external load and the cross-sectional dimensions of the part being designed. To calculate bending stresses in propeller blades, the extreme values of thrust and torsional moment on the propeller blade may be considered to be known or the maximum and minimum bending moments in the cross section may be considered to be known in design calculations of a specific cross section. Thus,

$$\sigma_{max} = \frac{M_{max}}{W}, \quad \sigma_{min} = \frac{M_{min}}{W}.$$

Substituting expressions for extreme values of stresses into (91), we obtain a formula for calculating the section modulus: /66

$$W \geqslant \frac{n_\sim}{\sigma_{-1}} \sqrt{\frac{M_{max}^2 - M_{max}M_{min}}{2}}$$

or

$$W \geqslant \frac{n_\sim M_{max}}{\sigma_{-1}} \sqrt{\frac{S-1}{2S}}, \tag{93}$$

where

$$S = \frac{M_{max}}{M_{min}}.$$

From formulae (91) and (93), it follows that for the evaluation of the cyclic strength of propeller blades, it is necessary to know the magnitude of constant and symmetrically fluctuating component of a load in an asymmetric cycle or to know the maximum and minimum stresses for this cycle.

To determine those stresses, it is expedient to proceed from those principles on which generally accepted calculation methods of static strength are based.

It was determined by experimental methods of studying the state of stress using models of ship propellers that, independently of their geometrical characteristics, the most stressed areas of blades are those with greater thickness.

This makes it possible to assume that it is expedient to perform strength calculations only for thicker cross sections and to use as the initial method the one discussed in Section 4. In such a case, the load of the blade caused by constant components of the thrust and torsional moment is determined by formulae (38), (45) or (40), (41), (47), (48), while the variable components are found by subsequent calculation of the amplitude values of fluctuating thrust and torsional moment using formula (84), as was discussed in Section 7. /67

The average value of the periodically changing component of an assymmetrical cycle of stresses is calculated by the following general formulae:

$$\sigma = \frac{(M_P + M_c)\cos\nu + M_T \sin\nu}{W}.$$

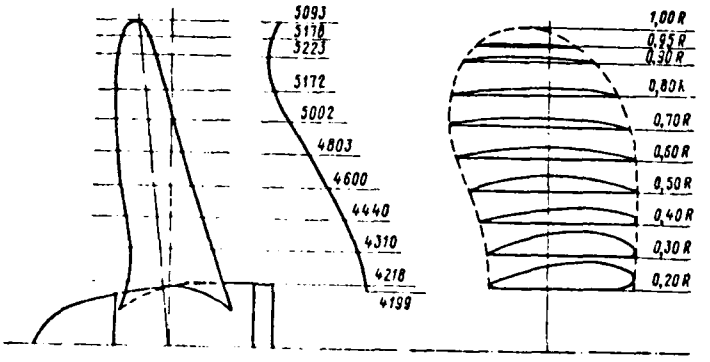

Fig. 30. Calculation of cyclic strength of propeller blades

The only difference is that in calculating average stresses, the bending moments M_D and M_T calculated for the average values of thrust and torsional moment of the blade are substituted into this formula. In calculating the maximum and minimum stresses (σ_{max}, σ_{min}) of an assymmetric cycle, the values of bending moments obtained for the operation of a propeller under conditions of a non-uniform velocity field are substituted into this formula.

To illustrate the practical application of the method discussed for determining the cyclic strength of propeller blades, let us perform this calculation for a single-shaft tanker with a closed-type stern, tonnage of 42,000t, power of the main engine 10,200 HP, and cruising speed of 15.5 knots at 102 rpm of the propeller.

Figure 30 illustrates additional information concerning the shape of the propeller blade.

Calculation of the cyclic strength of propeller blades comprises calculation of amplitude values of the thrust and torsional moment at the propeller blade in operation in a non-uniform velocity field behind the ship hull and calculation of the static and cyclic strength of the propeller blade.

Calculation of coefficients of thrust and torsional moment for conditions of operation in a non-uniform velocity field is presented in Table 9. Characteristics of non-uniformity of the velocity field (coefficients of nominal axial ψ_a and tangential ψ_τ wake at the equivalent radius equal 0.67R) obtained as a result of model tests of a tanker in an experimental basin are illustrated in Fig. 31, a, b.

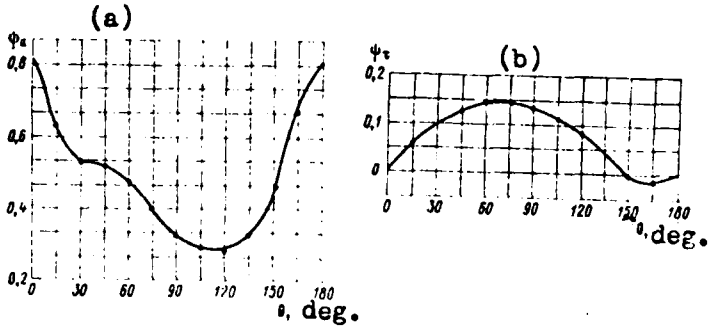

Fig. 31. Coefficients of wake

Table 9. Calculation of Coefficients of Thrust and Torsional Moment Created by a Propeller Blade Under Conditions of Operation In a Non-Uniform Velocity Field Behind the Ship Hull

Calculation formulae	θ degrees												
	0	30	60	90	120	150	180	210	240	270	300	330	360
$\bar{V}_{aR_0} = 1 - \bar{w}_{aR_0}$	0.19	0.45	0.52	0.67	0.72	0.55	0.19	0.55	0.72	0.67	0.52	0.45	0.19
$\bar{V}_{\tau R_0} = \bar{w}_{\tau R_0}$	0	−0.095	−0.145	−0.130	−0.075	0.005	0	−0.005	0.075	0.130	0.145	0.095	0
$1 - 1.5 \frac{\lambda}{\pi \bar{R}_0} \bar{V}_{\tau R_0}$	1	1.049	1.075	1.067	1.039	1.003	1	0.997	0.961	0.933	0.925	0.951	1
$\lambda_{p\theta} = \lambda \frac{\bar{V}_{aR_0}}{1 - 1.5 \frac{\lambda}{\pi R_0} \bar{V}_{\tau R_0}}$	0.137	0.310	0.349	0.453	0.501	0.396	0.137	0.398	0.541	0.519	0.406	0.342	0.137
$\bar{K}_1 = f(\lambda_{p\theta})$ при $\lambda_p = \lambda_{p\theta}$	0.263	0.226	0.213	0.176	0.158	0.196	0.263	0.196	0.141	0.150	0.193	0.215	0.263
$\bar{K}_2 = f(\lambda_{p\theta})$ при $\lambda_p = \lambda_{p\theta}$	0.0320	0.0272	0.0261	0.0230	0.0214	0.0247	0.0320	0.0247	0.0200	0.0207	0.0244	0.0264	0.0320
$\left(1 - 1.5 \frac{\lambda}{\pi \bar{R}_0} V_\tau\right)^2$	1	1.100	1.155	1.140	1.080	1.006	1	0.993	0.923	0.871	0.955	0.903	1
$K_1 = \frac{1}{Z}\left(1 - 1.5 \frac{\lambda}{\pi \bar{R}_0} \bar{V}_\tau\right)^2 \bar{K}_1$	0.0658	0.0620	0.0615	0.0503	0.0428	0.0493	0.0658	0.0488	0.0325	0.0328	0.0413	0.0485	0.0658
$K_2 = \frac{1}{Z}\left(1 - 1.5 \frac{\lambda}{\pi \bar{R}_0} V_\tau\right)^2 \bar{K}_2$	0.00800	0.00748	0.00754	0.00655	0.00578	0.00622	0.00800	0.00613	0.00402	0.00451	0.00522	0.00596	0.00800

Note: $\Delta K_1 = \frac{1}{2}\left(K_{1\max} - K_{1\min}\right) = 0.0166$; $\Delta K_2 = \frac{1}{2}\left(K_{2\max} - K_{2\min}\right) = 0.00175$.

Also necessary for the calculations are the curves of propeller action in free water. /68

Initial Data for Calculating the Coefficients of Thrust and Torsional Moment for Operation of a Propeller in a Non-Uniform Velocity Field:

Ship speed

V_s, knots 15.5

V, m/sec 7.98

Rotational speed

n_m, rpm 102

n, rp sec 1.7

Propeller diameter D, m 6.5

Number of blades in propeller, Z 4

Equivalent radius, $\bar{R}_0$ 0.67

Advance/diameter ratio (determined by speed of the ship)

$\lambda = \frac{V}{nD}$ 0.722

Figure 32 illustrates a comparison between results of calculations performed according to the discussed method (after recalculating on stresses actually present in the blade) and stresses measured in the blade of a real propeller operating in a non-uniform velocity field behind the hull of a tanker. By comparing curves 1 and 2, it follows that the character of variation of stresses in the propeller blade determined by both experiments and calculations is the same and that their amplitude values are also in satisfactory agreement. /69

The amplitude values of thrust and torsional moment fluctuations on the propeller blade are necessary (in the form of dimensionless coefficients) as initial data for performing the following stage of calculation, i.e., calculation of the static and cyclic strength of blades. To perform these calculations, the following data are needed:

Propeller diameter, m . . . . . D

Number of blades . . . . . Z

Rotational speed, rpm . . . . . n

Constant component of coefficient of thrust . . . K_1 /70

Constant component of coefficient of moment . . . K_2

Amplitude of fluctuation of coefficient of thrust (from Table 9) . . . . . $\Delta K_1 = \frac{1}{2}(K_{1\max} - K_{1\min})$

Amplitude of fluctuation of coefficient of moment (from Table 9) . . . . . $\Delta K_2 = \frac{1}{2}(K_{2\max} - K_{2\min})$

Relative radius of propeller hub . . . . . $\bar{r}_o$

Propeller material:

tensile strength, kg/cm^2 . . . . . σ_b

yield point, kg/cm^2 . . . . . σ_s

fatigue limit in corrosive medium . . . . . σ_{-1K}

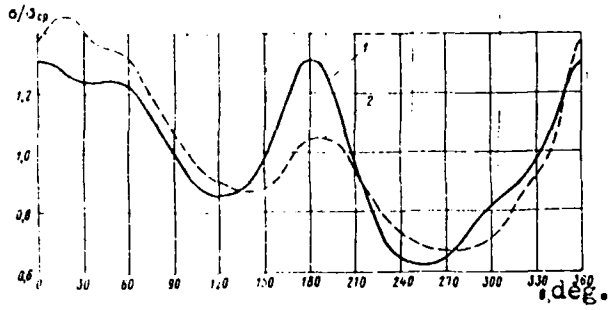

Fig. 32. Graph of changes of stresses in the root section of a propeller blade of full size during one revolution of the propeller: 1. by calculation; 2. experimental data.

Calculation is carried out in the following sequence:

Geometrical Characteristics of the Cross Section Being Checked:

Relative radius . . . . . r_p

Width . . . . . b

Maximum thickness, m . . . . . e_m

Pitch ratio . . . . . H/D

Pitch angle, degrees . . . . . $\nu = \arctan \frac{H/D}{r_p}$

Section modulus in respect to the main central axis for point C, m^3 . . . . . $W_\xi(C)$, Table 2 or (59)

/71

Determining Stresses Resulting From Acting Forces

Coefficient of bending moment caused by action of axial forces . . . . . $G_P(\bar{r}_0, \bar{r}_p)$ (Fig.14)

Coefficient of bending moment caused by action of tangential forces . . . . . $G_T(\bar{r}_0, \bar{r}_p)$ (Fig.14)

Constant component of bending moment caused by axial forces, kg-m . . . . . $M_P = \frac{K_1 \rho n^2 D^5}{2Z} G_P$

Constant component of bending moment caused by tangential forces, kg-m . . $M_T = \frac{K_2 \rho n^2 D^5}{Z} G_T$

Bending moment caused by centrifugal force, kg-m . . . . . M_c [(22) or (23)]

Bending moment caused by variable component of axial forces, kg-m . . . $\Delta M_P = \frac{\Delta K_1 \rho n^2 D^5}{2} G_P$

Bending moment caused by variable component of tangential forces, kg-m . $\Delta M_T = \Delta K_2 \rho n^2 D^5 G_T$

Compression stress at point C caused by constant component of acting forces, kg/cm^2 . . . . . $\sigma_m = \frac{(M_P + M_c)\cos\nu + M_T \sin\nu}{W_\xi(C)} \cdot 10^{-4}$

Amplitude of variable stress at point C, kg/cm^2 . . . . . $\sigma_a = \frac{\Delta M_P \cos\nu + \Delta M_T \sin\nu}{W_\xi(C)} \cdot 10^{-4}$

Determining the Safety Factor

Safety factor of static strength in respect to tensile strength . . . . . $n_b = \frac{\sigma_b}{\sigma_m}$

Safety factor of static strength in respect to yield point (taking into account the action of variable forces) $n_s = \frac{\sigma_s}{\sigma_m + \sigma_a}$

Safety factor of cyclic strength . . . . $n_\sigma = \frac{\sigma_{-1,k}}{\sqrt{\sigma_m \sigma_a + \sigma_a^2}}$

Safety factors of static and cyclic strength of material are selected in accordance with recommendations discussed in the following paragraph.

Section 9. Determining the Safety Factor of Static and Cyclic Strength /72

In evaluating both the static and cyclic strength of propeller blades, it is necessary to establish permissible stresses or safety factors.

Rational selection of permissible stresses determines the creation of optimal, from an engineering point of view, design of a propeller with high hydrodynamic properties, possessing sufficient mechanical strength, and requiring minimum expenditures of material. Determining factors for substantiated selection of permissible stresses are reliable data on the mechanical properties of the propeller material and the magnitude of stresses emerging in the propeller blades under operational conditions.

In a general formulation of the problem, it is difficult to establish permissible stresses in design calculation of propeller blades. The complexity of solving this problem is connected with a wide variety of external forces acting on the blade and with the complex geometrical form of the blades. Changes in the mechanical properties of materials depending on manufacturing technology of propellers, propeller size (scale factor), presence of stress concentrators, effect of surrounding medium, etc., must be taken into account. With the present state of the art of analytical determination of stresses in propeller blades, the solution of a problem of this type is practically impossible.

Discussed below is an approximate method of establishing the safety factor which is based on a differentiated approach for selection of permissible stresses. The principles of this method were developed by Corresponding Member of the Academy of Sciences of the USSR I. A. Oding. The idea and main aspects of this method as applicable to general machine building are discussed in (22). The essence of the differential method consists in the fact that in determining permissible stresses, the general safety factor of the structure being designed is found as a product of partial coefficients which take into account the factors of technological and operational character which affect the strength of the structure. The general safety factor obtained in this way, ties design stresses σ_p with stresses σ_i, which characterize either the strength of the material or its deformability. Analytically this may be expressed by the formula: /73

$$\sigma_i = \sigma_p n. \qquad (94)$$

The differential method of determining the safety factor cannot be called a simple method since quite often difficulties may be encountered in establishing some of the partial coefficients. In such a case, the designer has to solve an additional and quite complex problem. However, the negative features of this method are fully compensated by the fact that the designer obtains a full idea about the elements which comprise the safety factor he is establishing. Among the initial data for calculating permissible stresses, of special importance are the so-called factor coefficients which influence the general safety factor.

It should be noted that the vast majority of these partial coefficients are not directly safety coefficients. They determine only the relative value of stresses which were not taken into account in strength calculations or of a decrease in strength of the part under consideration which was not taken into account by testing specimens of the same material.

There are many reasons for the strength decrease of propeller material as compared with the strength characteristics of a smooth specimen. These reasons are various in their character. The presence and importance of causes of strength decrease may be predetermined by the designer and taken into consideration by using factor coefficients in the calculations.

Following the above method (22), let us present the general safety factor of static n_s and cyclic $n_\sim$ strength as a product of partial coefficients:

$$n_s(n_\sim) = S_1 S_2 K_1 K_2 M T_1 T_2. \qquad (95)$$

Actually, the safety factor is provided by coefficients $S=S_1S_2$, where S_1 reflects the reliability of the propeller material and S_2 reflects the reliability of the ship propeller as a propulsive device as well as the conditions of its performance. Coefficients S_1 and S_2 are selected on the basis of experimental data, after which they are considered to be kind of legitimate. In selecting the value of partial coefficient S_1, one should distinguish between forged and cast metals. The strength of test specimens cut out of a cast, forged, or rolled blank of the part cannot fully and accurately characterize the strength of the manufactured part as a whole. There is even less reason to judge the strength of the entire part by the strength of a cast strip for specimens. A part, particularly one of complex geometry, does not possess the same strength in different areas. This is explained by the heterogeneity of material structure, segregation, beginning of rupture caused by non-uniform shrinking, formation of blowholes, pores, etc. These flaws are more pronounced in cast metals as compared with rolled or forged metals. /74

For example, (22) recommends assuming $S_1 = 1.1$ for forged metals and $S_1 = 1.3$ for cast metals, explaining this by the presence of more defects in cast metals, which lowers their strength by 30%.

According to the same recommendations, the value of coefficient S_2 may be assumed to be within the range $1.15 \leq S_2 \leq 1.30$. It should be kept in mind that in most cases the breakdown of propellers, such as breaking off of a propeller blade, will not result in a full stoppage of the ship, since the ship in such a case does not loose steerability and usually can reach the nearest port independently at a lower speed. However, ultimately it leads to an increase of expense and therefore, taking into consideration recommendations of (22), it is expedient to assume that the value of coefficient S_2 is equal to its upper limit, i.e., $S_2 = 1.30$.

The effect of design and calculation factors is characterized by the coefficient:

$$K = K_1K_2 \qquad (96)$$

where K_1 takes into account errors in calculating stresses and a possible increase of stresses in the blade due to pitching and rolling, because the propeller might be only partially submerged in rough sea, or with the presence of trim difference. In addition, coefficient K_1 is distinguished for constant and variable components of hydrodynamic load and stresses caused by this load.

Analyses of stress measurements in blades of actual propellers demonstrate that constant components of actual maximum stresses may differ from those calculated by about 20% (using the method discussed in Section 4). Therefore, the minimum value of coefficient K_1 for the constant component of hydrodynamic load and the respective part of stresses in the cross section of the blade being considered may be assumed to be equal to 1.2.

The average errors in calculating the variable component may exceed those in calculating the constant component of hydrodynamic load. In addition, pitching and rolling of the ship in rough seas and incomplete submersion of propeller blades lead to an increase in amplitude values of the fluctuating hydrodynamic load. Therefore, it seems advisable to assume as a minimum value of coefficient K_1 for the variable component of the load and respective stresses, $K_1 = 1.3$.

Coefficient K_2 in formula (96) takes into account special features of design character which influence the possibility of stress concentrations in propeller blades. In determining numerical values of coefficient K_2, the current tendency of making considerably more strict the requirements which should be met in the design and manufacturing technology of ship propellers, especially in respect to their surface finish and the prevention of erosion damage of blades because of cavitation, is taken into consideration. The analysis of the above factors as applied to propellers of seagoing transport ships makes it possible to assume coefficient $K_2 = 1$. /75

The effect of the overall dimensions of parts or structures on their strength is taken into account by coefficient M, called the coefficient of scale effect. This coefficient can be determined fully and with required precision only by judging the results of experiments. It should be kept in mind that the coefficient of scale effect is of ambiguous character, i.e., its values for static and cyclically fluctuating forces are considerably different. For example, according to experiments on a number of steel brands and copper alloys, the decrease of static strength with increases in part size does not exceed 10 - 15%. Therefore, when a structure is subjected to static loads only, the coefficient M may be assumed to be within the range of 1.1 - 1.15.

Completely different results were obtained in determining the cyclic strength of test specimens of various dimensions. In all studies concerning the effect of the scale factor of test specimens on their cyclic strength, a univalent conclusion was reached, namely that with increases in the overall dimensions of a specimen the characteristic of cyclic strength, i.e., fatigue limit, decreases.

The reason for this phenomenon has not yet been determined accurately. However, this phenomenon cannot be disregarded. In Figure 33, a, curves of the decrease in fatigue limit are presented which show the dependence of the fatigue limit on the diameter of test specimens. Curve 1 was obtained by Ler in testing a round specimen in cyclic bending. Curve 2 was suggested by Faulhaber and is based on his experiments in bending round steel specimens. Curve 3 was obtained by Meilender and represents the dependence of the fatigue limit on the diameter of a specimen in torsion. Finally, Curve 4 was plotted according to results of cyclic bending tests and was suggested by Uzhik.

Figure 33, b, illustrates curves that show the effect of the overall dimensions of specimens on their strength. These curves were obtained by S. V. Serensen and represent in the best way the modern test data.

According to tradition, until now the strength of ship propeller blades was calculated only for the action of averaged hydrodynamic loads. Therefore, in publications concerning studies of the physical and mechanical properties of propeller materials, the effect of the overall dimensions of specimens on the fatigue properties of materials was not reflected at all. However, individual studies of the cyclic strength of copper alloy specimens with cross sections which, in area, differ by one order from standard size specimens demonstrate that in this case also a decrease in fatigue strength takes place, /76
the same way as was observed in the case of steel specimens. Thus, coefficient M, taking into account the scale effect in evaluating the cyclic strength of the material of propellers of various diameters (and therefore of various blade thicknesses) may be assumed to be within the range of 1.0 - 1.5.

The effect of technological factors on the state of stress of the workpiece is determined by coefficient $T = T_1 T_2$, where T_1 takes into consideration the surface finish and T_2 takes into account the presence of residual stresses.

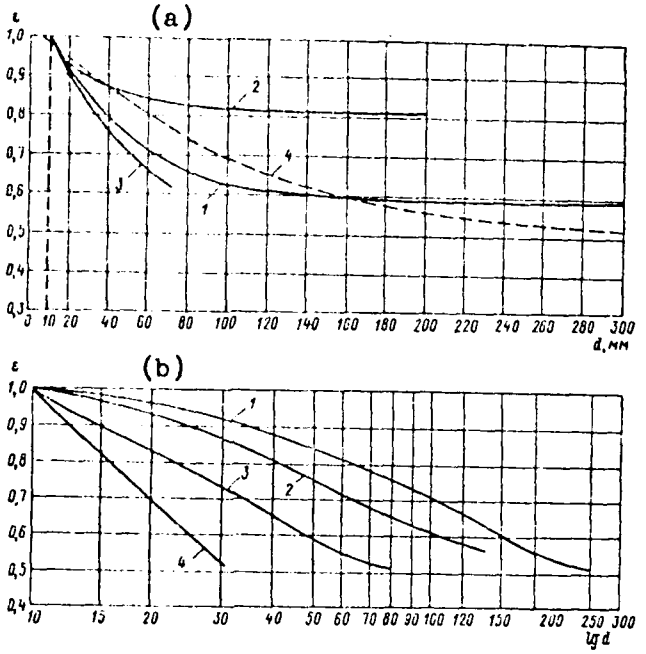

Fig. 33. Diagrams illustrating the decrease of fatigue limit in bending depending on the specimen diameter and the presence of stress concentrators: a. curves of fatigue limit decrease depending on the specimen diameter; b. curves of the effect of overall dimensions of specimens on their fatigue limit. 1. carbon steel without stress concentrators; 2. alloy steel without stress concentrators; 3. carbon steel with an average stress concentration; 4. alloy steel with high stress concentration.

The effect of surface damages and the quality of surface machining on the general strength of a structure subjected to alternating load is quite considerable. It was proven with sufficient reliability that this effect is more pronounced for materials with higher strength. /77
Table 10 shows the variation of relative values (in percent) of the fatigue limit of various steels in bending depending on the surface finish of specimens. In accordance with (22), the value of coefficient T_1 may be approximately determined using the equation $T_1 = 1 + \alpha(\sigma_{-1})$, where (σ_{-1}) - absolute value of the material's fatigue limit in symmetrical reversed bending; α - coefficient depending on the surface finish of the workpiece (for polished surface $\alpha = 0$; for ground surface - 0.004; for surfaces with negligible traces of cutting tool - 0.006; for roughly machined surface - 0.01; for corroded surface - 0.02).

Since for propellers made of LMtsZh55-3-1 the value σ_{-1}=9 kg/mm^2, coefficient α may be assumed to be 0.005. Therefore we obtain

$$T = 1 + 0.005 \cdot 9 \approx 1.05$$

Coefficient T_2 also should be used in calculations of both the static and cyclic character of acting forces. In contrast to other coefficients, coefficient T_2 may be above and below one. This depends on the sign of residual deformations in the cross section where acting stresses are determined. If the stress signs coincide the value of T_2 will exceed one, while in case of opposite signs coefficient T_2 may be less than one.

Under actual conditions, residual stresses may be eliminated by stress relief heat treatment. Technical specifications and instructions make performance of this operation compulsory. However, as a rule, it is impossible to fully eliminate residual stresses even with slow cooling after soaking.

Table 10. Dependence of the Fatigue Limit (%) of Steels in Reversed Bending on the Surface Finish of Test Specimens

Surface finish	Tensile strength, σ_b, kg/mm^2		
	47	95	142
Fine polishing	100	100	100
Rough polishing or superfinish	95	93	90
Fine grinding or fine machining with cutting tool	93	90	88
Rough grinding or rough machining	90	80	70
Rolled with presence of scale	70	50	35
In presence of corrosion in fresh water	60	35	20
In presence of corrosion in salt water	40	23	13

It was determined experimentally that in steel shafts, which are of a simple geometrical form, residual stresses after normalizing may reach 15 - 20% of the yield point (22). It may be assumed that these stresses will be even higher in a ship propeller of complex geometrical form. Individual measurements of these stresses on completely machined propeller blades confirm this assumption, showing that in some cases the magnitude of residual stresses reaches 30 - 40% of the yield point. This makes it possible to conclude that with the present state of the art of the manufacturing technology of propellers and in the absence of reliable and sufficiently complete information on the level of residual stresses in propellers of various diameters, the minimum value of coefficient T_2 should be assumed to be 1.3. /78

The above considerations make it possible to establish approximate values of partial coefficients which determine the general safety factor.

Substituting assumed values of partial coefficients into expression (95), we obtain a coefficient of static strength:

$$n_s = S_1 S_2 K_1 K_2 M T_1 T_2 = 1{,}3 \cdot 1{,}3 \cdot 1{,}2 \cdot 1 \cdot 1{,}15 \cdot 1 \cdot 1{,}3 = 3{,}04;$$

coefficient of cyclic strength

$$n = S_1 S_2 K_1 K_2 M T_1 T_2 = 1{,}3 \cdot 1{,}3 \cdot 1{,}3 \cdot 1 \cdot 1{,}2 \cdot 1{,}05 \cdot 1{,}3 = 3{,}60.$$

The values of general safety factors obtained should be considered to be the lowest values. The most reliable data concerning the value of the necessary safety factor may be obtained either by testing models of propellers under conditions approaching those of actual service or by systematic measuring of stresses in full size propellers under various service conditions. This does not mean that strength calculations without taking into account the form of the workpiece, loading regimes, dynamic strength properties and consequent strength safety factors established by verifying calculations of propellers designed and being used. Such a conditional calculation does not make it possible to evaluate the effect on strength of the most important factors which are always present under service conditions. As a result, such a calculation does not make it possible to correctly select means for increasing the strength of a workpiece being designed.

It is expedient to establish the relation between the calculated static strength safety factor in respect to the yield point and the safety factor usually used in respect to the tensile strength of material.

For example, for LMtsZh55-3-1 brass the tensile strength σ_b = 48 kg/mm^2 while its yield point is σ_s = 19 kg/mm^2. Taking into consideration that the safety factor in respect to the yield point n_s = 3.04, let us determine the magnitude of permissible stresses /79

$$\sigma_{доп} = \frac{\sigma_{s\,0.2}}{n_s} = \frac{19}{3{,}04} = 6{,}25 \quad \text{kg/mm}^2$$

From here, the static strength safety factor in respect to tensile strength:

$$n_b = \frac{\sigma_b}{\sigma_{доп}} = \frac{48}{6{,}25} = 7{,}7.$$

Thus, the value of safety factor n_b = 7.7 in respect to tensile strength corresponds to the value of safety factor n_s = 3.14 in respect to the yield point. The former is almost the same as the minimal value of the safety factor for brass and bronze propellers, which is accepted in all methods of strength calculations that meet the requirements of the Register of the USSR.

Section 10. Consideration of the Effect of Service Conditions in Determining External Forces Acting on Propeller Blades

In the process of exploitation, a ship is subjected to the action of wind and seaways. During cruising in rough seas, additional hydrodynamic forces emerge on the propeller blades due to the changing velocity field caused by the sea, ship pitching and rolling, and the disturbing action of the vibration of the ship hull.

In strict formulation, the problem of determining the hydrodynamic forces acting on the propeller of a ship moving in rough seas is extremely complex. In practice, it is more rational to solve the problem by taking into consideration factors which play a determinant role in the phenomenon being considered. In particular, it is possible to assume that during motion of a ship on the high seas, transverse velocities in the disk of the propeller due to pitching and rolling have a decisive effect on the appearance of additional hydrodynamic forces on the propeller. The sea itself and the effect of the stern part of the hull are assumed to be of little importance.

The effect of pitching and rolling of the ship on the hydrodynamics of the propellers is manifested first of all in the change of its operational regime in respect to average load and, as a result, in the higher resistance of the submerged part of the ship hull to rough seas, and also in the appearance of additional hydrodynamic forces during transverse displacement of the propeller in water.

Problems related to studies of the hydrodynamic characteristics of a propeller during rolling and pitching were discussed by I. Ya. Miniovich (2) and V. B. Lipis (19). I. Ya. Miniovich suggested formulae for the approximate calculation of hydrodynamic load components on a propeller during rolling and pitching which are based on the hypothesis of quasistationary state. In the work of /80
V. B. Lipis, the hydrodynamic characteristics of a propeller during rolling and pitching were determined taking into consideration the effect of the non-stationary state of the flow. V. B. Lipis also studied the hydrodynamic characteristics of a propeller during rolling and pitching taking into account the possible suction of air and incomplete submersion of the propeller.

Based on the physical concept of hydrodynamic action of propeller during rolling and pitching discussed in (20), it should be noted that rolling and pitching cause additional displacements of the propeller and as a result, the appearance of transverse velocities of water flow on the propeller.

These velocities may be considered to be directed perpendicularly to the axis of propeller rotation. Thus, during pitching and rolling a propeller operates under conditions of inclined flow with a varying angle of inclination.

The additional hydrodynamic load on propeller blades stipulated by operation of a propeller in a flow inclined in the vertical plane may be found using formulae obtained earlier (83). It is assumed that:

$$V_{aR} = V_p; \quad V_{tR_0} = -\bar{V}_B \sin\theta,$$

where θ - angular coordinate of the propeller blade;

$V_B = \frac{V_B}{V}$ - relative velocity of incident flow in the vertical plane.

Taking into account that the dependence of the coefficient of propeller thrust on the advance/diameter ratio within a relatively wide range of its changes approaches linear, we obtain:

$$\left.\begin{aligned} \Delta\bar{M}_p &= \left(1 - \frac{r_p}{R_0}\right)\frac{C}{2\pi z}(2K_1 + \lambda_p \operatorname{tg}\alpha_1)\cdot\lambda_v \sin\theta; \\ \lambda_v &= \frac{\pi L \psi_0}{\tau_k n D}\cos\frac{2\pi}{\tau_k}t, \end{aligned}\right\} \qquad (97)$$

where $\Delta\bar{M}_p = \frac{\Delta M_p}{\rho n^2 D^5}$ - coefficient of additional bending moment on propeller blade caused by pitching of the ship;

K_1 - coefficient of propeller thrust at designed regime;

λ_p - advance/diameter ratio of propeller at designed regime;

α_1 - inclination of propeller action curves $K_1(\lambda_p)$ to the axis;

λ_p - with design value of advance/diameter ratio;

L - ship length along waterline;

ψ_0 - amplitude of pitching;

$\tau_k \approx 2{,}4\,T$ - period of pitching (T-submersion of the ship).

Other designations are the same as in formulae (83).

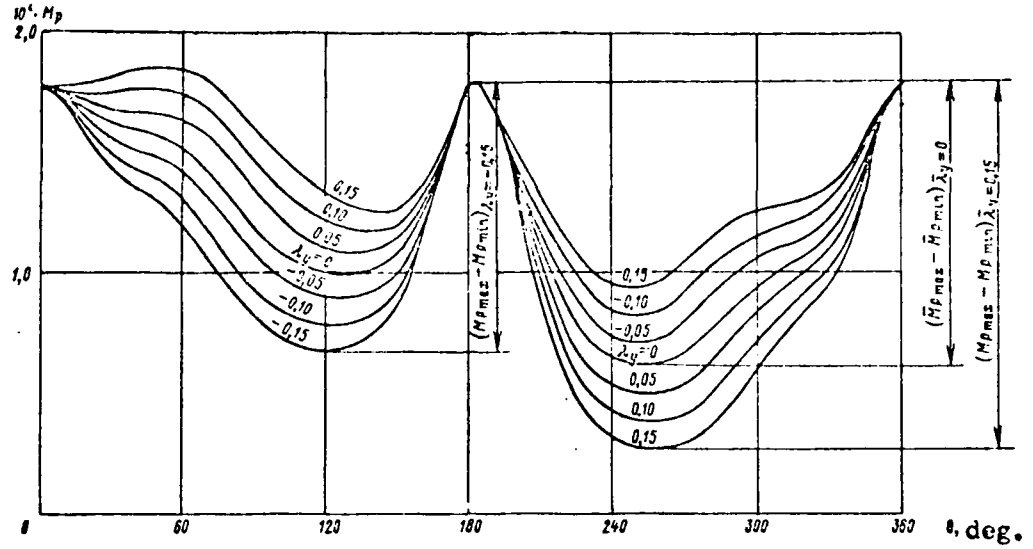

Fig. 34. Changing of bending moment depending on the angle of blade turn of a propeller operating at various values of parameter λ_y /81

The resultant hydrodynamic bending moment acting on the propeller blade of a ship moving in rough seas is found by summing up the moment determined for a calm sea and the additional moment caused by the action of ship rolling: /82

$$M_p(\theta) = M_{p_u}(\theta) + \Delta M_p(\theta).$$

Figure 34 shows the character of coefficient of moment $\bar{M}_p(\theta) = \frac{M_p(\theta)}{\rho n^2 D^5}$ variation, depending on the angle of propeller turn at various values of parameter λ_y, which can be considered as a relative vertical velocity.

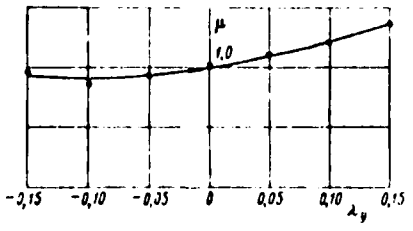

Fig. 35. Relative increase of variation of bending moment depending on λ_y

After coefficient of moment $\bar{M}_p(\theta)$ for a number of values of λ_y is found, it is possible to find the relative range of increase of bending moment change on the propeller blade, depending on λ_y (Fig. 35).

$$\mu = \frac{(\bar{M}_{P(0)_{max}} - \bar{M}_{P(0)_{min}})_{\lambda_y}}{(\bar{M}_{P(0)_{max}} - \bar{M}_{P(0)_{min}})_{\lambda_y=0}}$$

Function $\mu(\lambda_y)$ is approximated by a parabola of second power

$$\mu = a\lambda_y^2 + b\lambda_y + c;$$

in this case, the method of least squares is recommended for finding coefficients a, b, and c.

The value of relative vertical velocity λ_y is a linear function of the angle of pitching Ψ

$$\lambda_y = k\psi,$$

where

$$k = \frac{\pi L}{\tau_k n D}, \quad \psi = \psi_0 \cos\frac{2\pi}{\tau_k} t.$$

In accordance with the main aspects of the theory of pitching and rolling of ships on irregular seas (5), the normal law of distribution holds for angles of pitching:

$$f(\Psi) = \frac{1}{\sqrt{2\pi}\sigma_\psi} e^{-\frac{1}{2\sigma_\psi^2}\Psi},$$

where σ_ψ - mean square deviation, related to the average value of the angle of pitching according to equation $\sigma_\psi = 0.798\,\psi_0$.

Thus, μ will be a function of random variable Ψ, being at the same time a random variable of M /83

$$M = ak^2\Psi^2 + bk\Psi + c.$$

The numerical characteristics of function M are determined by the following general formulae of the theory of probability:

mathematical expectation $\hat{\mu} = \int_{-\infty}^{\infty} (ak^2\psi^2 + bk\psi + c) f(\Psi)\, d\psi,$

dispersion $D = \int_{-\infty}^{\infty} (ak^2\psi^2 + bk\psi + c - \hat{\mu})^2 f(\Psi)\, d\psi.$

after transformations of these equations we obtain

$$\hat{\mu} = ak^2\sigma_\psi^2 + c,$$

$$\sigma_\mu = k\sigma_\psi \sqrt{b^2 + 2a^2k^2\sigma_\psi^2}.$$

where $\sigma'_{\mu} = + \sqrt{D}$ - mean square deviation.

Since function $\mu(\lambda_y)$ in its meaning cannot be of smaller value than $\mu_{min} = c - \frac{b^2}{4a}$, its distribution, which is supposed to be normal, is truncated.

The numerical characteristics of the truncated normal distribution of function μ, which demonstrates the change of bending moment acting on a propeller blade during pitching and rolling of the ship, are found from relations:

$$\left.\begin{aligned} \hat{\mu} &= \hat{\mu}' + B\sigma'_{\mu}; \\ \sigma_{\mu} &= \sigma'_{\mu} \sqrt{1 - B^2 + At_1\varphi(t_1)}, \end{aligned}\right\} \qquad (98)$$

where μ' and σ'_{μ} - mathematical expectation and mean square deviation of initial non-truncated distribution, respectively.

Coefficients A and B are determined by equations:

$$A = \frac{1}{0{,}5 - \Phi_0(t_1)};$$

$$B = \frac{\varphi(t_1)}{0{,}5 - \Phi_0(t_1)}$$

under condition that

$$t_1 = -\frac{\hat{\mu}' - \mu_{min}}{\sigma'_{\mu}}.$$

The numerical values of functions $\Psi(t_1)$ and $\Phi_0(t_1)$ are tabulated and published in handbooks on probability calculations.

As an example, Figure 36 shows a graph of the dependence of /84
the relative (as compared with ship motion in calm water) increase of the average fluctuation range of the bending moment acting on the propeller blade of a high tonnage ship, on the average values of ship pitching amplitude.

The additional cyclic fluctuation of the hydrodynamic load acting on blades is observed also in the ballast transition of the ship. The submersion of a ship propeller, which is determined by the respective ship displacement, decreases to the extent that the blades are in the air. At the same time, the load on the blade which is not submerged drops to zero.

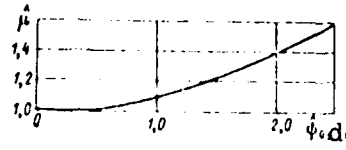

Fig. 36. Increase of the average values of the fluctuation range of the bending moment acting on the propeller blade of a high-tonnage ship as it depends on the average values of amplitude of ship pitching

The ballast transition of a ship in some cases represents a considerable part of the exploitation period of oil tankers and dry-cargo ships. However, incomplete submersion of propeller blades is most typical for the latter, since complete submersion of propeller blades for dry-cargo ships cannot be achieved due to the more limited fore-and-aft trimming system as compared with oil tankers.

A sufficiently accurate theoretical solution of the problem of determining the hydrodynamic forces acting on a propeller when it intersects the free surface is presented in (40). However, because of the extensive volume of computation, it is not acceptable for practical purposes. Therefore, an approximate solution which provides satisfactory results as compared to the results provided by the method discussed in (40) is discussed below. This method provides satisfactory results, particularly in determining extreme values of hydrodynamic load.

Let us proceed from the assumption that in the case of incomplete submersion of a propeller, the nominal velocity field will correspond to the case of complete propeller submersion, excluding the part of the propeller disk that projects out of the water, in which the hydrodynamic load equals zero.

Let us assume that distribution of thrust $\frac{dP}{dr}$ is changing along the radius according to linear law, while the distribution of tangential force $\frac{dT}{dr}$ along the radius is constant. Then, for a propeller of radius R which is submerged in respect to the water surface to depth R_1, we obtain:

for a completely submerged propeller ($R_1 > R$)

$$M_P = P(pR - r_p) \text{ и } M_T = \frac{M}{qR}(qR - r_p), \qquad (99)$$

where

$$p = \frac{2}{3}\cdot\frac{R^2 + Rr_p + r_p^2}{R(R + r_p)}; \quad q = \frac{R + r_p}{2R};$$

for a partially submerged blade ($R_1 < R$)

$$M_P' = P_1(p_1R_1 - r_p) \quad \text{and} \quad M_T' = \frac{M_1}{q_1R_1}(q_1R_1 - r_p), \tag{100}$$

where

$$P_1 = \frac{2}{3}\cdot\frac{R_1^2 + R_1r_p + r_p^2}{R_1(R_1 + r_p)}; \quad q_1 = \frac{R_1 + r_p}{2R_1}.$$

In formulae (99) and (100), the following designations are used:

M_P - bending moment caused by axial forces;

M_T - bending moment caused by tangential forces;

P - thrust of the propeller blade while $P_1 = \bar{h}^2P$, where $\bar{h} = \frac{R1}{R}$ $(R_1 < R)$;

M - torsional moment, $M_1 = \bar{h}^3M$;

r_p - distance from cross section being considered to the axis of propeller rotation.

From the above equations, we obtain:

$$\left.\begin{aligned} \mu_P &= \frac{M_P'}{M_P} = \bar{h}^2\frac{1 + \bar{r}_p}{\bar{h} + \bar{r}_p}\cdot\frac{2\bar{h}^2 - \bar{h}\bar{r}_p - \bar{r}_p^2}{2 - \bar{r}_p - \bar{r}_p^2}; \\ \mu_M &= \frac{M_T'}{M_T} = \bar{h}^3\frac{1 + \bar{r}_p}{1 - \bar{r}_p}\cdot\frac{\bar{h} - \bar{r}_p}{\bar{h} + \bar{r}_p}. \end{aligned}\right\} \tag{101}$$

Coefficients μ_P and μ_M determine the decrease of bending moments in the cross section being considered with relative propeller submersion to a depth of $\bar{h}$. Projecting of the propeller blade out of water and the decrease in hydrodynamic load begin at some angular position which depends on the value of $\bar{h}$. Only when $\theta = 0^\circ$ (360°) does the effect of incomplete submersion reach its extreme value. The dependence of coefficients μ_P and μ_M on the angular position of the blade θ at a given $\bar{h}$ is shown in Figure 37. A root cross section of the blade is being considered ($r_p = 0.20$).

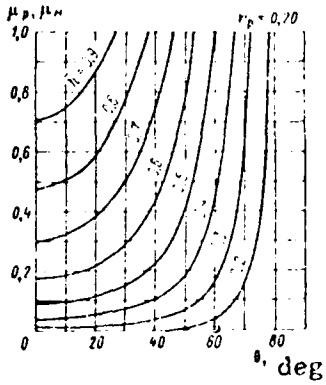

Fig. 37. Graph for determining coefficients μ_P and μ_M

This graph may be used for approximate evaluation of the effect of partial submersion of a propeller blade on the magnitude of the bending moment caused by the action of hydrodynamic forces in the critical cross section being considered. From Figure 37, it follows that partial submersion of a propeller blade affects considerably the variation of its dynamic load. For example, if 20% of the propeller blade is not submerged in water, the bending moment in the critical cross section decreases by more than 50%. /87

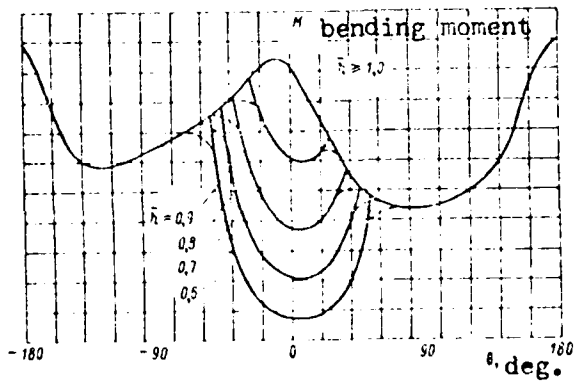

Fig. 38. Variation of hydrodynamic bending moment depending on angular position of propeller with various amount of submersion /86

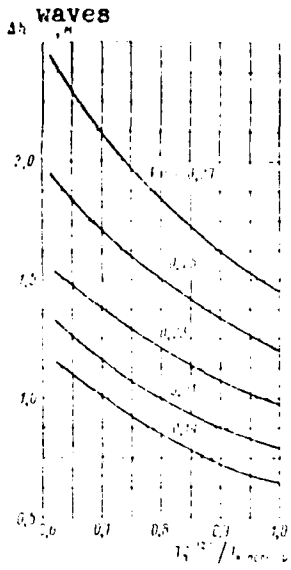

Fig. 39. Variation of submergence of a propeller during movement of a "Bezhitsa" type ship

As an example, Figure 38 shows the results of calculating the bending moment for full and partial submersion of a propeller blade. /87

Based on the results obtained by V. S. Shpakov, who studied the hydrodynamic load of a partially submerged propeller behind a ship hull, let us note that the actual submergence of the propeller axis $\bar{h}_{\varphi}$ at a given speed of the ship should be determined taking into account the wave ordinates in the area of the propeller disk, i.e.,

$$h_{\varphi} = h_{CT} + \Delta h_{waves}$$

where h_{φ} - actual submergence of the upper edge of the blade from the agitated water surface during ship motion;

h_{CT} - submergence of the upper edge of the blade from the water surface without motion of the ship;

h wave- wave ordinate in the area of the propeller disk measured from the still surface.

The simplest way to obtain wave ordinates in the area of the propeller disk for various hydrodynamic loads and corresponding speeds of the ship is by testing models in an experimental water basin or by using the data obtained for a sufficiently similar prototype of the ship in respect to main dimensions, stern lines, and the elements of the propulsion device.

For approximate evaluation of wave ordinates in the area of the propeller disk of a dry-cargo ship, a graph may be used which was plotted by V. S. Shpakov and is based on experimental data. The graph (Fig. 39) shows the dependence of wave ordinate h_{wave} on the submergence of the propeller and the relative speed (Froude number) of a "Bezhitsa" type ship.

Section 11. Determining External Forces During Impact of a Propeller Blade Against a Solid Object

Propellers of ice-breakers and ships navigating in contaminated waters are constantly subjected to impacts against blocks of ice or other floating objects.

According to the theory of impact, the problem of the impact of two bodies, includes the problem of their local deformations, but in respect to ship propellers this problem has not yet been properly solved. Therefore, researchers are analyzing this problem at the present time (7), (24).

N. N. Kabachinskiy and V. A. Belyayev performed an analysis of dynamic processes taking place in a propeller shaft-line system. However, in determining external forces during impact of a propeller blade against a solid object, they assumed that the blade is a thin, straight, homogeneous rod (4), (13) and the complex shape of a propeller blade was not taken into consideration.

The general dependence of impact forces on the geometrical characteristics of a propeller (diameter, pitch, blade contour, etc.) and on kinematic parameters (forward and rotational speed) was studied by S. V. Yakonovskiy (32), (33).

The impact of a ship propeller against a solid object is characterized by the impulse of impact forces (instantaneous impulse) acting on a propeller blade, the moment of this impulse, the angular velocity of propeller rotation after impact, and the kinetic energy lost as a result of impact.

To derive corresponding formulae, the following assumptions were made:

a propeller is a single body located at the end of an elastic shaft line;

the object colliding with the propeller is free and its mass is infinitely small as compared with the ship mass (after collision the forward motion of the ship V_o - const), the impact is absolutely inelastic;

changes of kinetic moment of rotating masses of the propeller do not cause changes of angular momentum of the whole ship.

At the same time, it is considered that the solid object is stationary and that the ship is moving only forward and its velocity vector is parallel to the propeller axis.

Figure 40 illustrates in the accepted coordinate system the instantaneous impulse during impact and the components of its moment.

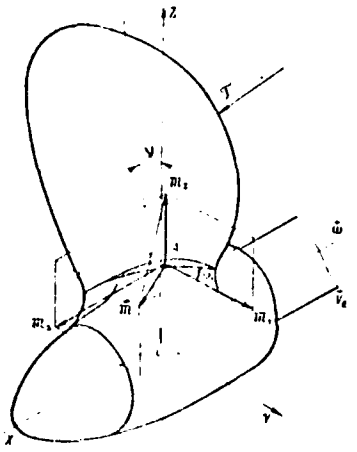

Fig. 40. Instantaneous impulse during collision and components of its moment

Below are given formulae of S. V. Yakonovskiy for the definition of characteristics of impact by the surface or edge of the blade as a function of geometrical and kinematic parameters of a propeller.

In these formulae the following designations are used:

n_1 and n_2 - frequency of propeller rotation per second before and after the impact, respectively;

$D = 2R$ - propeller diameter, m;

$\bar{r} = \frac{r}{R}$ - relative radius of impact point;

V_{ox} - ship speed, m/sec, (forward motion with the sign "-" and reverse with the sign "+");

$\lambda_1 = \frac{V_{ox}}{n_1 D}$ - advance/diameter ratio before the impact; /89

μ - adduced mass of the block of ice, kg·sec^2/m;

I_X - moment of inertia of the mass of propeller and the attached mass of water, kgcm·sec^2;

ω_1 - angular velocity of propeller rotation before impact, 1/sec, (forward motion with "-" sign and reverse with "+" sign);

r - radius of impact point, m;

α - polar angle between the straight line from the center of propeller rotation to the point of impact application at the blade edge and the axis CY in the plane of normal projection of the propeller, radian;

φ_A - pitch angle of the root cross section of the blade which is determined by the formula:

$$\operatorname{tg}\varphi_A = \frac{H}{2\pi r_A},$$

where

H - propeller pitch, m;

r_A - distance between root cross section and axis of rotation, m;

X_A, Y_A, Z_A - coordinates of point A in respect to which moments are calculated;

ν - angle of blade inclination, degrees.

At the moment of impact of blade surface:

instantaneous impulse

$$S = -\mu \frac{(n_1 H - V_{0x})\cos\nu \sqrt{1 + \left(\frac{1}{\pi r}\right)^2 \cos^2\nu \left(\frac{H}{D}\right)^2}}{1 + \frac{1}{\pi^2}\cos^2\nu \left(\frac{H}{D}\right)^2 \left(\frac{1}{r^2} + \frac{\mu R^2}{I_x}\right)}, \qquad (102)$$

rotational speed of the propeller after impact:

$$n_2 = n_1 \frac{1 + \frac{1}{\pi^2}\cos^2\nu \left(\frac{H}{D}\right)^2 \left(\frac{1}{r^2} + \frac{\lambda}{\frac{H}{D}} \cdot \frac{\mu R^2}{I_x}\right)}{1 + \frac{1}{\pi^2}\cos^2\nu \left(\frac{H}{D}\right)^2 \left(\frac{1}{r^2} + \frac{\mu R^2}{I_x}\right)}. \qquad (103)$$

Components of a moment of instantaneous impulse in a general case are functions of angular coordinate φ; considering that the impact takes place along the median line of the blade, it may be assumed that $\varphi = \frac{\pi}{2}$.

The angular coordinate of point A in the root cross section of the blade is also approaching the value of $\frac{\pi}{2}$.

In such a case, the following formulae are obtained: /90

for components of the moment of instantaneous impulse

$$\left.\begin{aligned}
\mathfrak{M}_{x_A} &= -\frac{1}{2}\mu\frac{(n_1H - V_{0x})\frac{H}{\pi}\cos^2\nu\left(1-\frac{\bar{r}_A}{\bar{r}}\right)}{1+\frac{1}{\pi^2}\cos^2\nu\left(\frac{H}{D}\right)^2\left(\frac{1}{\bar{r}^2}+\frac{\mu R^2}{I_x}\right)};\\
\mathfrak{M}_{y_A} &= \mu R\frac{(\bar{r}-\bar{r}_A)(n_1H-V_{0x})}{1+\frac{1}{\pi^2}\cos^2\nu\left(\frac{H}{D}\right)^2\left(\frac{1}{\bar{r}^2}+\frac{\mu R^2}{I_x}\right)};\\
\mathfrak{M}_{z_A} &= -\frac{1}{2}\mu\frac{(n_1H-V_{0x})\frac{H}{\pi}\cos^2\nu\operatorname{tg}\nu\left(1-\frac{\bar{r}_A}{\bar{r}}\right)}{1+\frac{1}{\pi^2}\cos^2\nu\left(\frac{H}{D}\right)^2\left(\frac{1}{\bar{r}^2}+\frac{\mu R^2}{I_x}\right)};
\end{aligned}\right\} \qquad (104)$$

for energy lost as a result of impact

$$\Delta = \frac{1}{2}\mu\frac{(n_1H-V_{0x})^2\cos^2\nu}{1+\frac{1}{\pi^2}\cos^2\nu\left(\frac{H}{D}\right)^2\left(\frac{1}{\bar{r}^2}+\frac{\mu R^2}{I_x}\right)}. \qquad (105)$$

Equations of S. V. Yakonovskiy for the impact of the blade edge based on the general theory of interaction of a propeller and ice are cumbersome and therefore may be used only with utilization of computers.

According to this theory the most disadvantageous position of an ice block (solid object) which stipulates the maximum value of instantaneous impulse and the component of its moment $\mathfrak{M}_x$ is a position parallel to the axis of a propeller, which corresponds to the actual conditions when a propeller operates at regimes approaching mooring regimes. Mooring regimes are typical for ships navigating in ice.

For such a specific case, more convenient formulae were obtained which are used in practical calculations.

The angular velocity of propeller rotation after an impact

$$\omega_2 = \frac{\omega_1}{1 + \frac{\mu R^2}{I_x} \frac{\bar{r}^2 \left(\frac{d\bar{r}}{d\alpha}\right)^2}{\bar{r}^2 + \left(\frac{d\bar{r}}{d\alpha}\right)^2}}; \tag{106}$$

The geometrical meaning of a derivative $d\bar{r}/d\alpha$ is explained by Figure 41, and its value may be determined by the formula

$$\frac{d\bar{r}}{d\alpha} = \frac{r(\alpha)}{d\alpha} = \frac{r(\alpha)\, dr(\alpha)}{r(\alpha)\, d\alpha} = r(\alpha) \operatorname{tg} \gamma,$$

where γ - angle between tangential lines to the contour of normal projection of the blade and to the circle of radius $r(\alpha)$ at the point of impact M.

The instantaneous impact against the edge /91

$$\zeta = -\mu \frac{\omega_1 R \frac{d\bar{r}}{d\alpha} \sqrt{1 + \frac{1}{\bar{r}^2}\left(\frac{d\bar{r}}{d\alpha}\right)^2}}{1 + \left(\frac{d\bar{r}}{d\alpha}\right)^2 \left[\frac{1}{\bar{r}^2} + \frac{\mu R^2}{I_x}\right]}. \tag{107}$$

Components of the moment of instantaneous impulse in respect to the point on the axis located at a distance $l(x_A = -l,\ y_A = 0;\ Z_A = 0)$ from the coordinates origin

$$\left.\begin{aligned}
\mathfrak{M}_x &= -\mu \frac{\omega_1 R^2 \left(\frac{d\bar{r}}{d\alpha}\right)^2}{1 + \left(\frac{d\bar{r}}{d\alpha}\right)^2 \left[\frac{1}{\bar{r}^2} + \frac{\mu R^2}{I_x}\right]}; \\
\mathfrak{M}_y &= -\mu \frac{\omega_1 R^2 \left(\frac{d\bar{r}}{d\alpha}\right)^2}{1 + \left(\frac{d\bar{r}}{d\alpha}\right)^2 \left[\frac{1}{\bar{r}^2} + \frac{\mu R^2}{I_x}\right]} \times \\
&\times \left\{\left[\left(\alpha - \frac{\pi}{2}\right)\frac{1}{\pi} \cdot \frac{H}{D} + \bar{r} \operatorname{tg} \nu\right] + \frac{l}{R}\right\}\left(\frac{1}{\bar{r}} \cdot \frac{d\bar{r}}{d\alpha} \cos\alpha + \sin\alpha\right); \\
\mathfrak{M}_z &= -\mu \frac{\omega_1 R^2 \left(\frac{d\bar{r}}{d\alpha}\right)^2}{1 + \left(\frac{d\bar{r}}{d\alpha}\right)^2 \left[\frac{1}{\bar{r}^2} + \frac{\mu R^2}{I_x}\right]} \times \\
&\times \left\{\left[\left(\alpha - \frac{\pi}{2}\right)\frac{1}{\pi} \cdot \frac{H}{D} + \bar{r} \operatorname{tg} \nu\right] + \frac{l}{R}\right\}\left(\frac{1}{\bar{r}} \cdot \frac{d\bar{r}}{d\alpha} \sin\alpha + \cos\alpha\right).
\end{aligned}\right\} \tag{108}$$

The energy lost as a result of impact

$$\lambda = \frac{1}{2}\mu \frac{\omega_{1x}^2 R\left(\frac{dr}{d\alpha}\right)^2}{1+\left(\frac{dr}{d\alpha}\right)^2\left|\frac{1}{r^2}+\mu\frac{R^2}{I_x}\right|}. \tag{109}$$

After determining components of the moment of instantaneous impulse $\mathfrak{M}_x$ and $\mathfrak{M}_y$ by formulae (104) and (108), for impact against the blade surface or the edge, with the help of Figure 40 it is not difficult to deduce a formula for calculation of the bending moment in respect to the axis of minimum rigidity of the root cross section of the blade

$$\mathfrak{M}_{\eta_A} = \mathfrak{M}_{x_A}\sin\varphi_A - \mathfrak{M}_{y_A}\cos\varphi_A. \tag{110}$$

Quantities characterizing the collision of a propeller with a solid body are functions of many parameters (reduced mass of a solid body, radius of the impact point, etc.). Under service conditions these quantities are random values which are determined by using statistical data of experimental full size tests and applying the theory of probability. However, there are insufficient data available yet and therefore, solving of such problems is limited at present to some specific solutions. For example, the tensile strength of detachable blades and of parts fastening blades to the hub as well as the strength of a shaft-line subjected to impact loads may be determined by comparing them with the existing prototype with the help of conditional impulse of stresses /92

$$\sigma_{\eta_A}\Delta t = \frac{\mathfrak{M}_{\eta_A}}{W_A}.$$

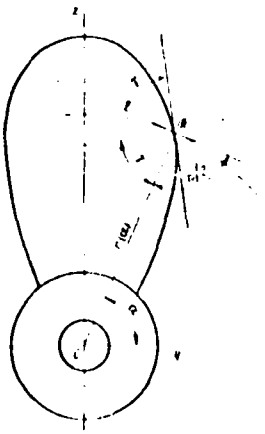

Fig. 41. Normal projection of blade contour and explanation of the geometrical meaning of the derivative dr/dα

It should be noted that formulae (104) and (108) are particularly important for understanding those loads to which studs fastening blades are subjected because of the action of each component of instantaneous impulse $\mathcal{W}_x$, $\mathcal{W}_y$ and $\mathcal{W}_z$. First of all, it concerns the continuously discussed problems on magnitudes of crumpling and shearing forces to which studs are subjected as a result of the vertical component of instantaneous impulse $\mathcal{W}_z$. In comparative calculations, μ is found by the formula $\frac{\mu R^2}{I_x} = 0.2 \div 1.0$, which is obtained as a result of data processing based on full size experimental tests.

Below is given an example of using the above dependences for comparative calculation in evaluating the strength of board propellers of two ice-breakers: one being designed and the second one of the "Moskva" type. Calculation was performed under the assumption that the ship propeller collides with an ice block of the same reduced mass as the propeller itself which is determined by the relation

$$\frac{\mu R^2}{I_x} = 0.4$$

for the ship being designed, which corresponds to the weight of the ice block of 2.1 ton. The most dangerous case is assumed for calculation, i.e., the ice-breaker is moving backward while the propeller is operating for forward motion. In such a case, impact against the blade surface is most probable.

Initial Data for Comparative Strength Calculation of Propellers of Two Ice-Breakers

	Ice-breaker being designed	"Moskva" ice-breaker
Diameter D, m	5.40	4.82
Pitch of the blade at a distance of 0.7R from axis of rotation H, m	4.30	3.86
Rotation speed at mooring regime n, rev/sec	- 1.92	- 1.83
Reduced mass of the ice block μ, kg·sec^2/m	$2.12 \cdot 10^2$	$2.12 \cdot 10^2$
Forward speed of ship V_o, m/sec	2.0	2.0
Distance between root section of the blade r_A from the axis of propeller rotation, m	1.0	0.8

/93

Initial Data for Comparative Strength Calculation of Propellers of Two Ice-Breakers

(Cont'd)

	Ice-breaker being designed	"Moskva" ice-breaker
Pitch of the root cross section H_A, m	3.45	3.20
Pitch angle of the root cross section φ_A, degrees	28° 40'	32° 00'
Blade inclination ν, degrees	0	0
Relative radius of the root cross section $\bar{r}_A$	0.370	0.336
Section modulus of the area of root cross section W, cm^3		
maximum	13,200	7,200
minimum	12,000	5,850
Moment of inertia of propeller with the adjoined mass of water I_x, $kg \cdot m \cdot sec^2$	$3.86 \cdot 10^3$	$2.22 \cdot 10^3$
Angular velocity of propeller rotation ω_1, sec^{-1}	- 12.1	- 11.5

The moment bending the blade in respect to the axis of minimum rigidity is determined with the help of formulae (104) and (110) assuming that:

$$\cos\nu = 1{,}0; \quad \pi^{-2} = 0{,}1 \quad \text{и} \quad \bar{r} = 1{,}0;$$

$$\mathfrak{M}_{\eta_A} = -\frac{\mu(n_1 H - V_0)(1-\bar{r}_A)}{1+0{,}1\left(\frac{H}{D}\right)^2\left(1+\frac{\mu R^2}{I_x}\right)}\left(\frac{1}{2}\cdot\frac{H}{\pi}\sin\varphi_A + R\cos\varphi_A\right).$$

Substituting numerical values into this equation, we obtain for the ice-breaker being designed:

$$\mathfrak{M}_{\eta_A} = -\frac{2{,}12\cdot 10^3(1{,}92\cdot 4{,}3 - 2)(1-0{,}37)}{1+0{,}1\cdot 0{,}635(1+0{,}4)} \times$$

$$\times\left(0{,}5\cdot\frac{4{,}3}{3{,}14}\cdot 0{,}482 + 2{,}7\cdot 0{,}876\right) = 3{,}38\cdot 10^3 \ \text{kg}\cdot\text{m}\cdot\text{sec},$$

For the "Moskva" ice-breaker:

$$\mathfrak{M}_{\eta_A} = \frac{2,12 \cdot 10^3 (-1,83 \cdot 3,86 - 2)(1 - 0,336)}{1 + 0,1 \cdot 0,613 (1 + 0,555)} \times$$
$$\times \left(0,5 \frac{3,86}{3,14} 0,533 + 2,41 \cdot 0,846\right) = 2,75 \cdot 10^3 \text{ kg} \cdot \text{m} \cdot \text{sec}.$$

The impulse of bending stresses (kg·sec/cm^2) as a result of blade impact amounts to:

	Ice-breaker being designed	"Moskva" ice-breaker
$\sigma_n \Delta t = \frac{\mathfrak{M}_{\eta_A}}{W_{max}}$	26.0	38.2
$\sigma_n \Delta t = \frac{\mathfrak{M}_{\eta_A}}{W_{min}}$	28.2	47.0

Table 11. Calculation of the Moment of Instant Impulse in Respect to Axis of Propeller During Impact Against the Blade Edge /94

No.	Designation and calculating formulae	Relative radius of the impact point $\bar{r}$						
		0.5	0.6	0.7	0.8	0.9	0.95	1.0
1	$\bar{r}^2$	0,25	0,36	0,49	0,64	0,81	0,902	1,0
2	tg γ	8,80	5,40	3,17	2,30	0,933	0,611	0
3	$d\bar{r}/d\alpha$ ($\bar{r}$. n. 2)	4,40	3,24	2,29	1,84	0,840	0,581	0
4	$\left(\frac{d\bar{r}}{d\alpha}\right)^2$	19,3	10,5	5,22	3,38	0,703	0,338	0
5	$\frac{1}{\bar{r}^2}$	4,00	2,78	2,04	1,56	1,23	1,11	1,0
6	n. 5 · $\frac{\mu R^2}{I_x}$	4,55	3,33	2,59	2,11	1,78	1,66	1,55
7	n. 4 × n. 6	87,7	35,0	13,5	7,13	1,25	0,56	0
8	1 + n. 7	88,7	36,0	14,5	8,13	2,25	1,56	1,0
9	$-\mu\omega_1 R^2 \times$ n. 4, кгс·м·с	$274 \cdot 10^3$	$149 \cdot 10^3$	$72,2 \cdot 10^3$	$48 \cdot 10^3$	$10 \cdot 10^3$	$4,8 \cdot 10^3$	0
10	$\mathfrak{M}_x$ = (n. 9 : n. 8)	$3,09 \cdot 10^3$	$4,14 \cdot 10^3$	$5,11 \cdot 10^3$	$5,91 \cdot 10^3$	$4,44 \cdot 10^3$	$3,08 \cdot 10^3$	0

Note: Auxiliary values: $-\mu\omega_1 R^2 = 142 \cdot 10^3$ kg·m·sec; $\frac{\mu R^2}{I_x} = 0.555$.

According to data of actual size tests of propellers operating in ice, the duration of impact $\Delta t = 0.02 \div 0.06$ sec. /95

Table 11 provides an example of calculation with the help of formula (108) in which the moment of instantaneous impulse $\mathfrak{M}_x$ was determined for the ice-breaker "Moskva" in respect to the propeller axis during impact of the propeller blade edge against the ice.

This calculation was performed for the case when the ship is moving forward and the propeller is rotating also for the forward motion of the ship ($V_{0X} < 0; \omega_1 < 0$).

Section 12. Method of Approximate Determination of the Frequency of Natural Bending Vibrations of Propeller Blades in Air and Water

In designing structures subjected to the action of periodical forces, it is necessary to calculate frequencies of natural vibrations in order to prevent the possibility of their coinciding with frequencies of exciting forces. As is known, in such a case, a resonance phenomenon takes place and as a result even low exciting forces may cause considerable variable stresses in a vibrating structure and cause failure within a relatively short time.

Let us discuss natural vibrations of a propeller blade taking place in a plane of minimum rigidity which is perpendicular to the chords of cross sections of a blade unfolded on the plane. Let us consider a blade as a cantilever beam with a variable cross section which is rigidly fastened at its end section.

Under such conditions, the equation of bending vibrations of the blade may be derived from the differential equation of the elastic line of the beam

$$EI\frac{d^2y}{dx^2} = -M(x), \tag{111}$$

where EI - is rigidity of the beam in bending;

M (x) - bending moment in any cross section of the beam.

If it is taken into consideration that in the case of natural vibrations it may be assumed that the blade is subjected to the action of inertia forces with an intensity of

$$q = \frac{d^2M(x)}{dx^2} = \frac{\gamma S}{g}\frac{d^2y}{dt^2}, \tag{112}$$

where γ - specific gravity of blade material;

g - acceleration of gravity;

S - cross sectional area of the blade, which varies along its length.

By substituting (112) into (111), we obtain the needed differential equation:

$$\frac{d^2}{dx^2}\left(EI\frac{d^2y}{dx^2}\right) = -\frac{\gamma S}{g}\cdot\frac{d^2y}{dt^2}. \qquad (113)$$

However, to this equation should be added boundary and initial conditions. Since in future only those characteristics of vibrations will be of interest which do not depend on the initial action, the initial conditions will not be taken into consideration in this solution. /96

Boundary conditions with the consideration that the blade is replaced by a cantilever rod may be represented as:

$$\text{with} \quad x = 0, \quad y = 0, \quad \frac{dy}{dx} = 0;$$

$$\text{with} \quad x = l, \quad EI\frac{d^2y}{dx^2} = 0, \quad \frac{d}{dy}\left(EI\frac{d^2y}{dx^2}\right) = 0,$$

where l - length of the blade.

Using the Fourier method for solving the formulated problem, when deflection y is sought in the form $y=f(x)\varphi(t)$, indicates that the motion being studied is a harmonic oscillation with a cyclic frequency p, which is determined by the expression

$$p^2 = \frac{\int_0^l EI\left(\frac{d^2f(x)}{dx^2}\right)^2 dx}{\frac{\gamma}{g}\int_0^l Sf(x)^2 dx}. \qquad (114)$$

Formula (114) makes it possible to find cyclic frequency if, with given functions I=I(x) and S=S(x), the law of distribution of blade deflections along its length (shape of vibrations f(x)) is known. It can be assumed that the shape of vibrations of a blade with a variable cross section is approximately the same as the shape of vibrations of a cantilever rod, for which it is accepted that:

$$f(x) = A\sin kx + B\cos kx + C\,\mathrm{sh}\,kx + D\,\mathrm{ch}\,kx; \qquad (115)$$

Constants A, B, C, and D are calculated from the boundary conditions for each root $k_i l$ of the characteristic equation.

Change of areas and moment of inertia of cross sections of the blade along its length is determined by the following dependences:

$$I(x) = I_0\left(1 - m_0\frac{x}{l} + m_1 \sin\frac{\pi x}{l}\right), \tag{116}$$

$$S(x) = S_0\left(1 - n_0\frac{x}{l} + n_1 \sin\frac{\pi x}{l}\right); \tag{117}$$

where n_0, n_1, m_0, and m_1 - numerical coefficients which can be found by formulae

$$n_0 = \frac{S_0 - S_l}{S_0}, \quad n_1 = \frac{1}{S_0}\left(\frac{S_0 + S_l}{2} - S_{1/2}\right);$$
$$m_0 = \frac{I_0 - I_l}{I_0}, \quad m_1 = \frac{1}{I_0}\left(\frac{I_0 + I_l}{2} - I_{1/2}\right),$$

in which S_0, $S_{1/2}$, S_1, I_0, $I_{1/2}$, I_1 - areas and moments of inertia of unfolded cylindrical cross sections of the blade at a radius r_0 (root cross section), at a radius corresponding to half of the blade length $r_{1/2}$ and at a radius r_1=R.

By substituting expressions (115), (116), and (117) into (114) /97
for any tone of frequencies of blade vibrations, we obtain

$$f_i = \frac{1}{2\pi}\left(\frac{\alpha_{0i}}{l}\right)^2 \sqrt{\frac{EI_0}{\rho S_0}} \sqrt{\frac{1 - m_0\beta_{i0} \pm m_1\beta_{i1}}{1 - n_0\gamma_{i0} \pm n_1\gamma_{i1}}}, \tag{118}$$

where $\alpha_{0i} = k_i l$ - parameters of the blade (cantilever beam) of a constant cross section with the area S_0 and moment of inertia I_0, which are determined by the equation of frequencies $\cos k_i l \operatorname{ch} k_i l = -1$.

The equation of frequencies has the following roots:

$k_1 l$	$k_2 l$	$k_3 l$	$k_4 l$	$k_5 l$	$k_6 l$
1,875	4,694	7,855	10,996	14,137	17,279

The factor in formula (118)

$$\sqrt{\frac{1 - m_0\beta_{i0} \pm m_1\beta_{i1}}{1 - n_0\gamma_{i0} \pm n_1\gamma_{i1}}} = \sqrt{K_i}$$

is a correcting coefficient which makes it possible to calculate vibration frequencies of the blade, which gets thinner toward the end, by the expression

$$f_i = \bar{f}_i \cdot \sqrt{K_i}.$$

Here f_i is the frequency of the i-th tone of the blade of length l, and of the constant straightened cylindrical cross section, the area of which is S_0 and the moment of inertia is I_0.

Constants β_{i0}, β_{i1}, γ_{i0}, and γ_{i1} for various shapes of vibrations of the blade are given in Table 12.

Table 12. Table of Auxiliary Coefficients

i	β_{i0}	γ_{i0}	β_{i1}	γ_{i1}
1	0,193	0,807	0,493	0,493
2	0,405	0,594	0,703	0,703
3	0,468	0,532	0,661	0,661
4	0,483	0,517	0,649	0,649
5	0,490	0,510	0,645	0,645
6	0,493	0,507	0,642	0,642

Designers are interested first of all in the first harmonics of natural bending vibrations or in the fundamental tone when, in the process of vibrations, the nodal line is positioned in the area of blade fastening in the hub while the antinode is formed at its tip. The minimum value of frequency which is determined by formula (118) and the smallest value of the root of the equation of frequencies $\alpha_{01} = 1.875$ correspond to the fundamental tone.

In such a case, for the vibration frequency of fundamental tone

$$f_1 = \frac{1}{6{,}28}\left(\frac{1{,}875}{l}\right)^2 \sqrt{\frac{EI_0}{\rho S_0}} \sqrt{\frac{1 - 0{,}193 n_0 \pm 0{,}493 |n_1|}{1 - 0{,}807 n_0 \pm 0{,}493 |n_1|}}. \qquad (119)$$

Values which are denoted by letters are determined by the geometrical characteristics of the blade and by the properties of the material of which the propeller is manufactured. /98

As an example, below is discussed calculation of the frequency of fundamental tone of blade vibration of a solid cast propeller.

Initial data for calculation

Propeller diameter D, m	5.2
Average pitch of propeller H, m	5.12
Area of unfolded blade A, m^2	13.8
Number of blades Z	5
Blade material	alcunic (aluminum-nickel bronze)
Modulus of elasticity E, kg/cm	$1.09 \cdot 10^6$
Density of propeller material γ, kg/cm^3	0.0075

Geometrical characteristics of the blade cross sections are determined by the drawing of the propeller and calculation according to the method discussed in Section 3.

Geometrical Characteristics of Cross Sections of the Blade

Blade Cross Section	l_i, cm	S, cm^2	I, cm^4
1	33.2	1,260	23,347
2	59.8	1,221	16,890
3	86.3	1,009	9,975
4	112.9	809	4,793
5	139.4	598	2,057
6	166.0	360	581
7	192.5	198	140
Root	0	1,260	31,000
Average	109.5	840	5,500
Tip of the blade	219.0	100	0

Using data in Table 2 (Section 3), n_0, n_1, m_0, m_1 are calculated and then, using formula (119), the frequency of fundamental tone vibration of the blade is calculated which will be 29.6 cycles.

It should be noted that the actual value of the frequency of natural vibrations of the blade measured under service conditions is 30.2 c. As seen from the above example, the deviation of calculated frequency from the experimental value does not exceed 2%.

Strictly speaking the formulae presented above are true only when the propeller is in a vacuum. In a medium having a certain density some volumes of the medium adjacent to the vibrating object will be involved in the vibration process and in this way, as it were, increase the mass of vibrating body.

Experiments demonstrated that frequencies of blade vibration in air and water differ considerably. Figure 42 illustrates oscillograms of attenuated natural vibrations of the blade of a /100
model of a propeller in air and in water. The oscillograms show that water decreases by half the frequencies of natural vibrations as compared with the frequency in air. Therefore, the vibration frequency for transport ship propellers is assumed to be approximately half of that in air. This ratio well coincides with results obtained by Ya. F. Shirila, who studied dynamic stresses in propeller blades of the ship "Pekari" (35) under actual operating conditions.

/99

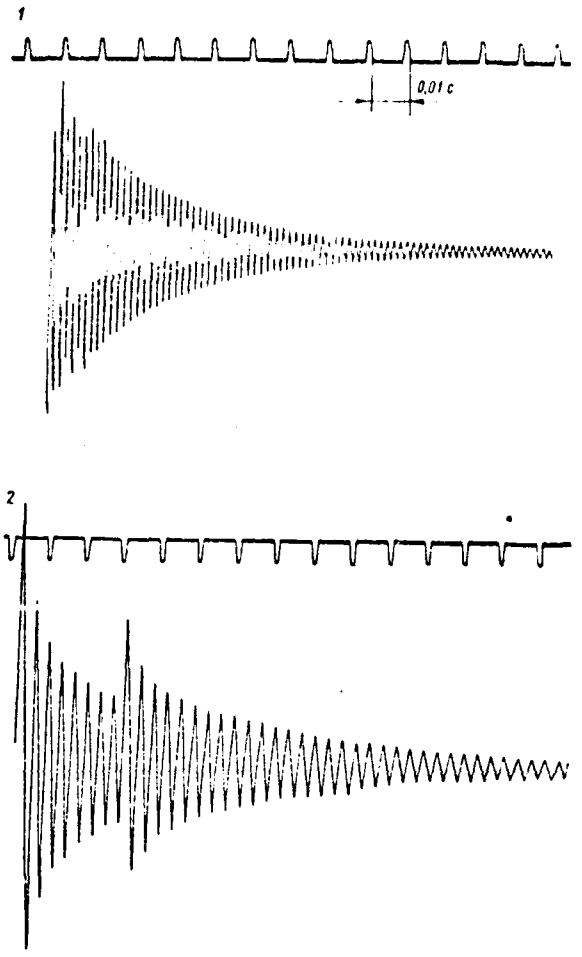

Fig. 42. Oscillograms of attenuated natural vibrations of the blade of a model of a propeller

1. in air; f = 578c; 2. in water; f = 288c.

It is advisable to determine frequencies of natural vibrations for all large size propellers (with diameter above 4-5 m). This is explained by the fact that natural vibrations of such propellers in water are relatively low, and in the case of high-speed engines, the appearance of resonance vibrations is possible.

CHAPTER III. EXPERIMENTAL STUDY OF THE STATE OF STRESS IN PROPELLER BLADES

Because analytic calculation of stresses in propeller blades is difficult due to their complex geometry and distribution of hydrodynamic forces, considerable attention is devoted at present to experimental studies of the state of stress in propeller blades. These studies make it possible to obtain data on the effect of individual geometric characteristics of marine propellers (disk ratio, pitch ratio, curvature of cross sections, etc.) on the magnitude of emerging stresses and to determine the areas with maximal stresses. The experimental method is also the most effective method for studies of the local strength of ship propellers, particularly those having wide blades. In addition, the results of experimental studies serve as a criterion for evaluating the correctness of several methods of approximate strength calculation. /100

It is obvious that the most reliable data on the state of stress in propeller blades may be obtained only by full scale experiments. However, such experiments are very laborious and complex in nature. Therefore, it is more rational to bring into accord measurements of actual propellers with measured stresses in models of propellers. Such stresses, confirmed by data obtained under actual operating conditions may be considered to be fully acceptable not only for making more accurate the existing approximate calculation methods, but also for development of new and more perfect calculation methods.

Section 13. Information from the Similarity Theory and Studies of the State of Stress in Propeller Blades Using Models of Propellers /101

Studies of the state of stress in propeller models with the purpose of using the results for actual operating propellers should be carried out in agreement with the law of physical similitude.

In a general case of similarity conditions, the modeling of the elastic-dynamic state of stress in propeller blades is reduced to maintaining the geometric similarity of the model and actual object as well as the similarity of deformations and principal stresses along three main axes. Naturally, in the case of testing models of propellers, the condition of hydrodynamic similarity of the model and actual object also have to be maintained. The scale of deformations and stresses should not depend on directions and the scale of normal stresses should be equal to the scale of tangential stresses, i.e., the following relations should be maintained:

$$\frac{\varepsilon_{iM}}{\varepsilon_{iH}} = 1; \quad \frac{\sigma_{iM}}{\sigma_{iH}} = \frac{E_M}{E_H}; \quad \frac{\sigma_M}{\sigma_H} = \frac{\tau_M}{\tau_H},$$

where ε - relative deformation;

σ - normal stresses;

τ - tangential stresses;

E - modulus of elasticity of material;

i=1,2,3 - index of principal directions of deformations and stresses.

Values with the "m" index correspond to the model and those with the "n" index concern the actual object.

Simultaneous similarity of deformations and stresses in a three-dimensional state of stress is possible only with equality of Poisson's ratio and moduli of elasticity (μ and E) of materials of a model and of actual object.

In the case of using isotropic materials for relative deformation of the model and the actual object in one of the principal directions in accordance with Hooke's law, it is possible to obtain

$$\left.\begin{aligned} \varepsilon_{1M} &= \frac{1}{E_M}[\sigma_{1M} - \mu_M(\sigma_{2M} + \sigma_{3M})]; \\ \varepsilon_{1H} &= \frac{1}{E_H}[\sigma_{1H} - \mu_H(\sigma_{2H} + \sigma_{3H})]. \end{aligned}\right\} \qquad (120)$$

from these equations

$$\frac{\varepsilon_{1M}}{\varepsilon_{1H}} = \frac{\frac{\sigma_{1M}}{E_M}\left[1 - \mu_H\left(\frac{\sigma_{2M}}{\sigma_{1M}} + \frac{\sigma_{3M}}{\sigma_{1M}}\right)\right]}{\frac{\sigma_{1H}}{E_H}\left[1 - \mu_H\left(\frac{\sigma_{2H}}{\sigma_{1H}} + \frac{\sigma_{3H}}{\sigma_{1H}}\right)\right]} = 1. \qquad (121)$$

With strict similarity of the ratios of stresses should be equal, i.e., /102

$$\frac{\sigma_{2M}}{\sigma_{1M}} = \frac{\sigma_{2H}}{\sigma_{1H}} = a, \quad \frac{\sigma_{3M}}{\sigma_{1M}} = \frac{\sigma_{3H}}{\sigma_{1H}} = b,$$

consequently

$$\frac{\varepsilon_{1M}}{\varepsilon_{1H}} = \frac{\frac{\sigma_{1M}}{E_M}[1 - \mu_M(a + b)]}{\frac{\sigma_{1H}}{E_H}[1 - \mu_H(a + b)]} = 1. \qquad (122)$$

The middle part of this equation may be equal to one only in the case when:

$\sigma_2 = \sigma_3 = 0$, $a = b$ или $\mu_H = \mu_M$.

The first case corresponds to uniaxial state of stress with the principal stress σ_1. The second case is equivalent to the condition that $\sigma_2 = -\sigma_3$ in deformation of pure slip caused by twisting the rod in respect to axis 1. Hence, the full similarity of the three-dimensional state of stress with simultaneous similarity of relative deformations is possible only with $\mu_H = \mu_M$.

Similar conclusions should be reached as a result of analyses of two other principal deformations ϵ_2 and ϵ_3.

Let us discuss simulation of the state of stress of a completely submerged propeller without presence of cavitation and assuming that the effect of the propeller's weight may be disregarded. The system of parameters which characterize the geometrical, elastic-dynamic, and hydrodynamic similarity of an actual propeller and its model includes the following parameters:

D - typical linear dimension of propeller (diameter);

E - modulus of elasticity of material;

μ - Poisson's ratio;

v - velocity of incident flow;

n - propeller rpm;

ν - coefficient of kinematic viscosity of liquid;

ρ - specific gravity of propeller material;

ρ_c - density of surrounding medium.

Out of the above eight parameters, of which only three have independent dimensions, it is possible to compose five dimensionless parameters or criteria of similarity, the numerical values of which in similar systems or phenomena should be the same:

$$\mu;\ \frac{\rho}{\rho_c};\ \frac{\rho n^2 D^2}{E};\ \frac{\rho_c v^2}{E};\ \frac{vD}{\nu}.$$

The last of the mentioned criteria of similarity is the Reynolds number. Since hydrodynamic studies of propeller models usually are carried out at high Reynolds numbers, which exceed certain critical values, it may be assumed that the phenomena of hydrodynamic character take place naturally, and it is therefore possible to exclude the Reynolds number from among the necessary criteria of similarity indicated above. /103

Maintaining equality of the four remaining criteria for the model and an actual object is compulsory in realization of full similarity of their elastic-dynamics state of stress.

The necessity of maintaining equality of the Poisson's ratio of the material of both the actual propeller and its model presents certain requirements in selecting material for the model. In most cases for studying state of stress models are made of the same material as the propellers themselves (brass, bronze). However, even in such a case, it is quite difficult to obtain similary of state of stress in a large size propeller and in its small model under laboratory conditions. Indeed, if $\rho_M = \rho_H$, $E_M = E_H$, and the model is tested in water ($\rho_{C.M} = \rho_{C.H}$), then from conditions of equality of the third and the fourth of the above listed criteria for a model and an actual object it follows that

$$n_M D_M = n_H D_H \text{ и } v_M = v_H,$$

i.e., velocities of flow under actual conditions and in the testing model should be the same and the ratio of angular velocities of the actual object and the model should be constant and equal to the linear scale.

Technical resources of regular laboratory equipment used for testing propeller models cannot provide equality of flow velocities for the model and the actual object. Velocities at which models are tested are usually lower than those in actual operation. As a result, relative deformations of blades and stresses emerging in them are also lower in simulation testing as compared with actual operating conditions. Therefore, tests of propeller models show that the model is, as it were, stronger than the actual propeller.

Because of these circumstances, special requirements are presented for measuring equipment used in testing models, since this equipment must provide for measuring extremely small relative deformations and low stresses.

The most expedient method of studying state of stress in propellers by means of testing models is measuring the relative deformation of blades with the help of strain gages. This method makes it possible to assume that the state of stress in a propeller blade is two-dimensional and that for the full characteristic of this state of stress it is necessary to determine principal deformations and the angle formed by the direction of one of them and one of the axes selected arbitrarily. Practically this task is reduced to measuring deformation in some three directions and a subsequent calculation of principal deformations and also their directions for all points at which strain gage sockets are located. /104

Measuring deformations of propeller blade model surfaces most often is performed with the help of wire strain gages forming rectangular sockets. A diagram of their distribution on the blade surface is shown in Figure 43. The total number of sockets on one model of a propeller reaches twenty, while the total of adhesively bonded strain gages reaches sixty. After bonding of strain gages, the areas of the blade surface occupied by strain gages and branching off conductors are coated with moisture protecting compound.

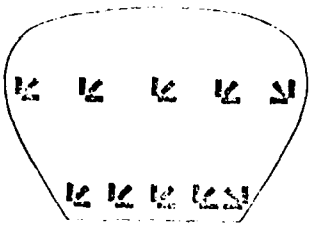

Fig. 43. Diagram of location of strain gage sockets on the surface of a propeller blade model

It should be noted that experiments in measuring deformations of propeller blades require development of high-quality current collectors which make it possible to transmit electric signals from sockets rotating together with the propeller to amplifying and recording devices.

As an example, Figure 44 illustrates oscillograms of relative deformations fixed at a certain points of a model propeller blade surface during operation in a uniform or inclined flow. Usually propellers of high-speed ships, such as gliding boats, hydrofoils, and others, operate in an inclined flow. In operation of a propeller in an inclined flow, deformations of its blades have two components on the oscillogram; a constant one and a clearly expressed variable component superposed on it (varying with frequency which is equal to revolutions of the propeller per unit of time). Oscillograms in Figure 44 show deformations in the course of change in propeller operation from the nominal regime to the full stop.

After deformations for the number of blade points measured in three directions are known, it is possible to determine the directions and amount of principal deformations in these points using rectangular strain gage sockets.

$$\left.\begin{aligned} \varepsilon_1 &= \frac{\varepsilon_0 + \varepsilon_{90}}{2} + \frac{1}{2}\sqrt{2}\sqrt{(\varepsilon_0-\varepsilon_{45})^2+(\varepsilon_{45}-\varepsilon_{90})^2};\\ \varepsilon_2 &= \frac{\varepsilon_0 + \varepsilon_{90}}{2} - \frac{1}{2}\sqrt{2}\sqrt{(\varepsilon_0-\varepsilon_{45})^2+(\varepsilon_{45}-\varepsilon_{90})^2}. \end{aligned}\right\} \qquad (123)$$

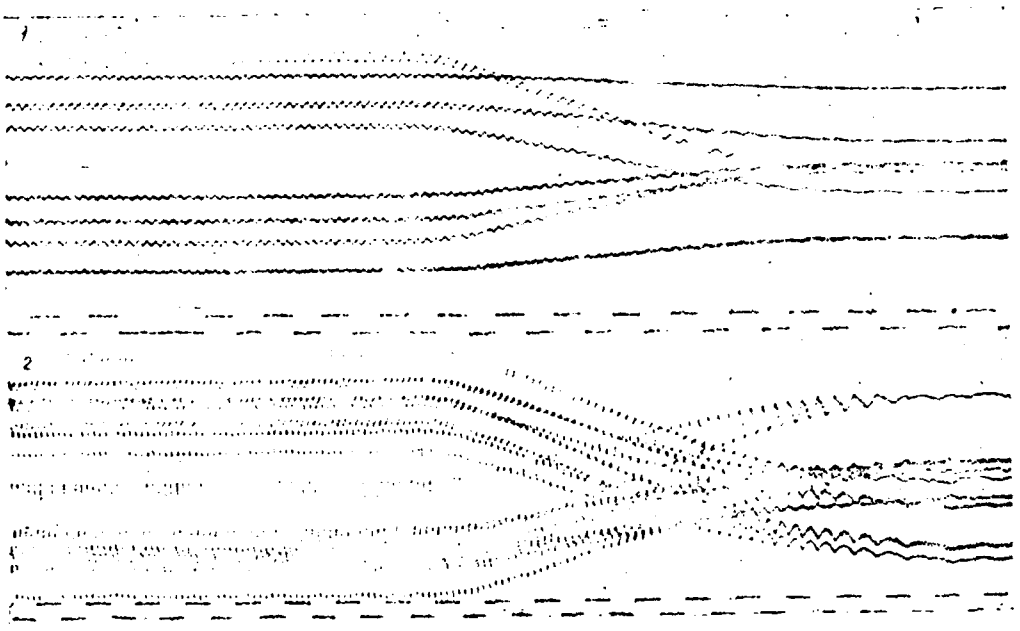

Fig. 44. Oscillogram of stresses emerging in a propeller blade during operation in a uniform (1) or inclined (2) flow

The principal stresses and their directions can be found from principal deformations with the help of Hooke's law for the two-dimensional state of stress

$$\left.\begin{aligned} \sigma_1 &= \frac{E}{1-\mu^2}(\varepsilon_1 + \mu\varepsilon_2); \\ \sigma_2 &= \frac{E}{1-\mu^2}(\varepsilon_2 + \mu\varepsilon_1); \\ \operatorname{tg} 2\varphi &= \frac{2\varepsilon_{45} - (\varepsilon_0 + \varepsilon_{90})}{\varepsilon_0 - \varepsilon_{90}}. \end{aligned}\right\} \qquad (124)$$

As an example, in Figure 45 is shown the distribution of maximum principal stresses along the intake side of a propeller blade in cross sections located at relative radii of 0.33 and 0.6. This diagram of stress distribution was obtained experimentally by means of tests in a cavitation tunnel.

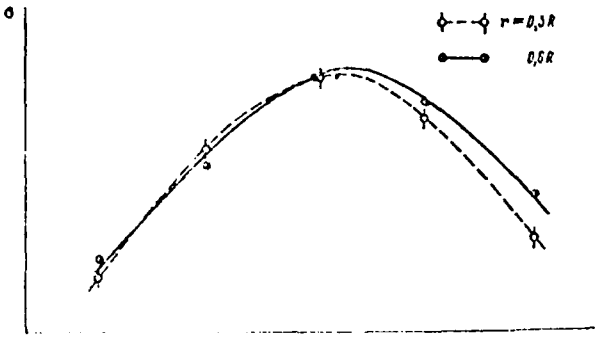

Fig. 45. Distribution of maximum principal stresses at the intake side of the blade of a propeller model ($z = 3$; $\frac{A}{A_0} = 0,55$; $\frac{H}{D} = 1,2$; $\frac{\delta}{D} = 0,015$), obtained in testing in a cavitation tunnel

Of particular interest are experimental studies of the state of stress of propeller models at which the external load of the blade is assigned by some schematized form of its distribution, such as pressure uniformly distributed on the blade surface or varying linearly along the radial and tangential directions.

A unit for simulation of uniformly distributed loads on the blade surface is shown in Figure 46; loads are created at the expense of excess pressure in a special rubber chamber which is located under the blade being tested within a hollow cylinder. In the course of experiment, stresses and elastic displacements (deflections) are recorded at certain points of the blade.

/107

Fig. 46. Experimental unit for creating uniformly distributed load on a propeller blade

Fig. 47. Experimental unit for static application of load on a blade according to a given law

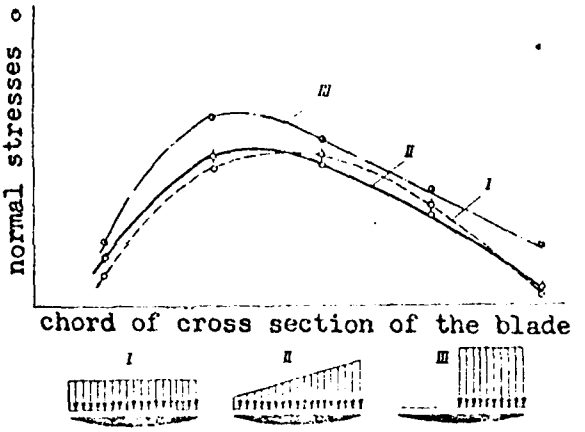

Fig. 48. Distribution of principal stresses in a root cross section of a propeller blade with various character of external forces application

I - load uniformly distributed along the chord of cross section; II - load varying according to a linear law; III - load higher in intensity uniformly distributed along half of the chord length

In the figure are shown strain gage sockets for measuring /108
relative deformations and dial indicators that show deflections.

The overall view of the unit for creating variable loads on blades which vary in both radial and tangential directions according to a prescribed law is presented in Figure 47. External forces are imitated by discrete loads which are applied to a sufficiently large number of cross sections close to each other. Stepped change of load obtained in this way may with sufficient accuracy be considered as continuous load change.

Figure 48 illustrates the distribution of principal stresses in a root section of the blade measured with the help of the above unit. In the course of experiment, the law of distribution of applied external forces was varied. In the same figure, diagrams of external forces application are included. The resultant of the external forces remains in all cases constant and the difference consisted only in the magnitude of torsional moments which cause mainly tangential stresses. As seen from these force diagrams, the difference between the uniform external load and that varying according to linear law does not lead to a considerable change in the distribution of normal stresses in a cross section of the blade under consideration. This and the other results of the

experiment confirm the hypothesis that in approximate methods of propeller strength evaluation it can be considered that the external load on the blade is uniformly distributed along the complete length of the chord of the blade.

Figure 49 illustrates a graph of changes in principal stresses at intake and forcing sides of the blade root cross section. There is also a curve of stresses plotted as a result of calculation by a method discussed in Section 4, where the blade is considered to be a cantilever beam. Satisfactory agreement of results of calculation and experiment by maximum stresses is a basis for considering that it is rightful to use approximate methods for practical strength calculations of ship propellers.

Experimental studies of propeller models make it possible to expose the weakest points of calculation methods being used. For example, experimental data show that cross sections of the blade have distorted neutral axes which probably approach the form of median lines of cross sections (see Fig. 49).

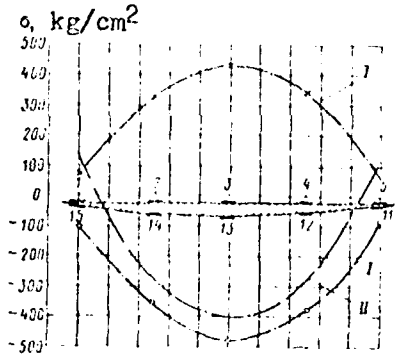

Fig. 49. Distribution of principal stresses at intake and forcing sides of the root cross section of the blade. I - experiment; II - calculation.

Although the supposition that the neutral axis of cross sections /109
is a straight line does not affect noticeably the magnitude of maximum stresses, utilization of this supposition in developing calculation methods for evaluating the local strength of a blade near its edges might lead to considerable errors.

Section 14. Full-Scale Tests of Propeller Blades With the Purpose of Determining the State of Stress in Them

Measuring stresses in the propeller blade of a full-scale object is an extremely complex problem from the point of view of technical realization of the experiment. One of the main problems is to provide reliable hydroinsulation of the stress pickups (deformations). As in the case of experiments with models, usually wire or semiconductor strain gage transducers are used in the form of rectangular sockets placed on propeller blades. They are subjected to the action of hydrodynamic pressures and high flow velocities which contributes to the breakdown of hydroinsulation of strain gages and which often makes these gages useless.

An inherent part of technical instrumentation used in experiments is a complicated current collector for transmitting signals from the rotating shaft line to recording devices. Current collectors under ship conditions have to be located in areas with increased humidity, which often require special measures to provide for their efficiency.

Finally, if the purpose of the experiment is to measure not only static but also dynamic stresses in propeller-blades, a serious problem emerges to eliminate in the transmitted signal distortions caused by vibrations of the main engine and stern part of the ship.

Because of purely technical difficulties and also because of the relatively high cost of preparations for such tests, only individual experiments have been carried out, which provided sufficiently explicit and reliable results.

Measurements of stresses in the propeller blade of a high-tonnage tanker were carried out by the Scientific Research Center for Ship Building and Marine Navigation with participation of the Experimental Water Basin in the Netherlands (45).

Under operating conditions, the propeller blade is subjected to the action of hydrodynamic load, load caused by the action of centrifugal forces and forces of weight, and also to the action of load caused by the vibration of the blades and propeller as a whole. The main subject of studies in (45) was static and dynamic stresses of a propeller blade caused by the action of hydrodynamic forces.

Tests were carried out on a tanker with a displacement of 42,000m^3 equipped with a steam turbine power unit with a capacity of 10,200 hp. This unit provided for a cruising speed of 15.5 knots at 102 rpm of the ship propeller (four blade, 6.53 m in diameter). A sketch of this propeller is shown in Fig. 30. In the course of experiments, stresses were measured in a root cross section of the blade at a relative radius of 0.25. Ten strain gage sockets were placed equally on both intake and forcing sides of the blade (Fig.50). /110

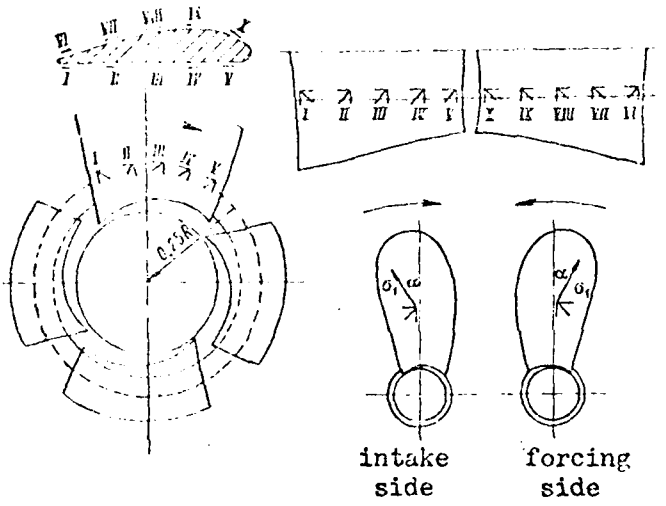

Fig. 50. Position of strain gage sockets along the profile of the propeller blade.

Each socket consisted of three strain gages positioned as is shown in Figure 43 and forming the active arms of an electric Winston bridge. Passive arms of the circuit are formed by temperature compensation strain gage pickups adhesively bonded on a special disk* in the propeller cone and precision resistances placed on a

*Disk and propeller are made of the same material.

shaft-line within the ship hull. Altogether, there were 30 bridges revolving together with the propeller shaft.

Table 13. Magnitude of Maximum Principal Stresses (kg/cm^2) in the Root Cross Section of a Propeller Blade

/111
-112

Angle of blade turn θ during operation of propeller, degrees	Forcing surface of the blade					Intake surface of the blade				
	Stresses at strain gage sockets (see Fig.50)									
	I	II	III	IV	V	VI	VII	VIII	IX	X
0	174	373	433	499	292	81	—254	—691	—626	121
10	180	393	465	520	305	82	—273	—723	—659	127
20	182	424	482	532	314	83	—286	—721	—612	127
30	181	429	482	529	313	89	—293	—716	—600	122
40	180	428	470	518	307	90	—298	—712	—584	121
50	182	425	462	520	303	91	—303	—707	—608	123
60	181	422	455	513	297	91	—296	—706	—568	120
70	176	401	429	426	280	95	—283	—686	—510	117
80	168	369	397	454	258	96	—268	—597	—457	114
90	158	337	371	419	238	95	—251	—553	—406	112
100	150	311	336	390	223	94	—236	—517	—363	112
110	141	288	308	355	213	93	—222	—477	—314	113
120	141	274	294	362	206	92	—214	—455	—332	114
130	139	269	288	358	203	91	—207	—466	—324	116
140	139	262	286	354	200	90	—201	—435	—318	117
150	139	260	284	352	201	89	—196	—429	—316	117
160	141	266	291	359	208	88	—196	—432	—333	117
170	146	283	323	387	221	87	—199	—464	—387	118
180	149	302	346	402	231	86	—207	—500	—426	120
190	152	313	357	445	238	87	—212	—521	—431	122
200	147	398	348	405	236	89	—210	—525	—391	123
210	143	288	310	371	215	92	—192	—451	—326	121
220	132	258	246	343	192	91	—180	—401	—247	119
230	126	253	241	320	182	91	—168	—368	—223	120
240	122	217	221	303	174	89	—159	—343	—217	121
250	118	203	201	294	166	37	—149	—327	—201	122
260	115	191	191	298	161	85	—140	—315	—193	122
270	114	186	194	286	160	81	—141	—306	—189	122
280	176	178	202	296	163	81	—146	—318	—203	122
290	118	192	210	301	170	80	—149	—335	—230	121
300	122	206	227	323	178	78	—154	—376	—256	119
310	130	223	250	355	197	75	—167	—381	—299	119
320	138	252	278	386	220	75	—160	—455	—370	119
330	147	278	316	415	236	76	—196	—522	—436	119
340	157	305	368	453	258	77	—214	—579	—503	119
350	167	337	408	489	278	79	—234	—641	—580	123
Average value	150	300	335	395	230	87	—215	—500	—400	121

Table 13 provides data on the magnitude and direction of maximum principal stresses measured during full-scale tests and depending on the angular position of the blade θ* during motion of the ship with full displacement and at 102 rpm of the propeller.

*Measuring of angle θ is done from the top position of the blade in the direction of propeller rotation.

Based on the test results, the following conclusions were reached: /113

central parts of the root cross section of the blade are subjected to maximum loads;

direction of maximum principal stress differs little from the radial direction; the second principal stress is perpendicular to the first one but is considerably smaller in magnitude;

the cyclic component may reach 80% of the average value of acting stress depending on the variation of non-uniformity of the velocity field in the area of the ship propeller; maximal value is observed in the zone of maximum wake while the minimum value is in the zone of minimum wake.

The average values of stresses obtained experimentally were compared (Fig. 51) with calculated values obtained by the methods of Taylor, Romsom, and Rosingh. Comparison demonstrates completely satisfactory agreement of calculated and experimental data.

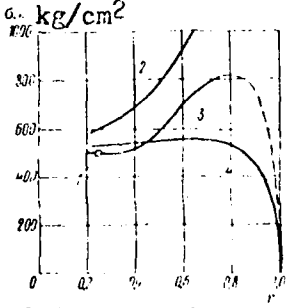

Fig. 51. Comparison of data obtained in full-scale experimental test with calculated results. 1 - experiment; 2 - calculation according to Taylor's method; 3 - calculation according to Romsom; 4 - calculation according to Rosingh.

Of special interest are full-scale tests of ship propellers carried out by Berlin University in cooperation with the Hamburg Shipbuilding Institute and Shipyard Hovaldswerke (35) for the purpose of studying stresses in propeller blades.

The propeller manufactured of aluminum-nickel bronze possessing high mechanical properties had the following parameters:

Diameter, m	4.8
Pitch ratio	1.055
Disk ratio	0.71
Number of blades	5

Tests were carried out on a refrigerator ship "Pekari" with a Diesel engine unit with a capacity of 11,400 hp at 142 rpm. of the propeller.

In the course of tests, deformations and stresses in the propeller blade during operation of the propeller and also frequencies of natural vibrations of the blade in air and water were determined.

Deformations were measured by strain gages bonded on the blade along the line of maximum thicknesses in cross sections at 0.28R, 0.45R, 0.68R, and 0.82R. Wires from the strain gage were lead out to the inside of the ship hull through the hollow propeller shaft and, with the help of a contact collector, were connected with the amplifier and automatic recorder. Blade deformations were measured at propeller rpm from n=60 to n=137 rpm. Directly before testing /114
at a full stop of the ship, the zero point of measurement was determined. Since the position of zero points varied, it was not possible to determine absolute values of the amount of deformations. However, results of measurements make it possible to derive a conception of variations of stresses amplitude as a result of propeller operation.

In Figure 52 is presented a graph illustrating the dependence of double amplitudes of normal stresses 2σ in the blade cross sections located at different distances from the axis of propeller rotation, on propeller rpm - n. The graph shows that an increase in n causes a change in stresses magnitude. At 137 rpm the maximum value of double amplitudes of stresses in a root section of the blade was approximately 160 kg/cm^2, while this stress variation at the cross section furthest from the hub was about 115 kg/cm^2. As was expected, the root cross section of the blade was subjected to maximum stresses.

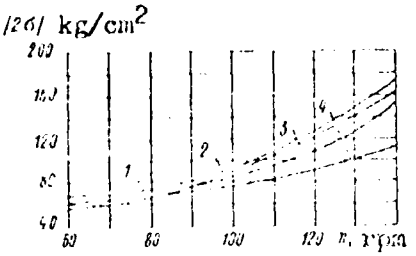

Fig. 52. Dependence of double amplitudes of normal stresses in a propeller blade on the rotational speed of the propeller.
1. r=0.28R; 2. r=0.45R; 3. r=0.68R;
4. r=0.82R.

Frequencies of natural bending vibrations of propeller blades were measured during docking of the ship. Vibrations (in air and with partial submersion of the propeller in water) were induced by an impact. The natural frequency of the first form of bending vibrations of the blade in water was found to be almost half that of the similar vibration frequency of the blade in air; more accurately,

$$f_{water} = 0.51\, f_{air}$$

and its value approaches the frequency of the 7th harmonics of hydrodynamic load. In spite of the fact that the coefficient of dynamic amplification in this case is within the range of 4-5, the resonance phenomenon is not dangerous here, since the amplitude of the 7th harmonics of hydrodynamic load during motion of a ship in calm water is very small. Measurements showed that in rough sea, amplitudes of hydrodynamic load may increase 3-4 fold. Magnitudes of stresses, calculated for maximum loads to which propeller blades of the ship "Pekari" might be subjected in the course of operation, are given in Table 14.

The blade material (aluminum-nickel bronze) possesses the following properties: tensile strength $\sigma_0^{'} = 6200 - 6800$ kg/cm^2 and fatigue limit in bending based on 10^5 cycles in sea water $\sigma_{-1k}^{'} = 800$ kg/cm^2. The average permissible stress of a zero cycle is 650 kg/cm^2 while the magnitude of respective maximum stress is 1300 kg/cm^2. This range of stresses is lower than that shown in Table 14, which indicates the possibility of a premature breakdown of the propeller blade.

Table 14. Stresses (kg/cm^2) Emerging in Propeller Blades Of The Ship "Pekari" During Its Exploitation /115

Side of the blade	Average stationary load	Variable load			Total load
		Caused by gas on the water basin	Caused by non-uniformity of the flow at the propeller disk	Caused by cavitations	
Intake	−650	± 135	(−1015) - 633	+400	(−2130) - 419
Forcing	502	± 95	732 - (−441)	± 210	1510 - (247)

Based on the obtained results (35), it is concluded that the blade thickness should be selected based on consideration of the fatigue strength of the blade material.

CHAPTER IV. STRENGTH OF ASSEMBLED SHIP PROPELLERS

Propellers with blades which are not cast as one piece with the hub but are fastened to the hub by one method or another are of the type of so-called assembled propellers; to this type belong also propellers with detachable blades.

Assembled propellers with blades fastened to the hub by means of a flange joint are the most widely used (Fig. 53).

Section 15. Determining External Forces in Strength Calculations of Assembled Propellers

Strength calculation of the blade-hub joint may be performed by taking into account either operational loads, i.e., external forces to which propeller blades are subjected during operational conditions, or maximal loads.

Operational load on the blade is calculated by formulae given in Chapter I and II, depending on the method used (static or cyclic character of external forces acting on the blade).

In calculations of the static and cyclic strength of flange joints, centrifugal forces of inertia and bending moments caused by them should also be taken into account. The magnitude of centrifugal force is a function of the total mass of the blade including the flange. The method of determining the bending moment which acts on the studs as a result of centrifugal forces may be the same as that used for strength calculations of solid cast propellers (see Section 2). /116

Flange joints of blades with the hub are considered to be heavily loaded bolt-type joints with a prestrain which has a considerable effect on the characteristics of the load cycle to which studs are subjected $r_{st} = \frac{\sigma_{min}}{\sigma_{max}}$ as compared with the characteristics of a variable load acting on a propeller blade and decreasing the amplitude of load pulsation.

This fact makes it possible to perform calculations of the cyclic strength of a flange joint principally for single-shaft ships with greater nonuniformity of the velocity field in the propeller disk and a high value of load coefficient in respect to thrust.

Strength calculation of flange joints of propeller blades with the hub is particularly necessary for ships navigating in ice and for ice breakers as well as for ships navigating in waters contaminated with solid objects.

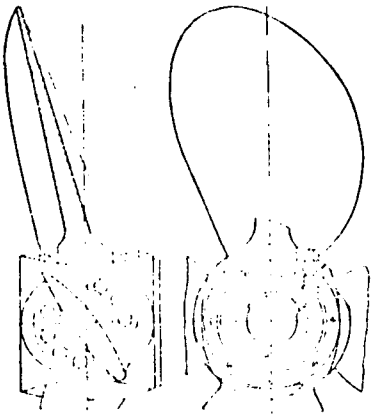

Fig. 53. Ship propeller with detachable blades

In full-scale studies of the character of ship propeller interaction with ice carried out by S. V. Yakonovskiy and M. N. Nikitin on the ice breakers "Kapitan Voronin" and "Kapitan Melekhov", it was determined that the number of collisions of the propeller with ice is a random number which varies within the range between 3 and 8 for one revolution of the propeller. Nominal duration of one impact is about 0.03 - 0.06 second and the stresses in propeller blades may reach 1000 kg/cm^2 which is 10 to 15 fold higher than the stress level during operation in clean water.

The extremely complex dynamics of the propeller impact have not yet been sufficiently studied and therefore, in strength calculations of propellers with detachable blades of ships for ice navigation, towboats, and ice breakers, various assumptions are made (12). To these conditional calculations also belong calculations of studs by taking into account maximum loads.

Determination of the dimensions of sufficiently strong studs for fastening blades to the hub, taking into account maximal loads, is based on the principle that in designing the structural complex "propeller - propeller shaft" there must be maintained a certain /117
arrangement of mutual strength of all elements of the structural complex (disregarding navigation conditions in ice or clear water) (10), (18).

The weakest link in this complex is the blade. In the case of a blade breaking in the plane of minimum rigidity, the fastening studs and propeller shaft should not have plastic deformations, i.e., stresses appearing in them should not exceed the yield point of the material.

Breakdown of the blade may be caused not only by the impact force acting in the direction perpendicular to the plane of minimum rigidity of the blade but also by a force directed under an angle to this plane. Under certain conditions force vectors causing breaking of the blade may also coincide with the line perpendicular to the plane of maximum rigidity. As a rule, the strength of the blade in the direction of maximum rigidity exceeds the strength of the propeller shaft. However, because the total section modulus of all studs of the flange joint in respect to the axis in the plane of maximum rigidity of the blade is practically equal to the total section modulus of all studs of the flange joint in respect to the axis in the plane of minimum rigidity and in some cases is even lower than that, the propeller shaft as a result does not break down.

However, with the extensive fluctuation of hydrodynamic forces on propeller blades and also under the action of impact forces, calculation by taking into account maximum static loads might not provide for sufficient fatigue strength of studs, and an additional corresponding verifying calculation will be necessary (see Section 8).

Section 16. Strength Calculation of Flanged Joints of Assembled Propellers

Flange joints of blades with the hub of the assembled ship propeller are considered to be in the group of parts joined by studs. Calculation of such joints consists in determining forces acting on the stud subjected to the highest load and strength calculation of this stud.

When a joint of several parts is subjected to the action of bending moment, the studs are subjected to unequal loads. The magnitude of the design calculation load depends to a large extent on the following principal premises (8) on which strength calculations of flange joints of propellers are based.

1. Both parts -- flange of the blade and the hub -- possess very high rigidity. Therefore, it may be assumed that there are no deformations of parts at the contact surfaces because of preliminary tightening of studs, and the turn of the supporting surface of the blade flange as a result of bending moment application will take place in respect to the flange edge or in respect to the line connecting the outer studs.

2. Both parts being joined, or at least one of them, possess certain pliability (the blade flange has several cutouts, the blade is made of nonferrous metal, the area of the supporting surface on the hub is small). In such a case, after the moment is applied, /118
one part of the butt joint will be subjected to additional load

while the load on the other part will decrease. The turn of the blade will take place in respect to the axis which passes through the center of gravity of the working part of the contact area, which is sufficiently close to the general center of gravity of cross sectional areas of all studs clamping the blade to the hub.

In strength calculations by maximum stresses, it is considered that the "axis of overturning" passes through most remotely located studs. This almost always happens in reality. In calculations on operational loads, the second premise is usually used.

It should be taken into account that in the latter case, the magnitude of maximum (calculation) load, which falls on the most heavily loaded stud, is higher, since in turning the flange in respect to the axis passing through the common center of gravity of cross sections of all studs, the tension forces are received only by some of the studs. This to some extent increases the margin of safety of the joint as a whole.

The simplest and the most widely used method of strength calculations of studs fastening propeller blades under condition of static action of forces is calculation by maximum load, which is discussed in detail in (9).

Based on the mutual arrangement of blades and studs strength, as a result of calculation, the necessary diameter of studs is determined for a given number of studs and their positioning on the blade flange (Fig. 54).

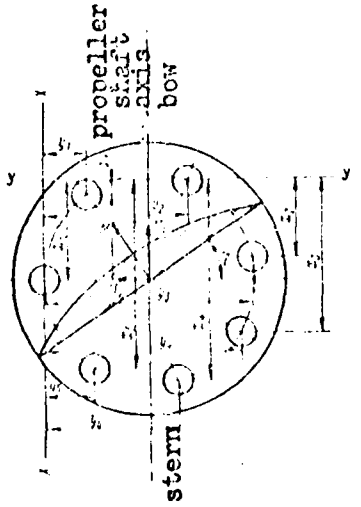

Fig. 54. Schematic diagram of the blade flange and "overturning" axis

It is supposed that the blade is "overtuning" in respect to axes X-X and Y-Y, which pass through the outer studs (see Fig. 54). Moments in respect to these axes M_x and M_y are components of a moment which causes breaking of the blade at its root cross section.

$$M = W\sigma_{b.s} = \alpha_\eta b e^2 \sigma_{b.s}, \qquad (125)$$

where W - section modulus of the blade cross section in respect to the axis of minimum rigidity;

α_η - coefficient from Table 6;

b - blade width in the root cross section;

e - blade thickness in the same cross section; /119

$\sigma_{b.s}$ - tensile strength of blade material.

Calculation of Stud Diameter (13)

Designations

Coordinates of center of gravity of studs cross sections, cm	$x_1, x_2, \ldots, x_{n-1}, x_n;$ $y_1, y_2, \ldots, y_{n-1}, y_n$
Tensile strength of blade material, kg/cm^2	σ_{bs}
Maximum bending moment, kg·cm	$M = \sigma_{bs} W$
Components of bending moment, kg/cm	$M_x = M \sin\varphi;\ M_y = M\cos\varphi$
Number of studs	n
Arbitrary coordinates of center of gravity of studs, cm	$x = \frac{x_1 + x_2 + \ldots + x_{n-1} + x_n}{n}$ $y = \frac{y_1 + y_2 + \ldots + y_{n-1} + y_n}{n}$
Tension force in the stud, kg	$Q = \frac{M_x}{y} + \frac{M_y}{x}$
Yield point of stud material, kg/cm^2	σ_{sm}
Cross sectional area of the stud, cm^2	$F_m = \frac{Q}{\sigma_{sm}}$
Stud diameter, cm	$d = \sqrt{\frac{F_m}{0.785}}$

Position of studs on the flange is shown in Figure 54.

Calculation is performed for determining stud diameter and dimensions of other elements of the flange joint of propellers also for other ships for any conditions of navigation in ice. Propellers subjected to low loads and diameters not exceeding 4.0 m do not require any additional calculation; they require only verifying calculation in accordance with requirements of the Register of the USSR.

Another calculation method for determining the static strength of studs, which much more precisely takes into account the real operational conditions and which in some cases is used as the second approximation, was suggested by Professor V. A. Dmitriyev (8), (15). As a result, the magnitude of stresses in the elements of the flange joint is determined, the dimensions of which were determined in the first approximation by the calculation based on the maximum stresses.

Such calculation is performed for propellers operating in a relatively uniform velocity field with negligible fluctuation of hydrodynamic forces acting on the blades (two-shaft ships, single-shaft ship with block coefficient $\delta \leq 0.8$).

It is assumed that the propeller blade is subjected to the load of hydrodynamic forces P_1 and T_1 and at the center of gravity to the load of centrifugal force P_c (Figure 55). These forces are considered to be constant in their magnitude and direction disregarding the position of the propeller blade in the flow. It is also presumed that the contact surface remains flat after load is applied and the turning of this surface occurs in relation to the axis passing through the center of gravity of the contact surface sufficiently close to the general center of gravity of the cross sections of all studs; at the same time, it is presumed that the load to which each individual stud is subjected is proportional to the distance between the stud and the axis of turning. /120.

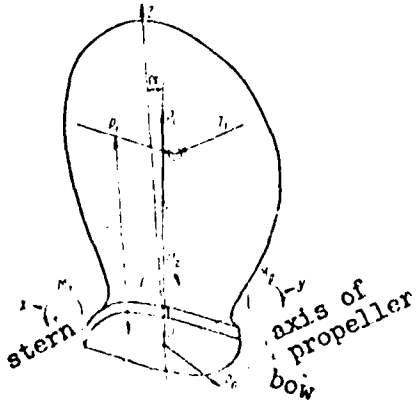

Fig. 55. Forces acting on the propeller blade during operation of a propeller

External action on the blade comprises the action of the following moments and forces at the flange contact: moment M_p from the action of thrust forces in XOZ plane, moment M_T from the action of tangential force in YOZ plane, and the moment M_z from the action of hydrodynamic forces in respect to OZ axis (see Fig. 55); centrifugal force P_c, which is perpendicular to the flange plane* and the transverse force P_t acting in the plane of contact.

*Some deviation between direction of centrifugal force action and the OZ axis is disregarded since it little affects calculation results.

The transverse force $P_t = \sqrt{P_T^2 + P_T^2}$ does not affect the strength of studs since this force is absorbed by the centering projection located on the blade flange (see Fig. 53). It was determined by calculations that shearing and crumpling stresses in the centering projection are very low and it is not necessary to perform strength calculations for this projection.

Moment M_z created by hydrodynamic forces* is neutralized by the

*As a result of forces of ice, see p.134.

moment of friction forces in the contact surface as a result of tightening of nuts fastening the blade under condition that the design and assembly of the flanged joint were properly performed. This makes it possible to rightfully disregard consideration of M_z in strength calculation.

Hence, the contact surface of the joint is subjected to the action of moments M_p and M_T and the centrifugal force P_c. The M_p and M_T moments are calculated by the formulae:

$$M_p = P_t l \text{ и } M_T = T_t l,$$

where l - distance between the point at which thrust and tangential forces are applied and the contact surface of the blade and the hub (see Fig. 55).

Figure 56 illustrates an arbitrary diagram of the flange in which coordinates of the studs in respect to X-X and Y-Y axes are indicated and a scheme of load application is shown. /121

When a joint with a number of studs is subjected to the simultaneous action of various forces and moments, a principle of superimposing may be used, according to which the stress in the n-th stud is

$$Q_n = Q_z + Q_{M_y} + Q_{M_x} = \frac{P_z}{n} + \frac{M_y x_n}{\sum_{n=1}^{n} x_n^2} + \frac{M_x y_n}{\sum_{n=1}^{n} y_n^2} \qquad (126)$$

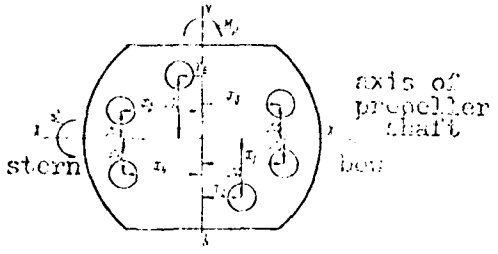

Fig. 56. Arbitrary diagram of the blade flange for strength calculations according to Professor V. A. Dmitriyev's method

Calculation is performed in the form of Table 15 and as a result, the stud of the flange joint which is subjected to a maximum load is determined.

Table 15. Determination of Forces Acting on Studs of a Flanged Joint

Sequential number of the stud within the flange	x_n, cm	y_n, cm	$M_y x_n$, kg·cm	$M_x y_n$, kg·cm	x_n^2, cm²	y_n^2, cm²	$\frac{M_y x_n}{\sum x_n^2}$, kg	$\frac{M_x y_n}{\sum y_n^2}$, kg	$Q_n = \frac{P_z}{n} + \frac{M_y x_n}{\sum x_n^2} + \frac{M_x y_n}{\sum y_n^2}$, kg
1	2	3	4	5	6	7	8	9	10
					$\sum x_n^2$	$\sum y_n^2$			

For reliable and long service life of the joint, of great importance is preliminary tightening of the studs fastening the blade, which provides for the absence of a gap between contact surfaces of the blade and hub.

This tightening force Q_3, kg - is recommended to be $(0,5 \div 0,6)\, \sigma_{adm} F_m$.

After calculating forces, the following values are determined: /122

rigidity of the flange coefficient (Fig. 57)

$$c_\Phi = \frac{E_\Phi F_\Phi}{t_\Phi} = \frac{\pi (D^2 - d_0^2) E_\Phi}{4 t_\Phi}, \qquad (127)$$

where E_Φ - modulus of elasticity of the flange material, kg/cm^2;

d_0 - diameter of holes on the flange for studs, cm;

D - diameter of contact surface of the nut, cm;

t_Φ - thickness of the flange under the nut, cm;

$F_{r.\Phi}$ - area of contact surface between the nut and the flange, cm^2;

coefficient of flange rigidity (see Fig. 57)

$$c_m = \frac{E_m F_m}{l_m} = \frac{\pi d^2 E_m}{4 l_m}, \qquad (128)$$

where d - diameter of the stud, cm;

$l_m = t_\Phi + 0.3\, d$ - effective length of the stud, cm;

E_m - modulus of elasticity of stud material, kg/cm^2;

and also the force of final tightening

$$Q_3' = Q_3 - Q_p \frac{c_\Phi}{c_\Phi + c_m}. \qquad (129)$$

To guarantee tightness of the joint after operational load is applied, the final tightening must be above zero. The force of final tightening should be selected depending on the operational load $Q_3' \geq kQ_p$, where $k = 0.5 \div 0.6$.

After this, the design force for the stud which is subjected to the maximum stress is determined

$$Q = Q_p + Q_3'$$

Design stress in the stud cross section should be

$$\sigma_m = \frac{Q}{F_m} = (0,50 \div 0,67)\sigma_{adm}.$$

The force absorbed by the stud subjected to the maximum load makes it possible to evaluate the strength of the stud and nut thread and the strength of the propeller hub.

The maximum force on the first, maximally loaded turn of the thread is determined by formula

$$U_{max} = \frac{P_z k_H}{n_{B.t}} \text{ kg} \qquad (130)$$

where $k_H = 3$ - is load coefficient;

$n_{B.t}$ - number of thread turns in the nut.

The contact surface of a single thread being calculated to resist crumpling

$$F_{cm} = \pi d_c a \text{ cm}^2,$$

where d_c - median diameter of the thread, cm;

a - height of the thread, cm.

The unit crumpling load of one turn of the thread /123

$$\sigma_{cm} = \frac{U_{max}}{F_{cm}} \text{ kg/cm}^2$$

The permissible bearing load to which the thread is subjected should not exceed the yield point of material of the nut $\sigma_{cm} < \sigma_{s.t}$.

The rated shearing strength of a single turn of the thread is

$$\tau_{cp} = \frac{U_{max}}{F_{cp}} \text{ kg/cm}^2$$

where $$F_{cp} = \pi d_1 S,$$

where d_1 - is outer diameter of the thread in the nut, cm;

S - thread pitch.

The magnitude of the shear stress obtained in this way should satisfy the inequality

$$\tau_{cp} \leq 0,47\sigma_{s.t}$$

Similar calculations may be performed in evaluating the strength in the thread elements of the propeller hub.

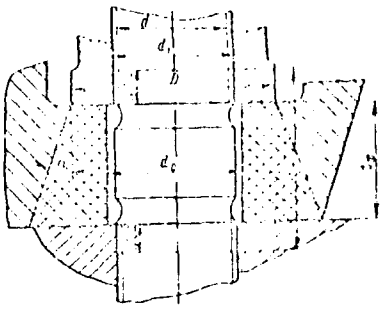

Fig. 57. Concerning calculation of the flange rigidity coefficient

In the case of strongly inclined propeller blades, when the action of the bending moment created by the centrifugal force P_c cannot be disregarded, calculation of the force acting on each individual stud is performed by the formula

$$Q_p = \frac{P_c}{n} + \frac{(M_p + M_c)x_i}{\sum_n x_i^2} + \frac{M_T y_i}{\sum_n y_i^2}.$$

However, as was mentioned previously, calculation of the static strength of studs fastening propeller blades is not always sufficient. The verifying calculation of cyclic strength of the blade joint, which is discussed below, includes determination of forces to which studs are subjected, determination of stresses to which the most loaded stud is subjected, and determination of the necessary safety factor.

If the maximum and minimum values of the thrust $P_{1\ max(min)}$ and the tangential force $T_{1\ max(min)}$ acting on the propeller blade are known, the value of the resultant of variable* hydrodynamic forces may be determined by the formula $P_n = \sqrt{P_1^2 + T_1^2}$.

*Among variable forces may be included impacts of blades against the ice, without affecting the following discussion.

The direction of the resultant force is changing due to non- /124
uniformity of the velocity field in respect to some average direction under an angle of

$$\beta = \text{arctang} \frac{T_1}{P_1}$$

to the axis of propeller rotation (Fig. 58).

Knowing the distance between the flange r_{fp} from the axis of propeller rotation, it is possible to determine moments created by hydrodynamic forces acting in the plane of flange contact by the formulae

$$M_{F_1} = P_1(r_p - r_{fp}) \approx P_1(0{,}7R - r_{fp});$$
$$M_{T_1} = T_1(r_p - r_{fp}) \approx T_1(0{,}7R - r_{fp}).$$

Knowing the weight of the blade together with the flange G, coordinates of the gravity force X_G and Y_G in the XOY coordinate system, and the distance of the center of gravity r_G from the axis of the propeller shaft (propeller), it is possible to calculate the magnitude of centrifugal force (with nominal rpm of the propeller)

$$P_c = \frac{G}{g}\left(\frac{2\pi n}{60}\right)^2 r_G,$$

which creates moments $M_{c_y} = P_c X_G$ and $M_{c_x} = P_c Y_G$ in respect to axes X and Y passing through the flange center. Then, the resulting overturning moment

$$M_{res} = \sqrt{(M_{F_1} + M_{c_y})^2 + (M_{T_1} + M_{c_x})^2},$$

while the direction of its vector forms the following angle with the Y axis (Fig. 59).

$$\beta_{res} = \operatorname{arctg}\frac{M_{T_1} + M_{c_x}}{M_{F_1} + M_{c_y}}.$$

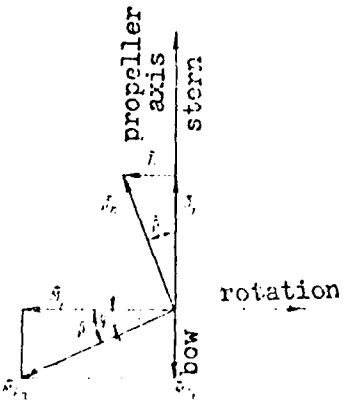

Fig. 58. Forces applied to the blade flange

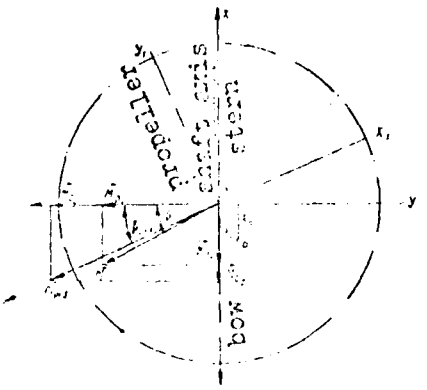

Fig. 59. Resultant overturning moment

To determine the variable cyclic load, the maximum and minimum values of the "overturning" moment ($M_{pe3\ max}$ and $M_{pe3\ min}$) are found. /125

The direction in which this moment is acting little depends on its magnitude. Therefore, it is assumed that

$$\beta = \beta_{pe3\,max} = \operatorname{arctg} \frac{M_{T_1\,max} + M_{c_x}}{M_{P_1\,max} + M_{c_y}}.$$

The threaded stud joint in the propeller is assembled with a prestrain. In order to determine the force acting on each stud during service of the flanged joint within the limits of elastic deformations, we find the coefficients of stud and flange couple rigidity which is equal to the sum of rigidities of both the stud and the flange, i.e.,

$$c_A = c_ш + c_ф. \tag{131}$$

The coefficient of stud rigidity is calculated by formula (128).

When the diameter of the stud varies along its length $l_ш$, its rigidity coefficient may be found by formula

$$c_ш = E_ш \sum_k \frac{l_{iш}}{F_{iш}} = E_ш \left(\frac{l_{1ш}}{F_{1ш}} + \frac{l_{2ш}}{F_{2ш}} + \ldots + \frac{l_{kш}}{F_{kш}} \right), \tag{132}$$

where $l_{iш}$ - length of stud portion with the cross section area $F_{iш}$.

In determining the rigidity coefficient of the flange it is assumed that under the action of force in the longitudinal direction of the stud, a uniform deformation in the cross section propagates within "the cone of influence" (see Fig. 57). Then, the coefficient of flange rigidity is calculated with the help of a more accurate formula

$$c_ф = \frac{E_ф \pi \left[(D + l_ф \operatorname{tg} \alpha)^2 - d^2 \right]}{4 l_ф}.$$

where D - diameter of contact surface of the nut;

α - angle between the stud axis and the generatrix of "the cone of influence" (see Fig. 57); it may be assumed that $\tan \alpha = 0.4 - 0.5$;

d_0 - diameter of holes for studs in the flange;

E_f - modulus of elasticity of the blade flange material.

With the help of formula (131) we find the rigidity coefficient for the elastic couple stud-flange C_A.

$$X_{i_0} = \frac{\sum_n C_A X_{i_f}}{\sum_n C_A} \quad \text{and} \quad Y_{i_0} = \frac{\sum_n C_A Y_{i_f}}{\sum_n C_A}.$$

The reaction force Q_{pM} of each elastic couple (stud-flange) is equal to the part of operational load caused by the action of that portion of resultant overturning moment created by external forces M_{pe} which is absorbed by each individual stud. Force Q_{pM} can be presented, as can any other force, in the form of a product of the total rigidity of the elastic couple (C_A) elements by the amount of deformation of parts ζ, i.e., $Q_{pM} = C_A \zeta$. /126

To calculate these deformations, it is necessary to determine the direction of the "overturning" axis of the bearing surface of the blade flange which, generally speaking, does not coincide with the X_1^* axis and is characterized by the angle α, and also to

*Direction of the X_1 axis coincides with the negative direction of the resultant M_{pe}.

determine the angle of turn α_k of the bearing surface (Fig. 60 and 61).

Omitting detailed discussions, below is the formula for calculating angle α.

$$\operatorname{tg}\alpha = \frac{\sum_n (Y_{i_f} - Y_{i_0}) X_{i_f}}{\sum_n (X_{i_f} - X_{i_0}) Y_{i_f}}. \qquad (133)$$

Auxiliary calculations with the use of this formula may be conveniently presented in tabular form (Table 16).

Angle α_k is calculated by formula

$$\alpha_k = \frac{M_p \cos\alpha}{\sum\limits_{i} (\eta_i - \eta_0)^2} \qquad (134)$$

Table 16. Table for Calculations With the Help of Formula (133)

Sequential numbers	X_{1i}	Y_{1i}	$X_{1i} - X_{10}$	$Y_{1i} - Y_{10}$	$(X_{1i} - X_{10})X_{1i}$	$(Y_{1i} - Y_{10})Y_{1i}$
1						
2						
3						
$n-1$						
n						
					Σ	Σ

(η_i see in Fig. 61), $\eta_0 = X_{10} \sin\alpha - Y_{10} \cos\alpha$).

The sum in the denominator of equation (134) may be also calculated conveniently in tabular form (Table 17).

The minimum and maximum values of α_k may be found with the help of formula (134) by substituting respective values of moments

$$M_{p\,max} = \sqrt{(M_{T_1\,max} + M_y)^2 + (M_{T_1\,max} + M_x)^2};$$
$$M_{p\,min} = \sqrt{(M_{T_1\,min} + M_y)^2 + (M_{T_1\,min} + M_x)^2};$$

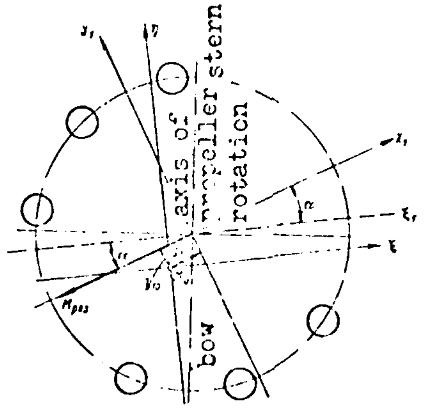

Fig. 60. Position of coordinate system /127

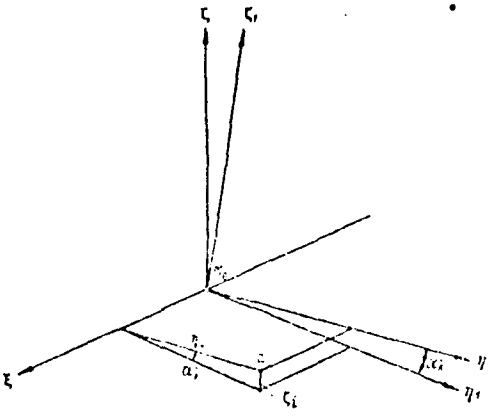

Fig. 61. Concerning calculation of overturning angle α and amount of deformations of the stud and flange ξ

Table 17. Table for Calculations With the Help of Formula (134) /128

Sequential numbers	η_i	η_i^2	$\eta_i\eta_0$	$\eta_i^2 - \eta_i\eta_0$
1 2 3 ... $n-1$ n				
				$\frac{\Sigma}{n}(\eta_i^2-\eta_i\eta_0)$

The portion of working load due the action of the resultant moment of external forces absorbed by each stud

$$Q_{pM} = \frac{M}{\frac{\Sigma}{n}(\eta_i^2-\eta_i\eta_0)}\eta_i$$

is calculated for all elastic couples (Table 18).

Table 18. Calculation of the Variation of Variable Stress Range for Each Stud

Sequential numbers	η_i	$Q_{pM_{max}}$	$Q_{pM_{min}}$	$Q_{pM_{max}} - Q_{pM_{min}}$
1 2 3 ... $n-1$ n				

After calculation is completed, a stud subjected to the action of load with a maximum fluctuation (in which the absolute value of the difference $Q_{pM\ max} - Q_{pM\ min}$ is greatest) and another stud which is subjected to a maximum tension force are selected.

The safety factor in respect to fatigue strength is determined only for the stud with a maximum load fluctuation.

For studs subjected to a maximum tensile load (sign " + "), the safety factor is determined in respect to the yield point ($\sigma'_{s\ b}$).

In the assembled structure the stud is subjected to the action of force

$$Q = (Q_3 - c_\varphi \xi) + Q_p,$$

where Q_3 - force of preliminary tightening; /129

$(Q_3 - c_\varphi \xi)$ - force of residual tightening;

Q_p - operational load.

Taking into account centrifugal force, the operational load

$$Q_p = Q_{pM} + \frac{P_c}{n},$$

maximum force absorbed by the stud $Q_{p_{max}} = Q_{pM_{max}} + \frac{P_c}{n}$,

minimum load absorbed by the stud $Q_{p_{min}} = Q_{pM_{min}} + \frac{P_c}{n}$.

After this, the amplitude of the fluctuating component of the load absorbed by the stud can be determined

$$Q_a = 0{,}5\,(Q_{max} - Q_{min}) = \frac{c_w}{c_w + c_\varphi} \cdot \frac{Q_{p_{max}} - Q_{p_{min}}}{2}$$

and the average load

$$Q_m = 0{,}5\,(Q_{max} + Q_{min}) = \frac{c}{c_w + c_\varphi} \cdot \frac{Q_{p_{max}} + Q_{p_{min}}}{2}.$$

Knowing the cross sectional area of the stud F_{th}, we obtain respective values of stresses: the amplitude of cyclic stresses $\sigma'_a = \frac{Q_a}{F_w}$ and the average stress $\sigma'_m = \frac{Q_m}{F_{th}}$.

The safety coefficient in respect to fatigue strength should be determined only for the threaded portion of the stud, because stress concentration in this portion is the most dangerous; for this purpose, the following formula is used $n_{\sigma w} = \frac{\sigma_{-1}}{K_\sigma \sigma'_a + \psi_\sigma \sigma'_m}$.

where σ_{-1k} - fatigue limit of the stud taking into consideration the stress concentration in the threaded part of the stud.

For studs made of stainless steel, it may be assumed that $\sigma_{-1k} = 3.5$ kg/mm^2, which provides for $n_a \geq 2.5$.

In calculating the safety coefficient for the stud subjected to maximum tensile load it is necessary also to take into account that in addition to tensile stress, the maximum value of which

$$\sigma_{max} = \frac{Q_{max}}{F_{st}} = \frac{\pi d^2}{4}\left(Q_3 + \frac{c_{st}}{c_{st}+c_\phi} Q_{1max}\right),$$

there also emerge tangential stresses as a result of tightening M_{st} /130

$\tau = \frac{M_{st}}{0.2d^3}$. The magnitude of the moment of tightening M_{st} is determined by the following expression:

$$M_{st} = \sigma_3 \frac{\pi d^3}{8}\left(\frac{S}{\pi d_{cp}} + f'\right),$$

where σ_3 - stress in the stud caused by preliminary tightening;

S - thread pitch;

d_{cp} - inner diameter of thread of the stud;

f' - friction coefficient in the thread (friction between materials of the nut and the stud, see p. 135 of original text).

Reduced stress is calculated by the formula

$$\sigma_{np} = \sqrt{\sigma^2_{max} + 3\tau^2},$$

and the safety coefficient in tension according to the yield point will be $n_{s\sigma} = \frac{\sigma_{s\sigma}}{\sigma_{np}}$. For parts of threaded joints, the value of $n_{s\sigma}$ is assumed to be larger than or equal to 1.5 - 2.0.

The degree of preliminary tightening should also be checked since its loss, due to crumpling of surface irregularities, may lead to overload of studs by cyclic forces. The necessary degree of tightening for the stud subjected to maximum loads is determined by the ratio $\frac{Q_{p\,max}}{Q_3}$; at the same time, the preliminary tightening force should exceed the operating load by a factor of 2-3.

The contact pressure on the propeller hub by the contact surface of the nut should also be checked $p = \frac{Q_{max}}{F_{k.c}}$,

where contact surfaces of the nut and hub (see Fig. 57)

$$F_{1.c} = \frac{\pi}{4}(D^2 - d_0^2).$$

With the yield point of the hub material σ_{sc}, the safety factor in compression $n_{sc} = \frac{\sigma_{sc}}{p_r}$; usually $n_{sc} \geqslant 1.3$.

Recommendations for using certain brands of materials for the elements of flanged joints are given in Section 21.

The safety of ship navigation depends to a large extent on the reliability of propellers. Therefore, classification societies of many countries regulate the strength and size of studs for fastening detachable blades and also require fulfillment of certain rules in the design of flanged joints of blades with the hub. Published /131
rules include calculation formulae for determining the minimum permissible diameter of the stud or its minimum permissible cross sectional area. These formulae were obtained by making several assumptions and simplifications of operational conditions of flanged joints within a propeller structure. This makes it possible to simplify final expressions and make them more convenient for quick verifying calculations. In deducing these formulae, statistical material based on generalization of experience in manufacturing and operation of propellers with detachable blades was taken into consideration, which made it possible to avoid rough miscalculations during evaluation of stud strength.

In the rules of the USSR Register of 1971, the formula for determining the minimum permissible diameter of studs fastening blades to the hub is of the following form:

$$d = ae\sqrt{\frac{b\sigma_{b.n}}{d_m\sigma_{y.m}}} \text{ mm} \qquad (135)$$

where e - blade thickness* in the root cross section, mm;

*In the rules of the Register the blade thickness is denoted by "t".

b - width of the blade in the same cross section, m;

d_m - diameter of the circle on which the studs are located, m; for other positions of studs $d = 0.85\,l$, where l - distance (m) between the most remote studs (Fig. 62);

$\sigma_{b.n}$ - tensile strength of blade material, kg/mm^2;

$\sigma_{b\,w}$ - tensile strength of studs material, kg/mm^2;

a - coefficient the value of which is 0.34, 0.30, or 0.28, depending on the number of studs in the flange (3, 4, and 5, respectively) on the forcing side of the blade.

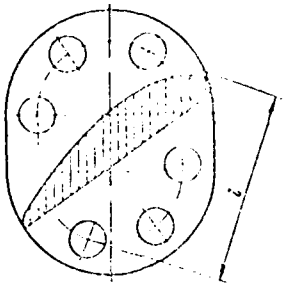

Fig. 62. Distance between most remote studs

In order to establish the level of requirements for the strength of studs calculated by the rules of the USSR Register, the American Bureau of Shipping, German Lloyd, and the Japanese Classification Society Nippon Kaigi Kichai, the diameter of studs was determined for more than 40 various designs of propellers.

For comparison of results, the average arithmetic values were found for the ratio of stud diameter found by respective formulae of foreign classification societies to the diameter found by formulae of the USSR Register:

Register USSR	1.0
American Bureau of Shipping	0.95
German Lloyd	0.90
Nippon Kaigi	0.97

/132

A comparison of these data shows that the difference in values is within 10%. The rules of Norwegian Veritas and British Lloyd do not contain formulae for calculating stud diameters.

Section 17. Some Design and Manufacturing Methods Providing For the Strength of Assembled Marine Propellers

Selection of dimensions and design of the elements of propellers is based on norms and recommendations compiled by the shipbuilding industry which make it possible to avoid rough miscalculations and provide for a reliable performance of ship propellers.

To determine in a first approximation the diameter of studs or their number for fastening detachable blades, an approximate formula derived by M. N. Nikitin may be used

$$d \approx \left| \frac{\quad}{\quad} \right| \qquad (136)$$

where n - number of studs on the forcing side of the blade; the other designations are the same as those used in Formulae (135).

In respect to design, the studs may be broken down into three main types (Fig. 63).

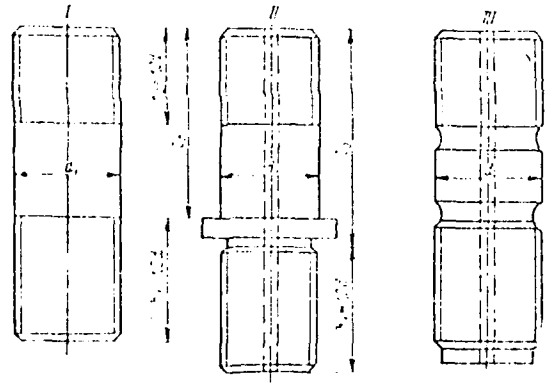

Fig. 63. Principal types of studs (I, II, III) used for fastening detachable blades

The first type of studs is the least perfect, since when it is screwed in as deep as possible into the deadend hole in the hub, the stud is stopped by the run off the thread where the thread is incomplete or crumpling of the thread or slight tears are present, which are extensive stress concentrators. In addition, the body of the stud has a sharp transition from the threaded to cylindrical part which causes non-uniformity of the state of stress and aggravates stress concentration. /133

The studs of the second type with a shoulder are more perfect. The shoulder or collar creates normal conditions of performance of individual threads and is supposed to prevent loss of the stud in case of its loosening. However, the collar does not prevent loosening of the stud since between the upper shoulder of the collar and the bearing surface of the flange there is always a gap of 0.3 - 0.5 mm.

When the fit of the stud in the blind hole is tight, the stress in the stud during the process of assembly and tightening to the limit may reach 0.2 - 0.3 of the yield point of the stud material.

Under the action of tightening force and operational load on the stud, its upper threads are subjected to the additional load, which for the studs of the first two types might result in overloading of the upper threads, appearance of plastic deformations, and localized fractures (64, a).

Studs of the third type differ from the first two types because they have relatively smooth transition of cross sections along their length and in the lowest end the stud has a projection which will touch the bottom of the blind hole in the hub.

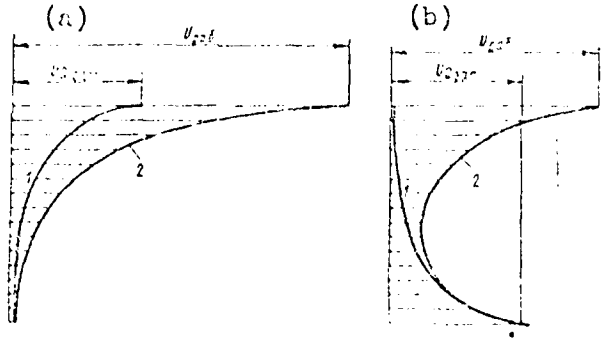

Fig. 64. Diagram of load distribution on the thread of different types of studs: a - studs of types I and II, b - studs of type III.

1. force absorbed by the thread during assembling of the stud in the hub; 2. total force acting on the thread during operation of the ship propeller.

In this case, the load is distributed between individual threads much more uniformly (Fig. 64, b), since during installation of the stud the threads at the lower end of the stud will be subjected to higher loads, while under the action of operational force the upper threads will be subjected to higher load. Under conditions of the general state of stress in flanged joints of a propeller, the loosening of one stud, as a rule, will cause overloading of other studs and rapid /134

breakdown and a loss of the whole blade regardless of whether a collar is provided on the stud or not. Therefore, in selecting the design of the elements of a flanged joint in ship propellers, all measures should be taken to prevent the possibility of even slight loosening of studs and appearance of dynamic stresses.

It is recommended to maintain for all three types of studs the following relationships of dimensions, which provide for the strength of threads in the hub and the nut and also for sufficient strength of the blade flange:

the length of the threaded part of the stud which is screwed into the hub should be no less than 1.2d;

the length of the threaded part of the stud for the nut and the thickness of the flange under the nut should be no less than 1.0d.

To provide for sufficient strength of the flanged joint, the studs are always installed tightly in the threaded holes in the hub; otherwise, under the action of variable load, mutual slips may take place between individual threads which will lead to a considerable friction decrease in the thread and to self loosening (9).

In ships, navigating under ice conditions, during impact of blades against the ice, the moment, which tries to turn the blade in respect to vertical axis, may reach a magnitude comparable with that of the propeller shaft and exceed the moment of friction forces between the blade flange and the bearing surface of the hub (32). In this case, the studs in the assembled propeller are absorbing shearing forces, which aggravates the tendency of the studs to self loosening. If studs are loosened, the load becomes of a dynamic character and the joint will break down.

From the experience of general machine building, it is known that the strength of the studs or bolts which fasten blades may be enhanced under the action of variable loads by roller burnishing of studs, bolts, and their thread.

With the proper rates and by using even the simplest technology, the fatigue strength of stud material may be increased by approximately 30% as compared with that before roller burnishing.

However, it should be noted that this manufacturing process until now has not been used for assembled propellers with a constant pitch.

The design of flanges of detachable propeller blades has a considerable effect on the propeller strength. Bearing surfaces of the blade flange and the hub exert considerable pressure against each other during tightening of nuts. In order to exclude the /135
possibility of loosening after preliminary tightening of the joint, which may be caused by plastic deformations of surface irregularities, the contact of bearing surfaces must be tight. Therefore contact surfaces should be scraped with a number of spots, no less than two on an area of 2.5 X 2.5 cm^2.

There is experience in machining the contact surfaces of blade flanges and propeller hubs of the atomic ice breaker "Lenin" (without manual finishing) with a very high surface finish of class 7 (▽ 7) and simultaneous inspection of surface flatness with a tolerance of 0.03 mm deviation from flatness in direction of concavity on the length of one meter. However, because of the complexity of inspection, this method did not receive wide use.

Nuts for fastening propeller blades are always made in the form of a screw cap in order to protect the screw joint from water. Controlled tightening of nuts is especially important for enhancing the strength of blade joints in assembled propellers. Analysis of the causes of propeller breakdowns showed that the main causes of stud failure were insufficient, excessive or, which is particularly dangerous, non-uniform tightening of nuts. The degree of tightness is controlled by the wrench torque or by the angle of nut turn.

To determine the torsional moment on the wrench, a known formula may be used:

$$M_{k.r} = Q_3 \frac{d_{cp}}{2} \operatorname{tg}(\psi + \rho) + \frac{1}{3} f Q_3 \frac{D^3 - d_{cp}^3}{D^2 - d_{cp}^2} \quad \text{kg·m} \qquad (137)$$

where Q_3 - force of preliminary tightening, kg;

d_{cp} - mean thread diameter, mm;

ψ - angle of lead of thread helix, degrees;

$$\operatorname{tg}\psi = \frac{S}{\pi d_{cp}},$$

where S - thread pitch, mm;

$\rho = \operatorname{arctg} \frac{f''}{\cos \frac{\alpha}{2}}$ - reduced friction angle, degrees;

f'' - friction coefficient in the thread;

α - angle of thread, degrees;

f - coefficient of friction between face of the nut and the blade;

$\bar{D}$ - outer diameter of contact surface of the nut, mm.

Values of friction coefficient are within the range of $f = 0.12 \div 0.13$ and $f = 0.15 \div 0.18$ but with the use of disulfide molybdenum lubricants decrease to 0.05.

For approximate calculation of the torsional moment on the wrench, the following formula may be used (21):

$$M_{кл} = 0{,}015 \frac{c^2 b d_{ш} \sigma_{b.ж}}{d_1 n} \quad \text{kg} \cdot \text{m} \qquad (138)$$

where c - blade thickness in the root cross section, cm; /136

b - blade width in the same cross section, m;

$d_{ш}$ - diameter of the circle on which centers of studs are located, cm; with the other locations of studs $d_{ш} = 0.85\ l$, where l - distance between most remote studs;

n - number of studs on the forcing side of the blade;

d_1 - outer diameter of the stud thread, cm;

$\sigma_{b.ж}$ - tensile strength of the blade material, kg/mm^2.

Since nuts are usually made of material with lower tensile strength as compared with material used for studs, it is recommended to perform a verifying strength calculation of the nut thread in shear (8); it is necessary that the following expression should hold

$$\tau_{ср} = 0{,}22 \frac{k_н d_1^2 \sigma_{s.ш}}{d H_г} \leq [\tau_{ср}], \qquad (139)$$

where $k_н = 2$ - coefficient of load for heavy thread with a number of threads along the nut height $n_г \approx 6$;

$k_н = 3$ - for fine thread with a number of threads along the nut height $n_г \approx 10$;

d_1 - outer diameter of the stud thread, mm;

$H_г$ - height of the threaded part of the nut, mm;

$\sigma_{s.ш}$ - yield point of the stud material, kg/mm^2;

$(\tau_{ср}) = 0.4\sigma_b'$ - permissible shearing stress for the material of the nut, kg/mm^2.

Section 18. Strength Calculation of Assembled Propellers Face of Traction

Plastic propellers may be designed as solid or assembled.

Strength calculation of such propellers comprises calculation of blade strength (for solid propellers) and calculation of general blade strength and strength of the blade joint with the hub (for assembled propellers).

Strength calculation of plastic blades is performed in the same way as is done for metal blades according to the methods discussed in Chapter I. However, properties of plastics are different from those of metals and design of plastic propellers differs in some features from that of metal propellers and differs in strength calculations as well.

In respect to strength properties, plastics differ from metals in the following:

wider variation of mechanical properties which depend extensively on their manufacturing technology, complex structure of material, and other factors;

anisotropy of mechanical properties of reinforced plastics; /137

dependence of strength of plastics in a structure on the effect of the surrounding medium, character of state of stress, and other factors.

Therefore, taking into account special features of synthetic materials, permissible stresses should be determined by the following formula:

$$|\sigma_i| \quad \frac{\sigma_{ik}}{n_i},$$

where (σ_i) - permissible stress for propeller blade material at nominal regime;

σ'_{ik} - maximum design stress in material of the structure;

n_i - safety strength factor, which depends on the design (nominal) regime.

Engineer K. P. Sidorov suggests any of the following regimes as a design regime for plastic propellers:

regime of static load of long duration which corresponds to specifications for ship exploitation (usually used in calculations of static strength);

regime of cyclic application of load, stipulated by non-uniformity of the velocity field in the propeller disk (mainly in cyclic strength calculations for a single-shaft ships);

regime of short duration overloads: reverse, maneuvering, collision, etc.

In these cases, the magnitude of the maximum stress in the propeller structure is calculated by one of the following formulae:

$$\sigma_{s} = k_{M} k_{v} k_{T} k_{t} \sigma_{0}'$$
$$\sigma_{-1K} = k_{M} k_{K} k_{T} k_{-1} \sigma_{0}'$$
$$\sigma_{0K} = k_{M} k_{K} k_{T} k_{c} \sigma_{0}'$$

where σ_{0}' - strength of plastic material in static bending of standard specimens in respect to the base kg/mm^2 (Table 19);

$k_{M}, k_{K}, k_{T}, k_{t}, k_{-1}, k_{c}$ - coefficients taking into account the effect of various factors on strength characteristics of pressure-molded material in manufactured parts (Table 20).

The strength safety coefficient is also selected in respect to the design regime characteristic of the operational conditions of propellers

$$n_{s} = n_{c} n_{M} n_{01}$$

or

$$n_{-1} = n_{M} n_{01}$$

or

$$n_{0} = n_{p} n_{c} n_{M} n_{01}$$

where $n_{p} = 2.0$ - coefficient taking into account an increase in the load on propeller blades during reverse;

$n_{c} = 1.3$ - coefficient taking into account the load increase during operation on the mooring regime;

Table 19. Mechanical Properties of Reinforced Plastics (Pressure-Molded Materials) Used for Marine Propellers

/136

Property	Brand of Material			
	СТ-1-С-30	СТ-1-Т/С-30	СТ-1-СК	СТ-1-К-25
Bending strength in static bending in respect to the base, σ_c, kg/cm^2	5000	5500	6000	6500
Compression strength in direction perpendicular to the layers, $\sigma_{c\perp}$, kg/cm^2	4000	4000	4000	4000
Shear strength in direction perpendicular to the layers, $\tau_{c\perp}$, kg/cm^2	1500	1700	1700	2000
Modulus of elasticity in bending in respect to the base, $E_{\parallel}$, kg/cm^2	$2.8 \cdot 10^5$	$3.0 \cdot 10^5$	$3.4 \cdot 10^5$	$4.0 \cdot 10^5$
Modulus of elasticity in compression, perpendicular to the layers, $E_{c\perp}$, kg/cm^2	$1.3 \cdot 10^5$	$1.3 \cdot 10^5$	$1.3 \cdot 10^5$	$1.3 \cdot 10^5$

NOTE: Non-stability of the modulus of elasticity of pressure-molded materials does not exceed 5%.

Table 20. Coefficients Taking into Account the Effect of [illegible] on the Strength of Metals Material [illegible] Type

Acting Factor	Coefficients	Range of Testing
Dependence of strength on variable factors	$k_t=0.8\cdot 2(1-0.065 \lg t)$ (static load) $k_{-1}=0.5\cdot 4(1-0.092 \lg N)$ (cyclic load)	$10^{-1} \leq t \leq 10^{4}$ hr. $10^{3} \leq N \leq 10^{7}$ cycles
Technological factor	$k_T=0.9\,\frac{1-0.135 \lg W}{1-0.075 \lg W}$	$10^{-1} \leq W \leq 10^{4}$ cm
Scale factor	$k_M=1-0.075 \lg W$	$10^{-1} \leq W \leq 10^{4}$ cm
Effect of surrounding medium (sea water)	$k_c = 0.90 \div 0.95$	-
Stress concentration	$k_k = 0.90 \div 0.95$	-

NOTE: 1. Coefficients k_T, k_M, k_c, k_k - given for static load.
2. t and N - service life of the specimen; W - section modulus of the specimen.

n_{II} = 1.5 - coefficient taking into account non-uniformity of the load on blades during one revolution of the propeller; /132

n_{III} = 1.6 - variational coefficient, taking into account the instability of strength characteristics of material and inaccuracies in calculating external forces.

Permissible stresses in plastic propellers for principal design regimes are calculated by the following formulae, respectively:

$$[\sigma_1] = \frac{\sigma'_s}{n_I};$$

$$[\sigma_{II}] = \frac{\sigma'_s}{n_I n_{II}};$$

$$[\sigma_{III}] = \frac{\sigma'_s}{n_{III}}.$$

Anisotropy of mechanical properties of pressure-molded materials (see Table 19) was the reason that plastic blades with flanges are not used in pressmolded propellers. Instead of the flange, propeller blades made of plastics are manufactured with a thick end which, in its cross section, has a dovetail shape (25) (Fig. 65). Blades are held in the dovetail slots of the hub by means of wedges; during operation of the propeller the dovetail root of the blade is subjected to the forces emerging in the root (Fig. 66). The magnitude of compression stresses emerging in the dovetail joint of the blade during propeller operation combined with stresses caused by preliminary tightening should not exceed the yield point σ'_s in prolonged static load.

According to test data, the yield point $\sigma'_s = 0.3\ \sigma'_{c\,\omega} \approx 1300$ kg/cm, depending on the type of pressure-molded material.

Data necessary for calculation of forces and stresses in the blade-hub joint:

Propeller diameter, m . . . . . D

Propeller pitch at $\bar{r} = 0.65$, m . . . . . h

Number of blades . . . . . Z

Thrust of propeller, kg . . . . . P

Tangential force, kg . . . . . T

Dimensions of the root part of the blade, mm

width . . . . . b

height . . . . . h

length of contact edge l

wedge angle, degrees . . . . . γ_{1K} G

Angle between the side and the base of the dovetail, degrees . . . . . β

length of the blade, mm L

Some of these data are shown in Fig. 65 and 66. /310

Calculation of forces and stresses in the joint of the blade with the hub is carried out in the following order:

Dimensions of the root cross section of the blade, mm:

maximum thickness . . . . . e_k

width . . . . . b_k

Angle between the axis of the dovetail and axis of propeller rotation . . . . . α

Resultant of external forces acting on the blade . $P_R = P_1 \sin\alpha + T_1 \cos\alpha$

Area of the contact side of the dovetail root of the blade . . . . . $F_{cp} = 0{,}5hl$

Area of the reactions on the dovetail in the joint area in the hub (see Fig. 66) . . . . . $x_{1,-1} = \frac{1}{6}\left(5b - \frac{h}{\operatorname{tg}\beta}\right)$;

$x_{1,1} = \frac{2}{3}\,b\sin\beta - \cos\beta\left(b - \frac{h}{\operatorname{tg}\beta}\right)$;

$x_{1,3} = L - 0{,}5R - \frac{h}{6}$

Maximum reaction in the dovetail joint R_3 . . $P_1 \; P_R \frac{x_{1,1}\sin(\alpha + \gamma_{1K}) + x_{1,3}}{x_{1,1}\cos\alpha + x_{1,1}} \times$

$\times \cos(90 - \alpha - \alpha_{(x,z)})$

Maximum contact stresses on the sides of the dovetail of the blade caused by operational loads (point A in Fig. 66) . . . . . $\sigma_A \frac{4P_1}{l_{cp}}$

Contact stresses on the side of the dovetail caused by shearing force . . . . . $\sigma_{cs} \frac{P_2}{l_{cp}}$

Contact stresses on the sides of the dovetail of the blade caused by preliminary tightening . . . $\begin{cases} \sigma_{cn} = n_1 \sigma_{cA} \\ \sigma_{cn} = n_1 (\sigma_c + \sigma_{cs}) \end{cases}$

Combined contact stresses at the point A (Fig.66) $\sigma_c = \sigma_{cn} + \sigma_c + \sigma_{cs}$

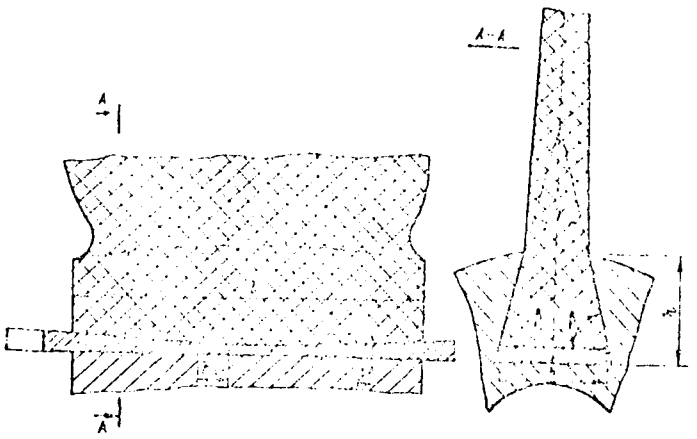

Fig. 65. Joint of plastic blade with the metal hub of propellers with a constant pitch /144

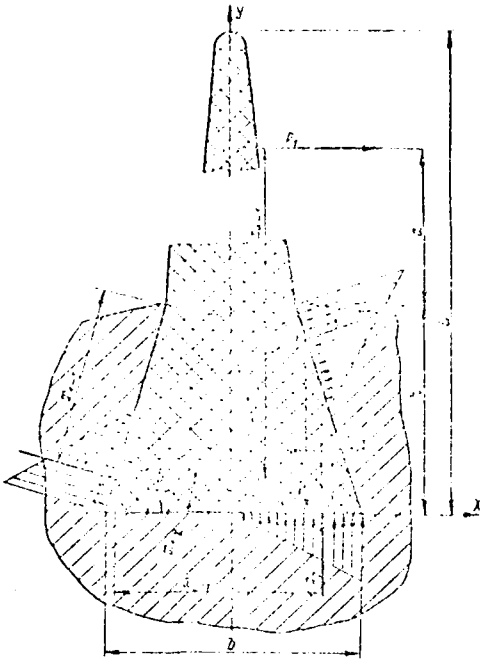

Fig. 66. Diagram of reactions in the blade-hub joint, which emerge under the action of external forces.

1, 2, 3, 4 - points at which resultant reaction forces and the thrust force are applied.

Coefficient of load increase on propeller blades with the change in rotation direction . . . . $n_p = \frac{\sigma_{b.w}}{\sigma_{b.w} + \sigma_b n_t + \sigma_c n_t}$ n_s /142

Area of root cross section of the blade . . . . . is determined by measuring with a planimeter or is calculated approximately by formulae $F_k \approx 0.6 b_k e_k$

Stresses in the root cross section of the blade caused by shearing force . . . . . $\tau_{sh} = \frac{P_n}{F_k}$

Safety factor in shear . . . . . $n_\tau = \frac{\tau_{-1}}{\tau_k} n_t$

Force of the wedge fit . . . . . $Q = 0.05 \sigma_{b.w} F_{tp}$

Depth of forcing in the wedge . . . . . $h_{cl} = \frac{b \sigma_{b.w}}{F_{cm} \cos\beta (\mu_{cm} + \mu_{cl})}$

Section 19. Strength Calculation of the Unit of Stud Installed in Blind Holes in the Hub [illegible]

In manufacturing and maintenance of propellers with detachable blades in some cases a method for installation of studs with a guaranteed tightness suggested by G. I. Petrov is used (Fig. 67).

Strength calculation begins with determining of necessary diameter of studs (see Sections 16 and 17). Knowing stud diameter, a force necessary to rupture the stud is determined by the formula

$$Q_0 = \sigma_{sm} \frac{\pi d^2}{4}.$$

As a rule, the hub of propellers with detachable blades is made of material possessing lower mechanical properties as compared with the stud material. Therefore, the maximum contact pressure on contact surfaces of the blind hole and the stud is selected in such a way as not to cause plastic deformations of the wall of the cylindrical hole

$$q = k\sigma_{sc},$$

where σ_{sc} - yield point of hub material, kp/cm^2;

k - coefficient taking into account the three-dimensional state of stress of material at the contact surface of the blind cylindrical hole in the hub (for calculations it may be assumed that k = 0.85).

The minimum diameter necessary for the part of the stud being fitted into the hub with a guaranteed tightness is calculated by the expression

$$d_0 = \frac{Q_p}{\pi q h f},$$

where h - height of the part of the stud fitted into the hub (see Fig. 67); /143

f - coefficient of friction between contacting surfaces of the stud and the hub.

Coefficient of friction for studs made of stainless steel and installed in a steel hub by means of cooling may be assumed to be within the range of 0.19 - 0.21 during axial displacement (8), (27).

The necessary diametrical tightness (interference), under condition that stress q is achieved on the contact surfaces, is calculated by the Lame formula

$$\delta = qd_0\left(\frac{C_m}{E_m} + \frac{C_c}{E_c}\right). \qquad (140)$$

where $E_ш$ and E_c – moduli of elasticity of the stud and hub, respectively. Coefficient of pliability of the stud

$$C_ш = \frac{d_ш^2 + d^2}{d_ш^2 - d^2} - \mu,$$

where d – diameter of through hole in the stud (see Fig. 67);

μ – Poisson's ratio of stud material.

However, calculation with the help of [illegible] formulas for blind holes with [illegible] ratio close to one, results in [illegible] error, since the rigidity of a cylindrical blind hole is far greater than the rigidity of a corresponding cylinder. Based on the analysis of experimental data on [illegible] joints of cylindrical parts fitted with interference into blind holes of small depth, the value of the coefficient of pliability of the hub c_c with a blind hole for the stud may be assumed to be equal in formula (140) to 0.5 – 0.6.

Practically, interference determined by formula (140) should be slightly higher, taking into consideration correction for crumpling of surface irregularities (8).

Necessary cooling temperature for the stud

$$t_1 = -\frac{2\delta}{\alpha d_ш} + t_0, \qquad (141)$$

where $\alpha = 8 \cdot 10^{-6}$ – coefficient of linear expansion of steel, deg^{-1};

t_0 – nominal temperature of the hub during assembly, deg.

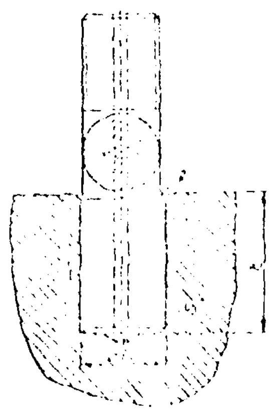

Fig. 67. Stud installed in a blind hole in the hub with a guaranteed tightness

Section 20. Strength Calculation of the [illegible] of Propeller Blades [illegible]

Propellers with detachable blades are finding wider and wider application. These blades are installed in the seats of a propeller hub with a guaranteed tightness (Fig. 68).

The suggested strength calculation makes it possible to determine the minimum dimensions of the root end of the blade, i.e., its seat in the hub.

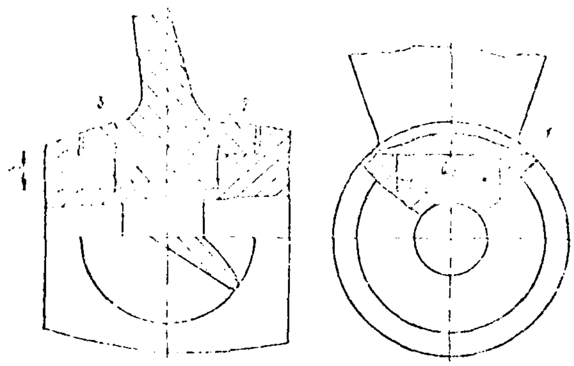

Fig. 68. Propeller with detachable blades, the root ends of which are installed in the hub with a guaranteed tightness.

1. cylindrical root end of the blade; 2. hole for oil supply in disassembly; 3. oil cavity.

The principle of this structure performance consists in the following: after equalization of temperatures of the root end of the blade and the hub during cooling in the course of assembly, on the contact surfaces emerges a considerable contact pressure because of a fit with interference (Fig. 69,a).

Under the action of bending moment, the root end of the blade tends to turn to a certain angle φ, while the walls of the seat in the hub resist that (Fig. 69,б).

As a result, in the elements of the joint emerge reactive forces which will lead to redistribution of contact pressure and will create an equilibrium moment of the opposite direction $M_{к.д}$ (9). At the same time, under the action of contact pressure, on the contact surfaces of the blade root and the hub will appear friction forces which create friction moment $M_{тр}$ of the same sign as the $M_{к.д}$.

Because the ratio of the blade root height h (see Fig. 68) to the diameter d_0 is small ($\frac{h}{d_0}$ = 0.5 ÷ 0.7), friction forces cannot be disregarded.

Hence, the condition of equilibrium may be written as /16[illegible]

$$M = M_{k.d} + M_{tr} \qquad (152)$$

where M - moment applied to the root end of the blade;

$M_{k.d}$ - equilibrium moment created by forces of contact pressure;

M_{tr} - equilibrium moment created by friction forces in the blade root seat in the hub.

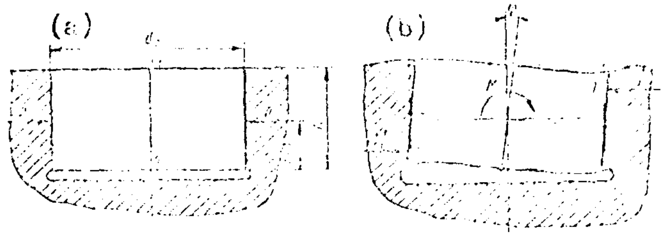

Fig. 69. Forces applied at the root end of the blade: a. after assembly of the propeller; b. under the action of bending moment.

The following principal assumptions were made in the calculation:

contact pressure emerging in the propeller assembly is uniformly distributed along the circumference of the root end of the blade and its height [illegible] const;

when the root end is subjected to the action of the moment M, redistribution of forces applied to the root end along its height will occur according to linear law (Fig. 70).

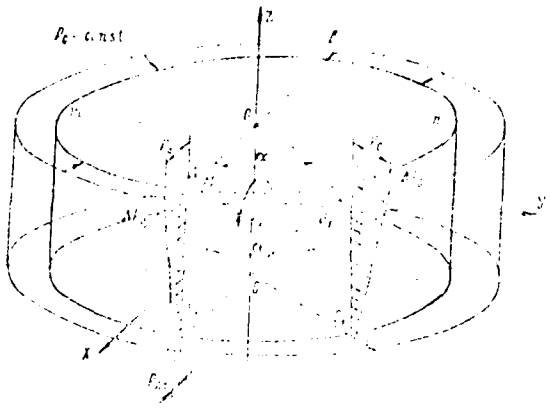

Fig. 70. Diagram of normal pressure on the cylindrical root of the blade after assembly

To provide for the possibility of replacing blades in case they /163
break down, the maximum contact pressure and corresponding radial stress should not exceed a certain magnitude σ'_{rm}, which eliminates the possibility of plastic deformations of walls of the hole in the hub.

In analogy with the distribution of pressures on mutually acting surfaces of journals and shafts, it is assumed that there is no contact pressure increase ΔP in horizontal cross sections of the blade root end as a function of angle α (see Fig. 70).

Then, the moment of contact pressure forces

$$M_{k.s} = 0{,}167\sigma_{rm}d_0h^2,$$

and the moment of friction forces

$$M_{tr} = 0{,}5f\sigma_{rm}d_0h.$$

In these equations, the maximum value of σ'_{rm} should not exceed $0.86\ \sigma'_{sc}$.

A formula for calculating the maximum moment absorbed by the joint, taking into consideration the dimensions of the seat in the hub and the mechanical properties of the propeller hub material, is in the form

$$M = 0{,}11\sigma_{sc}d_0h^2 + 0{,}43f\sigma_{sc}d_0h. \qquad (143)$$

where σ_{sc} - yield point of hub material;

d_o - diameter of the blade root end;

h - its height.

If some of the elements of propeller are known, such as number of blades Z, width of the root cross section of the blade b_p, dimensions of the cone of the propeller shaft, as well as some dimensions of the hub, which are selected according to design or manufacturing considerations, and the bending in the joint during breakdown of the blade at the root M_c, then the problem may be reduced to determining the dependence of d_o and h_o on some parameter m and some quantity $x_{1,2} = f(m)$.

When Z = 4 (number of blades in propellers most often used), $d_o = 2x$, and $h = (m-x)$, the expression (142) may be presented in the form

$$M = 2(A - 2B)x^3 - 4m(A - B)x^2 + 2Am^2x, \tag{144}$$

where $A = 0.144\ \sigma'_{sc}$, $B = 0.43\ f\sigma'_{sc}$.

This expression reaches the maximum with

$$x_{1,2} = \frac{2m(A - B) \pm m\sqrt{A^2 - 2AB + 4B^2}}{3(A - 2B)}.^{*}$$

*Negative root here does not have any meaning.

Substituting the value of M in expression (144) by M_c and the positive root x, we obtain the sought value of parameter m which determines the necessary minimum dimensions of d_o and h, which provide for the strength of the joint being designed.

The value of permissible contact pressure in assembling a propeller, taking into consideration the above assumptions, is $(p) = 0.43\ \sigma_{sc}$. /147

The interference (necessary for blind holes of small depths) is determined by formula (140) also with $C_c = 0.5$, while the necessary temperature of cooling is determined by equation (141).

BIBLIOGRAPHY

1. Aravin, B. P. New Materials and Technology of Casting Marine Propellers, Leningrad, "Sudostroyeniye", 1971, No. 10.

2. Bakht, Yu. V. Lovenfel'd, Ye. G., Kuretskiy, A. A. Grebnyye vinty reguliruyemogo shaga (Controllable Pitch Propellers), Leningrad, "Sudpromgiz" Publishing House, 1961.

3. Basin, A. M., Miniovich, I. Ya. Teoriya i raschet grebnykh vintov (Theory and Calculation of Marine Propellers), Leningrad, "Sudpromgiz" Publishing House, 1963.

4. Belyayev, V. A. Ob udare tverdogo tela o lopast' grebnogo vinta (Concerning Impact of a Solid Object Against a Propeller Blade) IN: Trudy A. A. Zhdadov Gor'kiy Polytechnic Institute, v. 14, no. 1, 1958.

5. Boroday, I. K., Netsvetayev, Yu. A. Kachka sudov na morskom volnenii (Pitching and Rolling of Ships on Rough Seas), Leningrad, "Sudostroyeniye", 1969.

6. Georgiyevskaya, Ye. P. Kavitatsionnaya eroziya grebnykh vintov i metody bor'by s ney (Cavitation Erosion of Propellers and Methods Of Its Prevention), Leningrad, "Sudostroyeniye", 1970.

7. Goldsmit, V. Udar. Teoriya i fizicheskiye svoystva soudaryayemykh tel (Impact. Theory and Physical Properties of Colliding Bodies), Moscow, "Stroyizdat" Publishing House, 1965.

8. Dmitriyev, V. A. et al. Theoriya mekhanizmov i mashin, detali mashin i pod'yemno-transportnyye mashiny (Theory of Mechanisms and Machines, Parts of Machines and Lifting and Transport Equipment), "Rechnoy Transport" Publishing House, 1963.

9. Dobrovol'skiy, V. A. Detali mashin (Parts of Machines), 7th edition, State Publishing House of Technical Literature, Ukr. SSR, 1954.

10. Zhuchenko, M. M., Ivanov, V. M. Sudovyye dvizhitel (Ship Propellers), Leningrad, "Sudpromigiz", 1956.

11. Ivanova, V. S. Ustalostnoye razrusheniye metallov (Fatigue Failure of Metals), State Scientific-Research Publishing House of Literature on Ferrous and Non-Ferrous Metallurgy, 1963.

12. Ignat'yev, M. A. Grebnyye vinty sudov ledovogo plavaniya (Propellers of Ships for Navigation in Ice), Leningrad, "Sudostroyeniye", 1966.

13. Kabachinskiy, N. N., Solov'yev, S. A. Zadachi opredeleniya napryazheniy v grebnom valu i grebnom vinte pri udare yego lopasti o tverdyy predmet (Problems of Determining Stresses in Propeller Shaft and Propeller During Impact of Its Blade Against a Solid Object). IN: Trudy A. A. Zhdanov Gor'kiy Polytechnic Institute, v. 9, no. 4, 1956.

14. Kartyshev, A. V. Grebnyye vinty iz chromamargantsevoy stali (Propellers Made of Chromium-Manganeze Steel), Leningrad, "Sudostroyeniye", 1969.

15. Katsman, F. M., Kudrevatyy, G. M. Konstruirovaniye vinto-rulevykh komplexov morskikh sudov (Design of Rudder-Propeller Units of Sea-Going Ships), Leningrad, "Sudpromgiz", 1963.

16. Katsman, F. M., Pustoshnyy, A. F., Shtumpf, V. M. Propul'sivnyye kachestva morskikh sudov (Propulsive Features of Sea-Going Ships), Leningrad, "Sudostroyeniye", 1972.

17. Kravchenko, P. Ye. Ustalostnaya prochnost' (Fatigue Strength), Moscow, "Vysshaya Shkola" Publishing House, 1960.

18. Lavrent'yev, V. M. Sudovyye dvizhiteli (Ship Propellers), "Morskoy Transport" Publishing House, 1949. /162

19. Lipis, V. B. K raschetu po vikhrevoy teorii deystviya grebnogo vinta pri kachke sudna (Concerning Calculation of the Propeller Action During Rolling and Pitching of the Ship Using Vortex Theory). IN: Trudy: TsNIIMF, no. 72, 1966.

20. Miniovich, I. Ya. Vliyaniye kachki korablya na gidrodinamicheskiye kharakteristiki grebnykh vintov (Effect of Pitching and Rolling of the Ship on Hydrodynamic Characteristics of Propellers). "Sudostroyeniye", no. 5, 1949.

21. Nikitin, M. N. Reliability of Fastening Detachable Propeller Blades. "Morskoy Flot", no. 3, 1970.

22. Oding, I. A. Dopuskayemyye napryazheniya v mashinostroyenii i tsiklicheskaya prochnost' metallov (Permissible Stresses in Machine Building and Cyclic Strength of Metals). Moscow, GNTI, 1962.

23. Papir, A. E. Osevyye nasosy vodometnykh dvizhiteley (Axial Pumps of Water-Jet Propellers). Leningrad, "Sudostroyeniye", 1965.

24. Perchenskiy, I. S. Ledovedeniye i ledotekhnika (Ice Science and Ice Technics), Leningrad, "Gidrometeoizdat" Publishing House, 1967.

25. Rozhkov, L. P., Sidorov, N. P. Selection and Calculation of Joints in Propellers With Detachable Plastic Blades. Technologiya sudostroyeniya, no. 8, 1964.

26. Romanov, V. V. Vliyaniye korrozionnoy sredy na tsiklicheskiyu prochnost' metallov (Effect of Corrosive Medium on Cyclic Strength of Metals). Moscow-Leningrad, "Nauka" Publishing House, 1969.

27. Rokhlin, A. G. Konicheskiye pressovye posadki grebnykh vintov i muft (Conical Press Fits of Propellers and Couplings), Leningrad, "Sudpromigiz", 1960.

28. Rusetskiy, A. A., Zhuchenko, M. M., Dubrovin, O. V. Sudovyye dvizhiteli (Ship Propellers), Leningrad, "Sudostroyeniye", 1971.

29. Rusetskiy, A. A. Gidrodinamika vinta reguliruyemogo shaga (Hydrodynamics of Controllable-Pitch Propeller). Leningrad, "Sudostroyeniye", 1968.

30. Sokolov, N. N., Lazarenko, S. P., Zhuravlev, V. I. Grebnye vinty iz alyuminiyevoy bronzy (Propellers Made of Aluminum Bronze). Leningrad, "Sudostroyeniye" 1971.

31. Sokolov, N. N., Rozen, M. P. Grebnyye vinty iz nerzhaveyushchey stali (Stainless Steel Propellers). Leningrad, "Sudpromgiz", 1960.

32. Yakonovskiy, S. V. External Forces Acting on a Propeller Blade During Navigation in Ice and Their Dependence on Geometrical and Kinematic Parameters of the Propeller. IN: Materialy po obmenu proizvodstvenno-tekhnicheskim opytom proektirovaniya morskikh sudov (Materials on Exchange of Industrial and Technical Experience in Design of Sea-Worthy Ships), no. 3, Leningrad, "sudostroyeniye", 1967.

33. Yakonovskiy, B. V. O vneshnikh silakh deystvuyushchikh na lopast' grebnogo vinta pri udare o led (Concerning External Forces Acting on the Propeller Blade During Impact Against Ice). In: Materials on Exchange of Experience. Trudy NTO SP, no. 62, 1964.

34. Register of the USSR. Pravila klassifikatsii i postroyki morskikh sudov (Rules for Classification and Building of Sea-Going Ships), Part 9, Moscow-Leningrad, "Transport" Publishing House, 1967.

35. Chirila, J. V. Dinamische Beanspruchung von Propellerflugeln auf dem Motorschiff "Pekari" Schiff und Hafen, 1970, no. 3.

36. Gutshe, F. Untersuchung von Schiffsschrauben in Schrager Anstromung Schiffbauforschung, Heft 3/4, 1964.

37. Hadler, J. B., Cheng, H. M. Analysis of Experimental Wake Data in Way of Propeller Plane of Single and Twin-Screw Ship Models. Transactions SNAME, vol. 73, 1965.

38. Keyser, R. and Arnoldus, W. Strength Calculation of Marine Propellers, International Shipbuilding Progress, 1959, no. 53.

39. Minsaas, K. J. Propeliteori, Skipmodelltanken Norges Tekniske Hogskole Trondheim, Skipsmodelltankens Meddelelse, 1967, no. 96.

40. Oberembt, H. Zur Bestimmung der instationaren Flugelkrafte bei einem Propeller mit aus dem wasser herausschlagenden Flugeln. Shiffstechnik, May 1970.

41. Romsom, J. Propeller Strength Calculation. The Marine Engineer and Naval Architect, 1952, no. 2-3.

42. Rosingh, W. H. C. E. Hoogbelaste Scheepsschroeven Spanningsmetingen en sterkteberekening, Ship en Werf, 1944, no. 11; 1945, no.12.

43. Sontvedt. Propeller induced exitation forces. Norske Veritas, Classification and Registry of Shipping, Publication, January 1971, no. 74.

44. Taylor, D. W. The speed and power of Ships. Washington, D. C., 1933.

45. Wereldsma, R. Stress measurements on a propeller blade of a 40,000 ton tanker on full scale. International Shipbuilding Progress, January 1961.